universität wien

MASTERARBEIT / MASTER'S THESIS

Titel der Masterarbeit / Title of the Master's Thesis

„The role of Sprouty3 in brain cancer-derived cells"

verfasst von / submitted by

Burcu Emine Çelik-Selvi, BSc

angestrebter akademischer Grad / in partial fulfilment of the requirements for the degree of

Master of Science (MSc)

Wien, 2019 / Vienna 2019

Studienkennzahl lt. Studienblatt / degree programme code as it appears on the student record sheet:	A 066 834
Studienrichtung lt. Studienblatt / degree programme as it appears on the student record sheet:	Masterstudium Molekulare Biologie
Betreut von / Supervisor:	Assoc. Prof. Dr. Hedwig Sutterlüty

DANKSAGUNG

Mein Dank gilt meiner Familie, insbesondere meiner Mutter Gülay, der ich diese Diplomarbeit widmen möchte. Danke Mama, dass du mich immer unterstützt und dieses Studium ermöglicht hast.

Dankbar bin ich meinem Mann Serdar, der an mich glaubt und mich mit seiner Bewunderung für meine Arbeit mit Stolz erfüllt. Eine wunderbare Zukunft mit dir ist mein besonderer Antrieb.

Meinen Geschwistern Hande und Berk, weil sie mich mit ihren ständigen Fragen über mein „zukünftiges Einkommen als Fertigstudierte“ motivieren und inspirieren.

Ein großes Dankeschön an Carmen und Matthias, weil ich auf sie zählen kann und sie mir immer den Rücken freihalten. Ohne euch wäre ich nicht so weit gekommen. Oma, Opa und Petra, weil sie mich mit offenen Armen empfangen haben.

Meinen Freundinnen Hülya, Asuman und Zeynep, die mich immer wieder aufmuntern und anspornen. Unsere angeregten Tee-Zeiten genieße ich immer wieder sehr.

Im Besonderen gilt mein Dank Assoc. Prof. Dr. Hedwig Sutterlüty-Fall, für das in mich gesetzte Vertrauen, sowie die geduldige und engagierte Betreuung meiner Diplomarbeit. Ich bin zutiefst dankbar für das freundliche, ja fast familiäre Arbeitsklima in der Gruppe. Weiters bedanke ich mich bei Jakob und Jihen für ihre exzellente Unterstützung und unvergessliche Zeit im Labor.

Ich bedanke mich auch bei den Bergers, sowie bei allen anderen Mitarbeitern des Krebsforschungsinstituts für ihre Unterstützung, insbesondere bei Gerald für die lehrreiche Einführung ins Live Cell Imaging und Silvia für die vielen netten Gespräche.

TABLE OF CONTENTS

1 Introduction

1.1 Brain cancer

Brain and central nervous system (CNS) cancers are identified as a rare but one of the most devastating forms of cancer. These tumor entities are diverse in terms of molecular defects, morphology and clinical behavior. Based on the data of the years 2011 to 2015, the incidence of a new brain tumor was 6.4 per 100,000 persons per year. The peak prevalence ranged between 55 and 64 years of age, with a slight male predominance. In 2018 it was estimated that there will be 23,880 new cases of brain and CNS cancer, leading to 16,830 deaths. These accounted for 1.4% of all new cases of cancer and 2.8% of all cancer deaths in the United States, being the tenth leading cause of cancer death with a five-year survival rate of 33.2% [1]. However, in infants and children pediatric brain tumors are the most common solid tumors and the second most common cancer after hematological malignancies. Accounting for approximate 20-25% of all primary pediatric tumors, brain and other CNS tumors are the leading cause of cancer-related death in this population [2].
Brain cancers present challenges in the determination of risk factors as there is no definitive cause that contribute to brain tumorigenesis. Multiple studies have proposed conflicting results on whether exposure to non-ionizing radiation as from cell phone usage increases brain tumor risk, though it is now accepted that the risk is likely negligible [3-6]. On the contrary, certain doses and forms of ionizing radiation, such as high-dose radiotherapy or radiation from A-bombs and nuclear tests are the only established environmental risk factor for CNS tumors [7-9]. Very little is known about the genetic risk factors for brain cancer and so far, multiple familiar cancer predisposition syndromes have been associated with brain tumors, including neurofibromatosis, Li-Fraumeni syndrome, tuberous sclerosis and Turcot's syndrome. These syndromes have in common that individuals inherit a germline mutation in tumor suppressor genes which are involved in downregulation of growth promoting signaling pathways in the cell, such as NF1 or NF2 (Neurofibromin 1/2) in neurofibromatosis, TSC1 or TSC2 (Tuberous Sclerosis Complex 1/2) in tuberous sclerosis or genes involved in DNA repair in the case of Turcot's syndrome and TP53 (Tumor protein p53) in Li-Fraumeni syndrome [10-12]. Tumors initiate when the remaining copy of the tumor suppressor is silenced or mutated, giving rise to cells with a growth advantage and allowing cancers to form. Apart

to these well-known syndromes, brain tumors are suggested to aggregate in families [13]. Additionally, genome-wide linkage studies of familial glioma point to the 15q23 locus [14]. Due to the delicate anatomy and physiology of the brain, therapeutic strategies employed for brain cancer treatment encounter several hurdles. Accompanied by poor prognosis and high relapse rate, the situation is further aggravated, leading to the high mortality rate in brain cancer.

1.2 Classification and types of brain cancer

Primary brain tumors consist of heterogenous neoplasms of glial and non-glial origin. The following section will mainly address those of glial origin as they represent the specialism of this study.

Gliomas, which arise from glial or precursor cells, are the most prevalent type of brain tumor in adults, accounting for 81% of malignant brain tumors. They include astrocytomas (AC), oligodendrogliomas (ODG) and ependymomas, which arise from astrocytes, oligodendrocytes (Fig. 1) and from the ependyma, respectively. Glioblastoma (GB), the most common astrocytic tumor and WHO Grade IV, accounts for 57% of all gliomas and has a five-year survival rate of 5.6% [15]. Regarded as a variant of GB, gliosarcoma (GS) is defined as a biphasic neoplasm of glial origin with mixed areas of malignant mesenchymal components [16]. Concerning pediatric tumors, neuroblastoma (NB) is the second most common solid tumor in children. NB arises from the developing sympathetic nervous system and exhibits unique characteristics such as high metastatic frequency or even spontaneous tumor regression of [17].

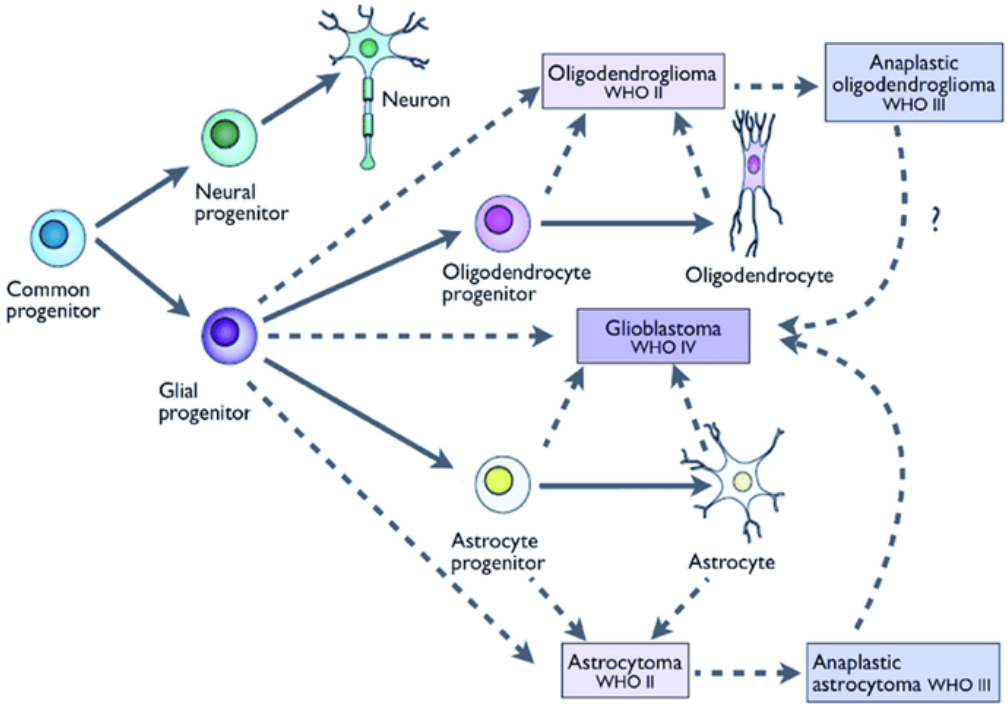

Fig. 1. Origin of primary brain tumors. Common progenitors produce neuronal and glial progenitors that differentiate into mature neurons, astrocytes and oligodendrocytes, which give rise to indicated gliomas. Modified from [18].

There are more than 150 different types of CNS tumors and unlike other types of cancer, primary brain and CNS tumors are not staged, but are classified according to a malignancy scale. Tumor types are assigned a grade, ranging from Grade I (least malignant) to Grade IV (most malignant). Table 1 demonstrates the 2016 World Health Organization Classification of Tumors of the Central Nervous System (2016 WHO CNS) by cell origin and predicted clinical behavior, based on histological characteristics such as cellularity, mitotic activity, pleomorphism, necrosis, endothelial proliferation as well as genetic and epigenetic biomarkers [19, 20].

Table 1. 2016 WHO grading of selected CNS tumors [20].

WHO grades of select CNS tumours	
Diffuse astrocytic and oligodendroglial tumours	
Diffuse astrocytoma, IDH-mutant	II
Anaplastic astrocytoma, IDH-mutant	III
Glioblastoma, IDH-wildtype	IV
Glioblastoma, IDH-mutant	IV
Diffuse midline glioma, H3 K27M–mutant	IV
Oligodendroglioma, IDH-mutant and 1p/19q-codeleted	II
Anaplastic oligodendroglioma, IDH-mutant and 1p/19q-codeleted	III
Other astrocytic tumours	
Pilocytic astrocytoma	I
Subependymal giant cell astrocytoma	I
Pleomorphic xanthoastrocytoma	II
Anaplastic pleomorphic xanthoastrocytoma	III
Ependymal tumours	
Subependymoma	I
Myxopapillary ependymoma	I
Ependymoma	II
Ependymoma, *RELA* fusion–positive	II or III
Anaplastic ependymoma	III
Other gliomas	
Angiocentric glioma	I
Chordoid glioma of third ventricle	II
Choroid plexus tumours	
Choroid plexus papilloma	I
Atypical choroid plexus papilloma	II
Choroid plexus carcinoma	III
Neuronal and mixed neuronal-glial tumours	
Dysembryoplastic neuroepithelial tumour	I
Gangliocytoma	I
Ganglioglioma	I
Anaplastic ganglioglioma	III
Dysplastic gangliocytoma of cerebellum (Lhermitte–Duclos)	I
Desmoplastic infantile astrocytoma and ganglioglioma	I
Papillary glioneuronal tumour	I
Rosette-forming glioneuronal tumour	I
Central neurocytoma	II
Extraventricular neurocytoma	II
Cerebellar liponeurocytoma	II
Tumours of the pineal region	
Pineocytoma	I
Pineal parenchymal tumour of intermediate differentiation	II or III
Pineoblastoma	IV
Papillary tumour of the pineal region	II or III
Embryonal tumours	
Medulloblastoma (all subtypes)	IV
Embryonal tumour with multilayered rosettes, C19MC-altered	IV
Medulloepithelioma	IV
CNS embryonal tumour, NOS	IV
Atypical teratoid/rhabdoid tumour	IV
CNS embryonal tumour with rhabdoid features	IV
Tumours of the cranial and paraspinal nerves	
Schwannoma	I
Neurofibroma	I
Perineurioma	I
Malignant peripheral nerve sheath tumour (MPNST)	II, III or IV
Meningiomas	
Meningioma	I
Atypical meningioma	II
Anaplastic (malignant) meningioma	III
Mesenchymal, non-meningothelial tumours	
Solitary fibrous tumour / haemangiopericytoma	I, II or III
Haemangioblastoma	I
Tumours of the sellar region	
Craniopharyngioma	I
Granular cell tumour	I
Pituicytoma	I
Spindle cell oncocytoma	I

Molecular signatures such as the genetic status of isocitrate dehydrogenase (IDH), the integrity status of chromosomes 1 and 19 (1p/19q) or the histone H3 K27M status aid to increase the diagnostic accuracy within diffuse glioma subtypes (Table 1).

Fig. 2 demonstrates a classification algorithm for gliomas. IDH1 and IDH2 are enzymes that convert isocitrate to α-KG (α-ketoglutarate). Mutations of IDH1 codon 132 and IDH2 codon 172 are an early event in gliomagenesis and contribute to neomorphic activity, resulting in conversion of α-KG to the oncometabolite D-2-hydroxyglutarate (2-HG), the accumulation of which may contribute to the glioma cytosine-phosphate-guanine (CpG) island methylator phenotype (G-CIMP) [21]. IDH wild-type (lacking the mutation) and IDH-mutant GBs are clinically distinct from each other. While IDH^{wt} GBs develop de novo and account for 90% of GBs, IDH^{mut} GB arise from astrocytomal precursor lesions. Furthermore, IDH^{mut} GBs are accompanied by frequent TP53 mutations and absence of EGFR amplification. Studies showed that the mean overall survival time of patients with $IDH1^{mut}$ GB was more than twice as long as that of patients with $IDH1^{wt}$ GB [22].

Astrocytomas typically develop in cells which harbor IDH1/2 mutations and subsequently acquire TP53 mutations (Fig. 2). About 65% of diffuse ACs carry a TP53 mutation in addition to IDH1/2 mutations, whereas 75% of ODGs contain a 1p/19q co-deletion, which is also a predictor of prolonged survival in patients. Notably, in diffuse gliomas TP53 mutation and loss of 1p/19q are mutually exclusive [23]. Recent studies additionally described mutations in the ATRX (α-Thalassemia X-Linked Mental Retardation Syndrome) gene which were found to be co-present with IDH1/2 and TP53 mutations in diffuse astrocytomas [24, 25].

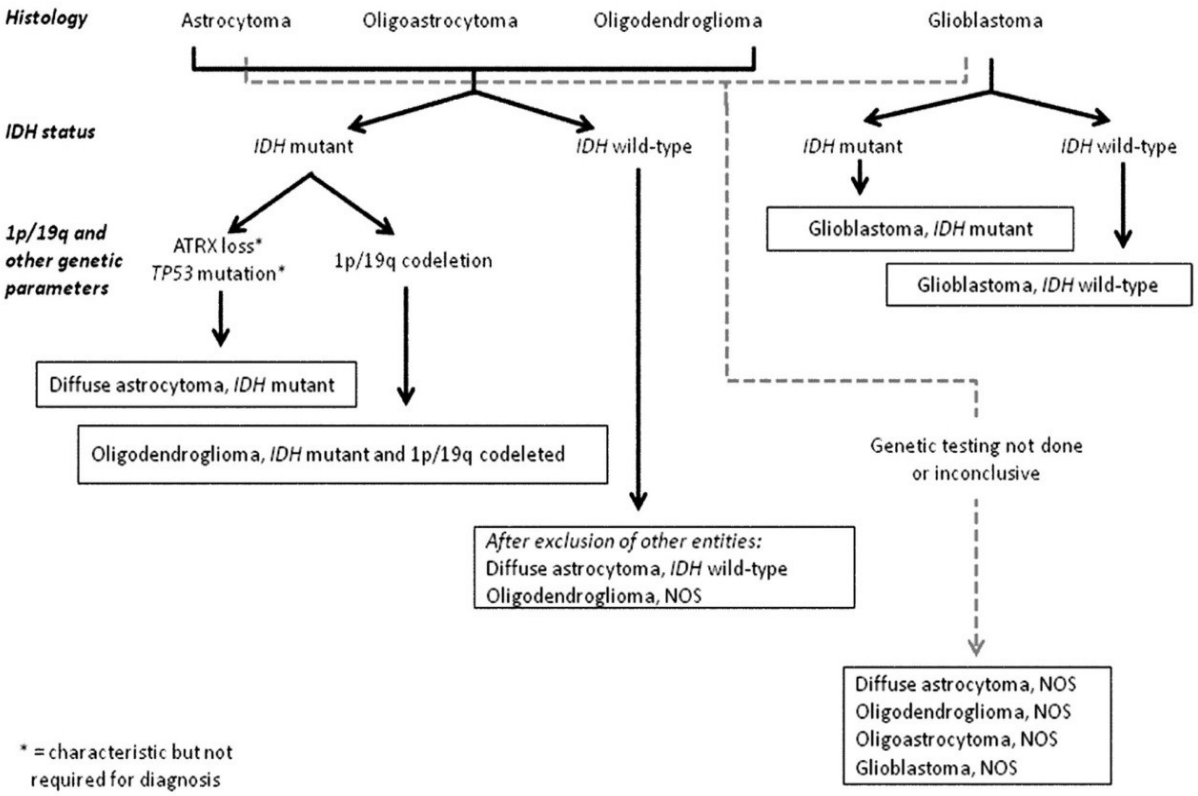

Fig. 2. 2016 CNS WHO algorithm for diffuse glioma. Classifications are based on histological appearance and genetics. NOS, not otherwise specified (tumor lacking a diagnostic mutation) [20].

1.3 Core pathway alterations in brain cancer

Decades of molecular studies have identified a highly interconnected network of aberrations in human malignancies as well as in GBs, involving three major pathways: (1) the dysregulation of growth factor signaling via amplification and mutational activation of receptor tyrosine kinase (RTK) genes, including the activation of the phosphatidyl inositol 3-kinase (PI3K) pathway, (2) the inactivation of the p53 and (3) retinoblastoma (RB) tumor suppressor pathways [26].

Fig. 3 summarizes whole-exome sequencing (WES) studies by the Cancer Genome Atlas Research Network (TCGA), describing that 90%, 86% and 79% of 291 GB samples harbored alterations of the RTK, TP53 and RB pathways, respectively, suggesting that dysregulation of these three pathways is a main requirement for glioblastoma pathogenesis. In addition to mutations of TP53 itself, inactivation of the p53 pathway occurred in the form of amplifications of its negative feedback regulators MDM2 (Mouse double minute 2 homolog) (7.6%) and MDM4 (Mouse double minute 4 homolog) (7.2%), severely compromising its tumor suppression ability by inducing apoptosis. Among the samples harboring RB pathway aberrations, the most common event was deletion of the CDKN2A or CDKN2B (Cyclin-dependent kinase Inhibitor 2A/B) locus (overall 61%), followed by amplification of the downstream CDK4 (Cyclin-dependent kinase 4) locus (14%), leading to loss of cell cycle control. The deletion of CDKN2A, which encodes the tumor suppressor p14ARF, disturbs both pathways as it targets the p53 inhibitory protein MDM2 for degradation. Considering the RTK genes, EGFR (epidermal growth factor receptor) (57%) was the most frequently activated, accompanied by mutations of PIK(3)K (25%), NF1 (10%) and alteration of PTEN (Phosphatase and Tensin homolog) (41%) [26, 27].

Since Sprouty proteins play a key role in RTK-mediated signaling, this pathway will be described in more detail in the following section.

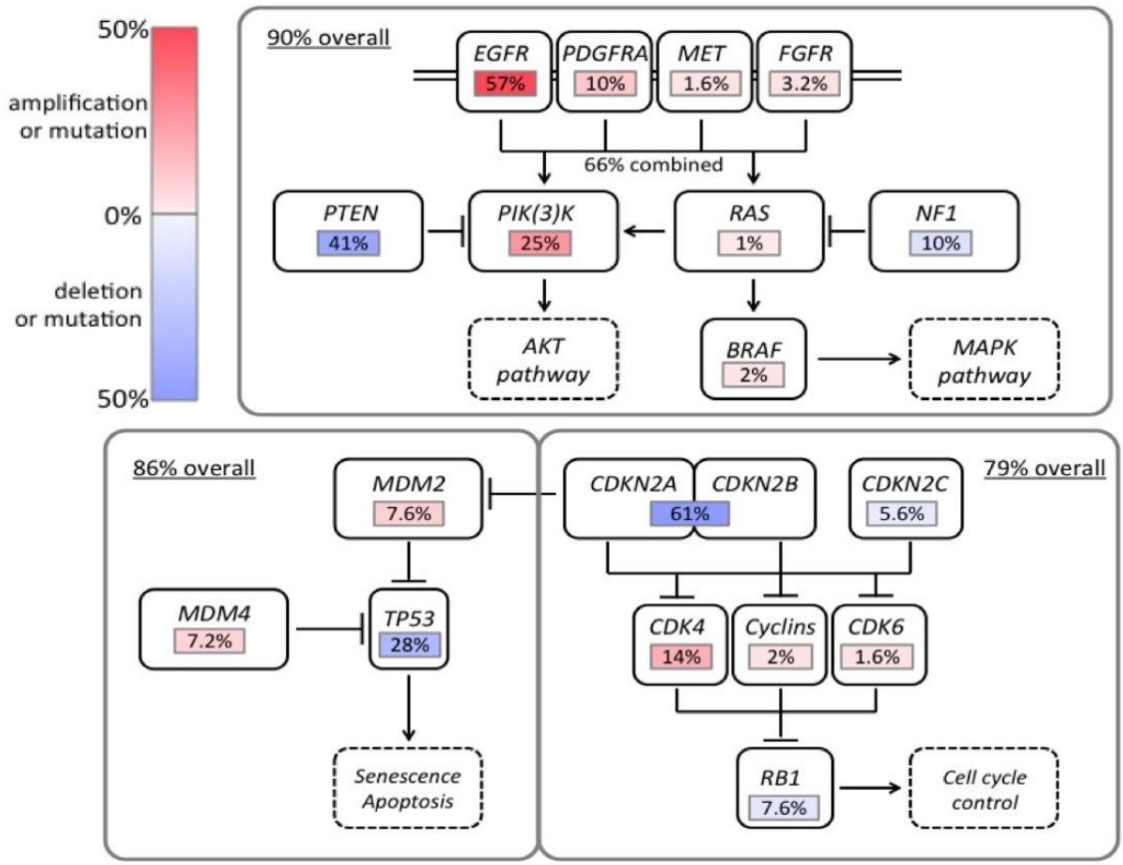

Fig. 3. Alterations of canonical PI3K/MAPK, p53 and RB regulatory pathways in GB [27].

1.4 Receptor tyrosine kinase (RTK) mediated signaling pathways

RTKs are essential components of signaling transduction that enable communication between cells via their environment. They act as cell surface receptors for growth factors, hormones, cytokines, neurotrophic factors and other extracellular signaling molecules. Therefore, RTKs have emerged as key regulators of critical cellular processes, such as differentiation, cell proliferation, metabolism, survival and cell migration.

All RTKs exhibit a similar molecular architecture and are organized into five fundamental structures: an extracellular (N-terminal) ligand-binding ectodomain, a single transmembrane helix (TM) and a cytoplasmic region composed of the juxtamembrane regulatory region (JM) followed by a protein tyrosine kinase (TK) domain plus a carboxy (C- terminal) region (Fig. 4) [28].

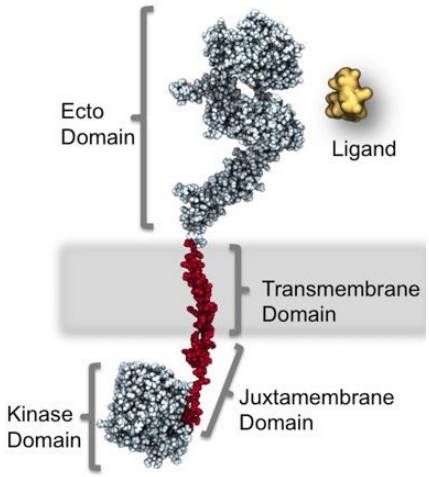

Fig. 4. Schematic representation of a generic RTK model. Depicted are an extracellular ligand binding ectodomain, a single transmembrane spanning helix, a basic JM region, and a kinase domain plus a C-terminal region (not shown). The TM and JM regions have been highlighted in red. Figure modified from [28].

The unique ligand-binding properties between different RTKs are determined by features in the variable ectodomain such as cysteine/leucine/glycine-rich motifs, fibronectin III-like repeats and immunoglobulin-like domains. Fig. 5 illustrates the structural diversity of the ectodomains and TK domains, which together organize the RTKs into twenty subfamilies with various members in humans, including, among others, fibroblast growth factor receptor (FGFR), epidermal growth factor receptor, insulin and insulin-like growth factor receptor (InsR, IGFR), platelet-derived growth factor receptor (PDGFR), vascular endothelial growth factor receptor (VEGFR), hepatocyte growth factor receptor (Met or HGFR) and the proto-oncogene Kit. Consistently with the key regulatory roles they play, RTKs are highly conversed in evolution from *C.elegans* to humans [29, 30].

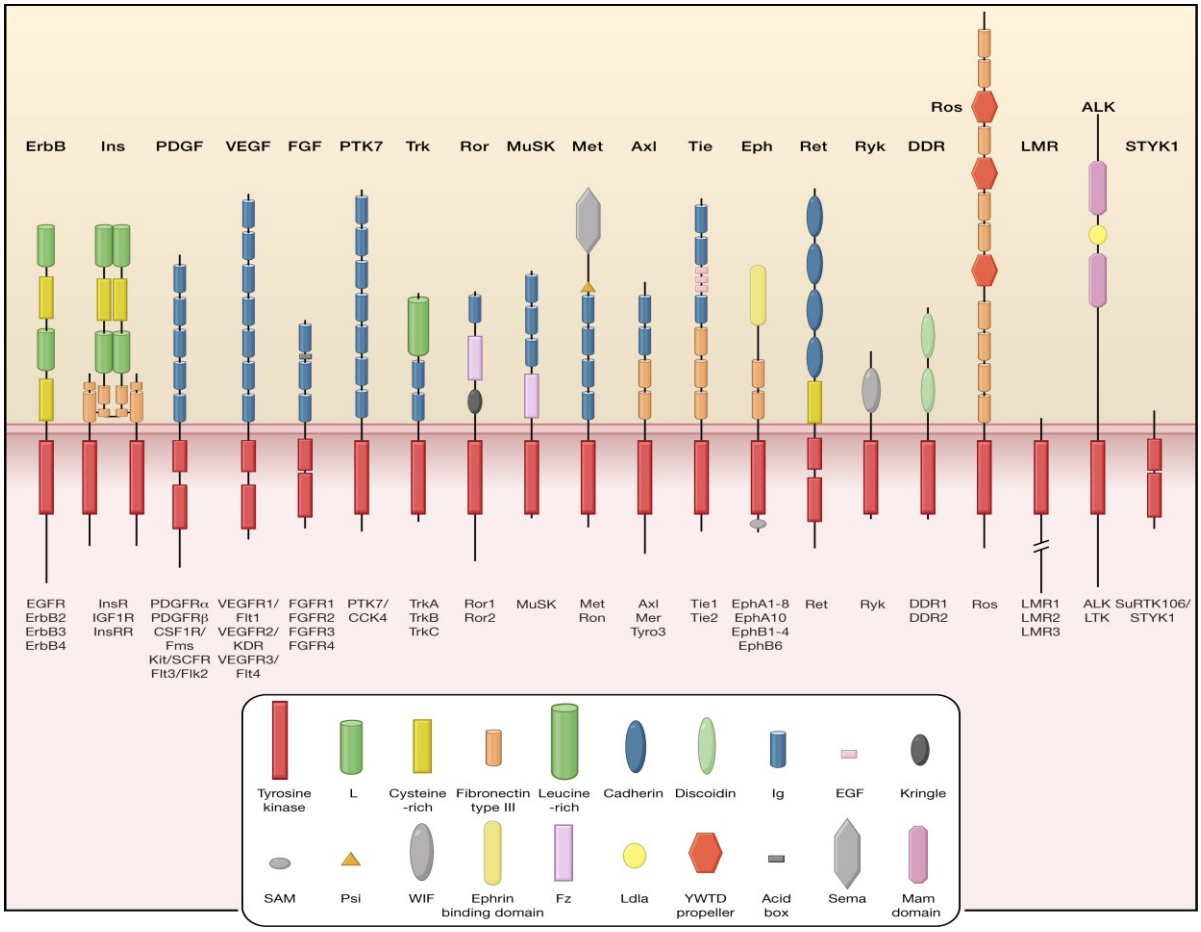

Fig. 5. Human receptor tyrosine kinases. The domain architecture of the 20 human subfamilies are shown schematically with family members listed beneath each receptor. Structural features in the variable ectodomains are marked according to the key. The intracellular TK domains are shown as red rectangles [30].

1.4.1 Activation of RTKs

Generally, ligand-binding activates RTKs by inducing receptor oligo- or dimerization, which stabilizes interactions between adjacent cytoplasmic domains and leads to activation of the kinase domain. This allows tyrosine residues in the cytoplasmic region of each receptor monomer to be trans-phosphorylated by its partner receptor. The phosphorylated receptor then serves as a site for assembly and activation of intracellular signaling proteins containing a Src-homology 2 (SH2) domain or phosphotyrosine-binding (PTB) domain. This allows membrane recruitment of phospholipase Cγ (PLC-γ), which becomes phosphorylated and activated, and phosphatidyl inositol 3-kinase (PI3K), which is brought to its substrates at the membrane. Other key recruited molecules are growth factor receptor-bound protein 2 (Grb2) and Son of Sevenless (Sos), causing activation of the Ras-Raf-MEK-ERK pathway. Activation of these three intercellular cascades transduce the signals to the nucleus to regulate the transcription of target genes (Fig. 6) [31].

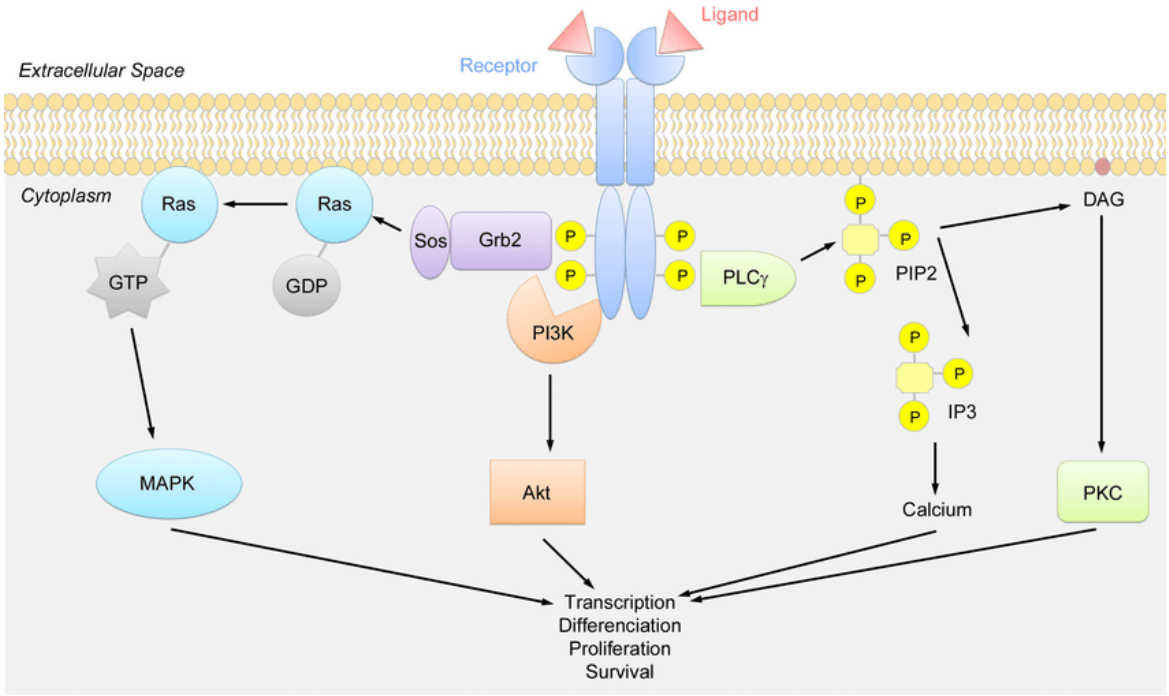

Fig. 6. Simplified schematic view of the RTK canonical signaling pathways. RTK are transmembrane receptors and interaction of dimers with their ligands induces a transphosphorylation on tyrosine residues of the intracellular domain. The phosphorylated cytoplasmic domain interacts with Grb2, PI3K and PLCγ. The integration of the activation of the three intracellular cascades leads to many different outputs at the cellular level [32].

1.4.2 The Ras/Raf/MAPK signaling cascade

Incoming signals registered via RTKs are relayed to the MAPK (mitogen-activated protein kinases) cascade via the Ras GTPase. By cycling between the inactive GDP-bound state and the active GTP-bound state, these proteins function as molecular switches. This cycle is controlled by guanine nucleotide exchange factors (GEFs) such as Sos, which catalyzes the conversion of inactive Ras-GDP to active Ras-GTP, and GTPase-activating proteins (GAPs) such as NF1, which terminate the active state by stimulating GTP hydrolysis [33].

Activated Ras then activates and transmits the signal to different effector proteins such as MLK3-, Raf- and MEK-kinases, which target the p38-, ERK1/2- and JNK signaling modules, respectively. The JNK and p38 pathways are activated in response to environmental stress or cytokines, whereas the MAPK/ERK (extracellularly regulated kinase) pathway responds to growth stimuli [34]. Another, less well-characterized class of stress-activated pathways is the ERK5 pathway, also termed as “Big MAP kinase 1” (Fig. 7) [35].

Ras-GTP stimulates serine/threonine-specific protein kinases belonging to the group of MAPKK kinases (MAP3K) including Raf and MEKKs (MEK kinase), which are at the top of the

three-tiered MAPK/ERK cascade [35]. MAPK3 then phosphorylates the downstream group of protein kinases, the MEK (MAP/ERK kinase) or MAP2Ks at two serine residues. MAP2Ks in turn phosphorylate the MAPKs ERK at a tyrosine and a threonine residue, classifying them as protein kinases with dual-specificity [36]. Inactivation of MAPKs occurs by dual-specificity protein phosphatases called MAPK phosphatases (MKP) which remove the activating phosphates on MAPKs [37].

ERKs ultimately deliver signals both to cytoplasmic and, upon dimerization, to nuclear substrates. ERK1/2 catalyzes phosphorylation and activation of over 150 substrates, including nuclear transcription factors such as c-Fos and Elk-1 (Fig. 7) [38].

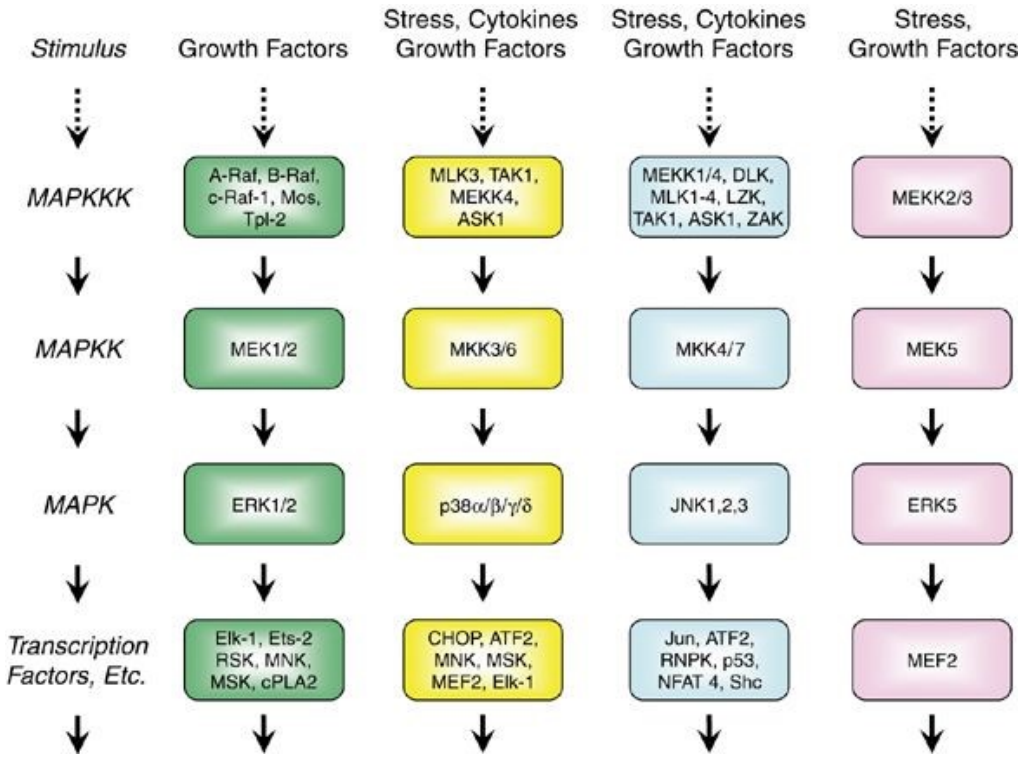

Fig. 7. Mammalian MAPK cascades. Four major MAP3K-MAP2K-MAPK protein kinases are depicted. The ERK (green) pathway is commonly activated by growth factors, the p38 (yellow), JNK (blue) and ERK5 (pink) pathways are additionally activated by cytokines or environmental stress, such as osmotic shock and ionizing radiation. Many of the substrates for MAPKs are nuclear transcription factors [39].

1.4.2.1 Deregulation in brain cancer

Gene amplification and mutations of EGFR enhance EGFR activation and occur in 57% of GBs as determined by the TCGA dataset [27]. Among EGFR mutants found in GB, the oncogenic EGFRΔIII (deletion of exons 2–7) was the most common and is thought to occur after amplification of $EGFR^{wt}$ [40]. EGFRΔIII arises from an in-frame deletion of 801 bp in the DNA se-

quence encoding the ligand-binding domain, rendering a truncated yet constitutively active receptor [41]. The kinase activity of EGFRΔIII is much weaker than that of ligand-activated full-length EGFR, but its weak constitutive kinase activity has been reported to be sufficient to deliver growth advantage to tumors [41]. EGFRΔIII in GB cells has also been shown to cross-talk with $EGFR^{wt}$ and thus to promote a more aggressive tumor phenotype through paracrine mechanisms [42].

Although mutations of the three Ras proto-oncogenes (K-RAS, H-RAS, N-RAS) are frequent in several cancer types to varying degrees, the Ras genes are rarely mutated in malignant and benign gliomas. The TCGA project reported a 1% mutation rate in the Ras genes and despite this low incidence, 10% of the GBs harbored inactivating mutations or deletions in the negative regulator of Ras, the NF1 gene. Any loss of its functionality will cause sustained intracellular levels of active Ras-GTP, resulting in prolonged activation of the Ras/Raf/MAPK signaling pathway [27].
Over 800 different mutations are known in the NF1 gene and gene product, with point mutations occurring in approximately 90% of cases and larger deletions occurring in about 10% of cases [43]. Mutation analysis of N-RAS, K-RAS and H-RAS in 93 gliomas, as reported by Jeuken et al., showed only one mutation, namely G10E in N-RAS, occurring in pure oligodendroglial tumors. However, findings of this and other groups indicate that Ras/Raf pathway activation in gliomas is achieved much more frequently by copy number gains rather than by activating Ras/Raf mutations [44, 45].

According to the dataset of the TCGA, BRAF activation mutations are not a frequent event in gliomas (2%) and never co-occurred with NF1 gene deletion [27]. The majority of BRAF mutations are located within the kinase domains of exons 11 and 15, affecting residues that stabilize the kinase in the inactive form. BRAF mutations provoke increased BRAF kinase activity and thus lead to constitutive activation of the ERK pathway [46]. In human malignancies, most BRAF mutations are missense mutations at the amino acid position 600, also referred to as $BRAF^{V600E}$, which accounts for 80% of all BRAF mutations [47]. However, analyses by various groups revealed a lower frequency of $BRAF^{V600E}$ mutation in gliomas. Davies et al. reported that 11% of 38 glioma cell lines carried the $BRAF^{V600E}$ mutation, whereas a study led by Knobbe et al. found that only three of 94 GBs (3.2%) carried the $BRAF^{V600E}$ gene. In line

with these observations, Basto et al. reported the presence of $BRAF^{V600E}$ in 6% of 34 GBs and 0% of 13 astrocytomas [47-49].

Recent breakthrough studies on pediatric low-grade astrocytomas uncovered genetic alterations of the BRAF gene involving copy number gains and rearrangements. A study by Pfister et al. evaluated 66 pediatric low-grade gliomas and found 44% of the tumors to carry BRAF gene duplication with increased downstream target genes expression [50]. In addition, comparative genomic hybridization studies revealed that gliomas carry extra copies of the $BRAF^{wt}$ gene and that this gain is more predominant in high-grade gliomas. A significant correlation could also be observed between activated MAPK and BRAF copy number gains [44]. The most common genetic abnormality and a clinical predictor for good outcome in pilocytic astrocytomas was found to be a BRAF duplication caused by BRAF-KIAA1549 fusion gene that mimics the constitutive kinase activity of oncogenic $BRAF^{V600E}$ [51].

1.4.3 The PI3K-Akt signaling pathway

PI3K and Akt play an evolutionarily conserved role in promoting cell, tissue and organismal growth downstream of growth factors. Stimulation of RTKs or G-protein-coupled receptors (GPCRs) lead to activation of PI3K bound via their regulatory subunit or adapter molecules like the insulin receptor substrate (IRS) protein (Fig. 8). This triggers the activation of PI3K and conversion of the phospholipid cell membrane components phosphatidylinositol 4,5-bisphosphate (PIP_2) to phosphatidylinositol 3,4,5-bisphosphate (PIP_3). PI3K activity is opposed by PTEN. Cytosolic Akt/protein kinase B (PKB) is recruited and engages PIP_3 at the plasma membrane through Pleckstrin Homology domain (PHD) binding, allowing phosphoinositide-dependent protein kinase 1 (PDK1) to access and phosphorylate T308 in the activation loop, leading to partial Akt/PKB activation. Maximal activation of Akt requires phosphorylation of S473 in the hydrophobic motif, primarily by the mechanistic target of rapamcyin complex 2 (mTORC2). Akt kinase inactivation takes place by actions of the two protein phosphatases Protein phosphatase 2A (PP2A) and PH domain leucine-rich repeat protein phosphatase (PHLPP). Similar to ERK, activated Akt phosphorylates downstream substrates involved in the regulation of diverse cellular functions, including multifunctional substrates such as GSK3, FoxO and mTORC1 [52].

The PI3K-AKT and Ras/MAPK pathways can cross-inhibit one another, but they can also act in a cooperative manner to robustly regulate key cellular processes involved in cell growth and proliferation [53].

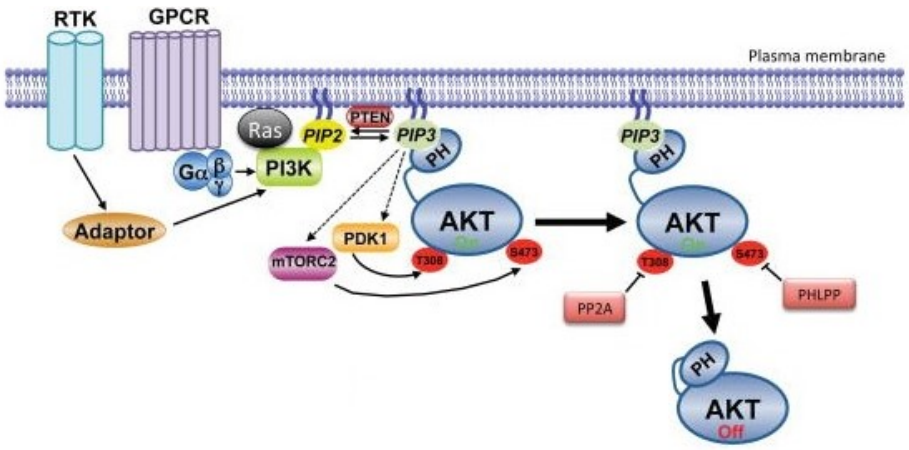

Fig. 8. Molecular mechanisms of Akt regulation. Stimulation of RTKs or GPCRs lead to activation of PI3K, leading to conversion of PIP2 to PIP3 at the plasma membrane. Cytosolic inactive AKT is recruited to the membrane and engages PIP3 through PH domain binding. This leads to phosphorylation of T308 and S473 by PDK1 and mTORC2, respectively, resulting in full activation. Signal termination is achieved by the PIP3 phosphatase PTEN, and the PP2A and PHLPP protein phosphatases. Modified from [52].

1.4.3.1 Deregulation in brain cancer

PTEN acts as a tumor suppressor gene, as it negatively regulates the PI3K-Akt pathway by blocking Akt activation via the reduction of intracellular levels of PIP_3. Loss of heterozygosity of chromosome 10, which causes deletions/mutations of PTEN, is a common event in GBs [54]. Akt activity is elevated in the absence of PTEN, leading to increased proliferation and inhibition of apoptosis.

According to the TCGA dataset, PI3K mutations were found in 63 of 251 GB samples (25.1%). These were mutually exclusive of PTEN mutations/deletions, with 59.4% of the GB samples harboring one or the other. Considering the RTK genes, 89.6% of the GBs had at least one alteration in the PI3K pathway. PTEN loss was associated with incremental increases in Akt pathway activity, while in $PI3K^{mut}$ samples, Akt activity was even lower than in samples lacking PI3K mutations [27].

1.4.4 The PLC-γ/Ca^{2+} pathway

Another highly conserved RTK signaling pathway is mediated by PLC-γ, which relays information from the activated receptor to downstream signaling cascades by production of second-messenger molecules (Fig. 6). Upon growth factor stimulation, PLC-γ is recruited to activated RTKs via SH2 domain-phosphotyrosine interactions and then subjected to phosphorylation by RTKs. As a consequence, activated PLC-γ hydrolyzes PIP_2 to form two second messengers - inositol (1,4,5)-trisphosphate (IP_3) and diacylglycerol (DAG). IP_3 activates calcium receptors on the endoplasmic reticulum, resulting in mobilization of intracellular Ca^{2+}, causing a cascade of intracellular changes and activity. Both Ca^{2+} and DAG work together to activate serine/threonine kinases of the protein kinase C (PKC) family, which in turn targets several substrates for phosphorylation. One of these targets is Raf1, which is, in this case, activated in a Ras-independent manner [55, 56].

1.5 Sprouty proteins

The Ras/Raf/MAPK signaling pathway plays a central role in the development of multicellular organisms as well as in signal transmission. Its activity is tightly controlled through complex actions of both positive and negative regulators that function at multiple levels of the signaling cascade. Sprouty (Spry) proteins represent a major class of modulators of RTK-dependent signaling pathways which function to attenuate or amplify the activated receptor signaling. Being in that position, Spry proteins are suggested to play an important role in human carcinogenesis.

The founding member of the Sprouty (Spry) family was discovered in a genetic screening in *Drosophila* as an antagonist of fibroblast growth factor signaling responsible for shaping the developing trachea [57]. Subsequent studies revealed four mammalian Spry proteins and one of them, Spry2, was found to exert similar functions to *dSpry* (Drosophila Sprouty) in modeling the branching of the mammalian lung [58].

1.5.1 Structure of Sprouty proteins

Based on sequence homology, orthologs of *dSpry* have been characterized in other species. In mammals, four Sprouty genes encoding for proteins Spry1-4 were identified with a molecular weight between 32-35 kDa [59].

Generally, in both *Drosophila* and mammals, all Spry proteins comprise conserved C-terminal cysteine-rich Spry domain and a highly divergent N-terminal domain, into which a conserved key tyrosine residue is located. While both termini are necessary for Spry activity, the C-terminus is thought to mediate Spry location while the N-terminus interacts with the SH2 domain of signaling molecules [60, 61].

Fig. 9 illustrates the structure of the human Spry1-4 proteins in more detail, showing the N-terminal invariant key tyrosine residue for each Spry isoform which is flanked by conserved residues, giving rise to the canonical Casitas B-lineage lymphoma (c-Cbl) binding domain (CBD). In the case of Spry2, the residues 52-59 represent the CBD [62]. Adjacent to it, the serine-rich motif (SRM) is situated. The C-terminal cysteine-rich domain (CRD), also known as the Spry (or translocation) domain, is embedded with a highly conserved motif that mediates binding to Raf1 (Raf1-binding domain, RBD). The CRD is shared by the structurally and functionally related Spred (Sprouty-related protein with EVH-1 domain) proteins [59].

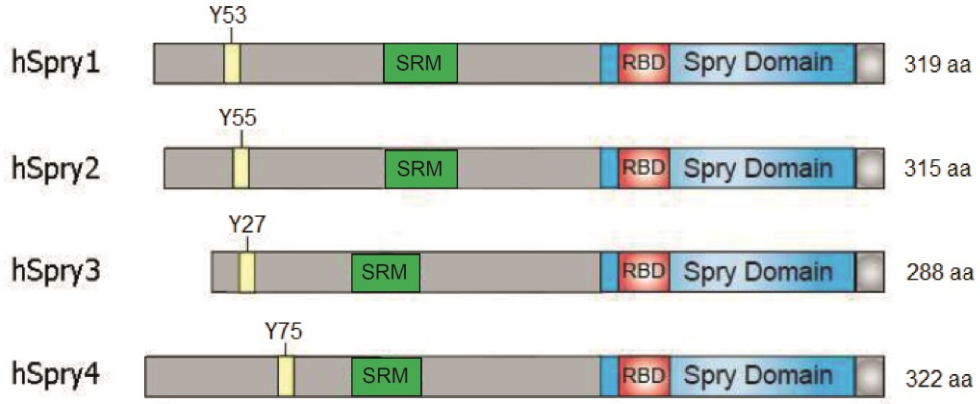

Fig. 9. Structure of Sprouty proteins. All Spry proteins have a conserved C-terminal cysteine-rich domain, also called Spry domain (blue), which in turn contains the RDB (Raf1 binding domain; red). The invariant key tyrosine (Y) residue, flanked by the CBD (c-Cbl binding domain; yellow), is located within the N-terminus and next to it the SRM (serine-rich motif; green) is situated. aa, amino acids. Modified from [59].

Besides translocation from the cytosol to the plasma membrane by binding to PIP_2, the C-terminal domain is also required for anchoring to the plasma membrane through palmitoylation, which was shown for Spry1 and Spry2 [63, 64]. Others have proposed that Spry

proteins may translocate to the plasma membrane via interactions through their C-terminal regions with caveolin-1 after serine phosphorylation in response to growth factor stimulation [64, 65]. Regardless of the mechanism, it is clear that translocation of Spry1 and Spry2 to the plasma membrane is an essential event for mediating their inhibitory role [60]. Additionally, the different Spry isoforms are thought to form homo-and hetero-oligomers through their CRDs [66, 67].

The sequence divergence between the N-terminal domains of Spry proteins might reflect their distinct biological functions and protein-interactions [68]. Spry activity is controlled by growth factor-dependent tyrosine phosphorylation. In the case of Spry2, rapid and reversible phosphorylation of tyrosine 55 (Tyr55) within the conserved N-terminal region contributes to its inhibitory activity on the Ras/MAPK pathway [66, 69]. The phosphorylation of the Tyr corresponding to Tyr55 of Spry2 in other Spry isoforms is also essential for some of their interactions with other proteins, as it allows Spry proteins to translocate to the plasma membrane and to interact with Grb2 and c-Cbl [70-72]. Notably, Spry1 and Spry2 are target to tyrosine phosphorylation in response to EGF and FGF stimulation, while Spry4 is phosphorylated upon FGF and insulin signaling. For Spry3, these events are not studied [59, 73, 74]. The Src family of kinases is involved in phosphorylating the key tyrosine, while Shp2 (SH2-domain containing tyrosine phosphatase 2) is responsible for dephosphorylation [75]. Adjacent to the key tyrosine residue, the SRM is thought to contribute to the stability of the three-dimensional disposition of the protein. Ser112 and Ser121 on Spry2 were shown to be phosphorylated by serine/threonine kinases such as Mnk1 (MAPK-interacting-kinase 1), contributing to the stability and integrity of Spry2 protein when compared to the unphosphorylated state [76]. In the proximity to the SRM, a substitution of proline at position 106 with serine in a Spry2 variant ($Spry2^{P106}$ to $Spry2^{S106}$) was also shown to carry a biological significance since Ser106 facilitated phosphorylation [77].

1.5.2 Expression and regulation of Spry proteins

With the exception of Spry3, which is suggested to have a restricted distribution in the brain and testis, Spry proteins are widely expressed in the developing embryo and in adult tissues [78, 79]. During embryonic development, Spry genes are expressed in intimate association with known sites of growth factor activity, especially FGF signaling, suggesting involvement

in negative feedback loops [79, 80]. A study led by Zhang et al. reported common but also distinct expression patterns for Spry1, 2 and 4 genes during mouse development. Spry1 and Spry2 were found to be expressed in the epithelium of the developing craniofacial area and trunk, while Spry4 was expressed in the mesenchymal or neuronal tissue. Yet in the lung, Spry1, 2 and 4 demonstrated expression primarily in the epithelial tissue. They concluded that expression in both epithelial and mesenchymal tissue suggests roles for these Sprys in the epithelial-mesenchymal interactions that govern organogenesis [81]. Spry3, a largely uncharacterized member of the Spry family, is highly expressed in central and peripheral nervous system ganglion cells in mouse and human, including cerebellar Purkinje cells and retinal ganglion cells [82]. Panagiotaki et al. reported that during axonal branching in *Xenopus* embryos, Spry3 expression is restricted to the trigeminal nerve and to both sensory and motor neurons in the spinal cord in a BDNF (brain-derived neurotrophin factor) - dependent manner [78].

Currently, the main role assigned to Spry is to inhibit Ras/Raf/MAPK signaling downstream of a wide range of growth factor stimuli depending on the cellular context and/or specific ligand [66]. As with negative feedback regulators of signaling pathways, Spry levels are tightly controlled through the same signaling pathway they regulate [83]. Among these growth factors that can induce Spry activity are EGF (epidermal growth factor), FGF (fibroblast growth factor), PDGF (platelet-derived growth factor), VEGF (vascular endothelial growth factor), HGF (hepatocyte growth factor), GDNF (glial-derived growth factor), BDNF (brain-derived neurotrophic factor) and nerve growth factor [75, 78]. Other stimuli like insulin, stem cell factor/kit ligand (SCF) and T-cell receptor activation were also shown to stimulate Spry activity [75].

Besides transcriptional regulation through RTK-signaling, Spry proteins are further regulated on multiple levels, especially through differential localization, posttranslational modification and regulation of proteins levels [59, 64, 70, 84, 85]. Fig. 10 summarizes the interactions of hSpry2 with a variety of binding partners such as adaptor proteins, phosphatases, kinases and ligases, as well as their functional outcomes.

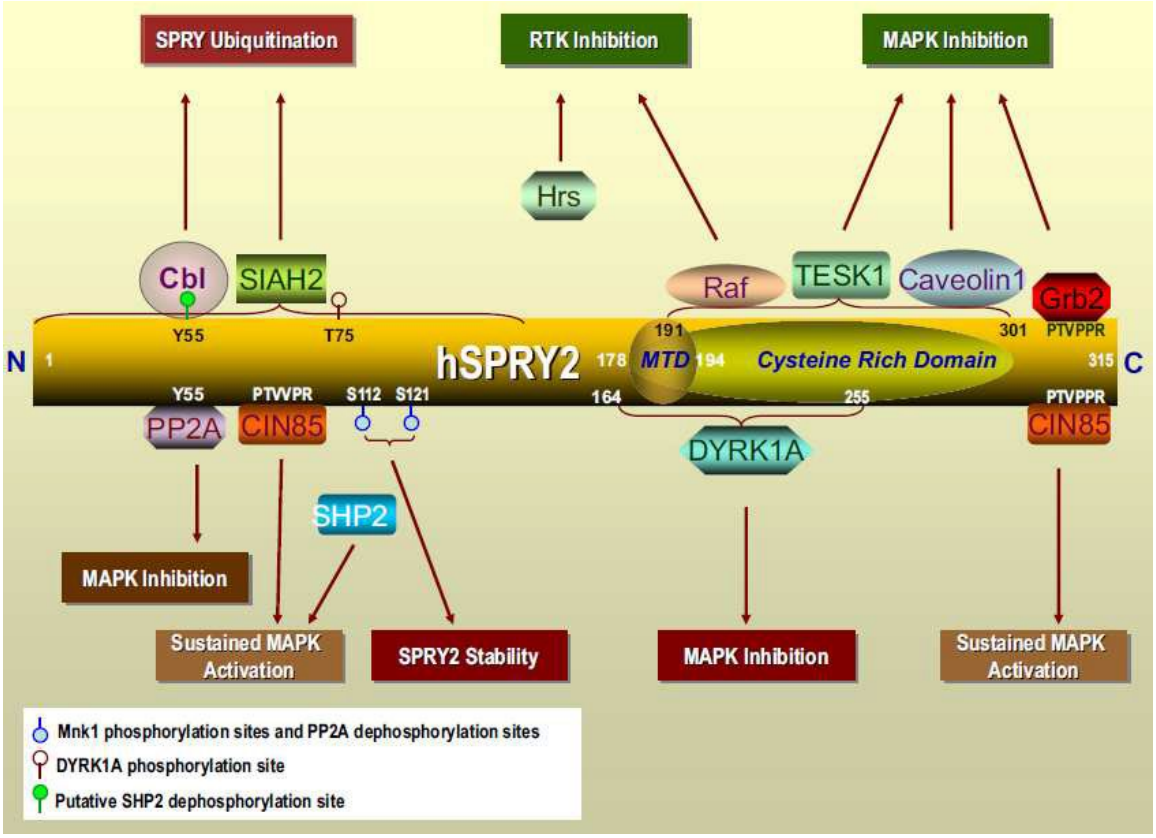

Fig. 10. Schematic representation of binding partners of hSpry2 and the functional consequences of each interaction. Interaction sites of Hrs and Shp2 are not clear. Physical interaction of PTP1B (Protein tyrosine phosphatase 1B) and PTEN with Spry2 have not been observed. MTD, membrane translocation domain [86].

Posttranslational phosphorylation of Tyr55 on Spry2 does not only contribute to the inhibition of the Ras/Raf/MAPK pathway through Grb2 binding, but also serves as a docking site for the SH2 domain of the E3-ubiquitin ligase c-Cbl (canonical casitas B-lineage lymphoma). As their presence in the cell is required only in a time restricted manner, Spry proteins are targeted for c-Cbl-directed ubiquitination and subsequently proteasomal degradation in a growth factor-dependent manner. Additionally, in the case of Spry2, this process is further regulated by Ser112 and Ser121 phosphorylation by Mnk1 (MAP Kinase Interacting Serine/Threonine Kinase 1). Serine phosphorylation decreases phosphorylation of Tyr55 and therefore binding of and ubiquitination by c-Cbl. On the contrary, when Spry2 is not phosphorylated on Ser112 and Ser121, phosphorylation of Tyr55 is enhanced with a subsequent increase in c-Cbl binding, leading to increased Spry2 ubiquitination and degradation [76]. Other E3-ubiquitin ligases such as SIAH2 (Seven In Absentia Homolog 2) and NEDD4 (neural precursor cell expressed developmentally downregulated protein 4) were shown to polyubiquitinate and regulate Spry2 levels as well [72, 87].

Generally, it appears that besides Tyr55 there are at least 19 phosphorylation sites on Spry2 and that some of the residues which are phosphorylated on Spry2 are also conserved in other Spry isoforms. However, whether these sites are likewise target to phosphorylation or how phosphorylation modulates the functions of the other Spry isoforms remains largely unknown [86].

1.5.3 Modes of action of Spry in RTK signaling

The molecular basis for the mode of action of Spry proteins has been difficult to determine, as the functional role of the various Spry isoforms varies depending on the growth factor pathway, ligand, cell type and species. Fig. 11 demonstrates examples on how Spry interacts with essential elements of the RTK-MAPK cascade and how these interactions modulate growth factor signaling.

In the absence of growth factors, RTKs exist in an unphosphorylated and unstimulated state. As a result, signal transduction to the nucleus and transcription of growth-factor-responsive genes are off. Spry proteins, whose synthesis can be induced by tissue-specific transcription factors, are present in the cytoplasm [88-90]. Canonical RTK activation leads to a phosphorylation cascade of MAPKs, resulting in phosphorylated and activated ERK (Fig. 11a), which translocates to the nucleus and in turn activates a variety of target proteins, transcription factors or the transcription of target genes, one of which being Spry [59].

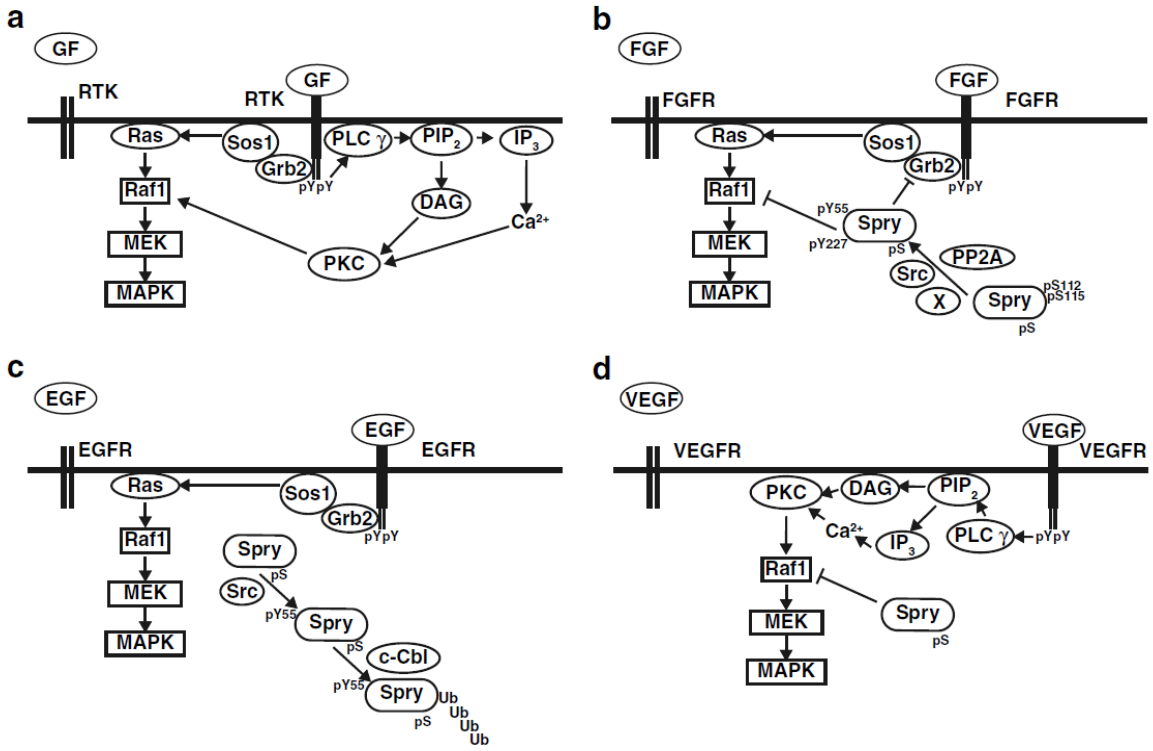

Fig. 11. Spry mechanisms of action in growth factor signaling pathways. (a) Canonical signal transduction in the absence of Spry. (b) Spry-mediated inhibition of FGF signaling. (c) Spry-mediated potentiation of EGF signaling. (d) Spry-mediated inhibition of VEGF signaling [75].

Generally, all mammalian Spry proteins, although to varying degrees, are able to inhibit FGF-induced MAPK activation [65, 67, 73]. In absence of FGFR activation, Spry is phosphorylated on Ser/Thr residues [64, 91]. Upon FGF stimulation as shown in Fig. 11b, Spry translocates to the plasma membrane in a phospholipid-dependent manner [64] where highly conserved serines 112 and 115 are dephosphorylated likely by PP2A [91]. Responsible for binding to PP2A is, in the case of Spry2, the N-terminal region around Tyr55. Therefore, PP2A competes with c-Cbl for binding to this region when Tyr55 is phosphorylated, suggesting that PP2A and c-Cbl interact with distinct pools of Spry proteins, thus balancing the biological activity of Spry [91]. Another phosphatase, PTEN, although a physical interaction with Spry2 has not been observed, was found to be necessary for Spry2-mediated inhibition of cell proliferation [92]. Concurrently, Spry phosphorylation at Tyr55 by a Src-like kinase and by an unknown kinase at Tyr227 are required for Spry to inhibit FGF-induced activation of MAPK [69]. Hence, for Spry2-mediated inhibition of FGFR signaling, both tyrosine phosphorylation and serine dephosphorylation are required. Finally, a protein tyrosine phosphatase, likely Shp2, returns Spry to a dephosphorylated state [75].

Furthermore, proteins involved in RTK-signaling like Raf1 and adaptor proteins Grb2 or Gap1 (Ras GTPase-activating protein) were identified to directly interact with Spry proteins, suggesting that Spry proteins generally exert their function via interfering with Ras activation, Raf induction or receptor degradation [59, 93-95]. In some cases, Spry binding to Grb2 is sufficient for inhibition, while in others, Grb2 association is not required [73, 96]. Binding of Spry2 to the SH2 domain of Grb2 sequesters Grb2 away from Sos, thereby inhibiting the Erk1/2 pathway. Moreover, growth factor-mediated phosphorylation of Tyr55 on Spry2 alters its conformation to reveal a cryptic PXXPXR motif in the C-terminus that serves to bind the SH3 domain of Grb2. Since this motif is exclusive to Spry2, this additional interaction of Spry2 with Grb2 is not performed by other Spry isoforms [73, 93]. Spry2 was also found to associate with Gap1 and this association substantially decreased after FGF stimulation in mammalian cells. Nonetheless it is not clear if this reversible interaction contributes directly to the negative regulation of MAPK activation [94]. Another option is Spry binding to Sos1 and eventually to Raf1, terminating MAPK activity. Interestingly, a combinatorial set of Spry isoforms have been reported to interact with each other to attenuate FGF-induced MAPK activation. In a heterodimer of Spry1 and Spry4, Spry1 binds to Grb2, while Spry4 interacts with Sos1, being the most potent combination for inhibiting FGF2-induced MAPK activation [67].

Besides Mnk1, other kinases are suggested to bind and promptly modulate Spry2 function. DYRK1A (dual-specificity tyrosine-phosphorylated and -regulated kinase 1A) has been shown to interact with and phosphorylate Spry2 on Thr75 and to negatively affect the inhibitory function of Spry2 [97]. Another kinase, TESK1 (testicular protein kinase 1), was identified as a binding partner of Spry2 and Spry4. Independent of its kinase activity, TESK1 attenuated the inhibitory actions of Spry2 at many levels [98-100].

In the context of EGF signaling (Fig. 11c), Spry2 is likewise Tyr55 phosphorylated and competes with EGFR for binding to c-Cbl. As previously described, through sequestration with c-Cbl, Spry2 as well as Spry1 are able to prevent c-Cbl mediated receptor degradation of EGFRs or FGFRs, resulting in sustained signaling activity. This shows that Spry modulation of RTK signaling is very pliable. On the other hand, Spry4, despite having a Tyr residue equivalent to Tyr55 in Spry2, does not interfere with downregulation of EGFRs. This is perhaps due to the fact that Spry4 does not contain the threonine residue directly next to Tyr55 which is important for c-Cbl binding [76, 101, 102].

In the case of VEGF signaling and PLC-γ/PKC activation (Fig. 11d), Spry interacts with Raf1 via its conserved RBD and thus inhibits activation of ERK. Tyrosine phosphorylation of Spry is not required in this instance as Raf is activated in a Ras-independent manner by PKC [95, 103]. Although the interactions of Spry with Grb2, Raf1 and Gap1 provide a framework for understanding how Spry modulate signaling downstream of RTKs, other functional attributes of Spry cannot be explained solely on the basis of these interactions. This indicates that there might be alternative mechanisms that are used by Spry to antagonize RTK signaling.

1.5.4 Sprouty and cancer

Given their critical role as modulators of RTK signaling and crosstalk-mediators between ERK and other signaling pathways for maintaining control of cellular behavior, Spry proteins and their utility as a biological marker, tumor suppressor and oncogene have been studied by different investigators.

Consistent with the role of Spry2 in inhibiting both Erk1/2 signaling and proliferation, Spry2 expression was reported to be significantly decreased in hepatocellular and lung carcinomas [104, 105]. In mice, inhibition of the biological activity of Spry2 accelerated activated β-catenin-induced Erk1/2 activation to confer neoplastic phenotype in the liver, signifying that loss of Spry2 function contributes to hepatic tumorigenesis [106]. Likewise, Sutterlüty et al. reported reduced Spry2 expression in NSCLC (non-small cell lung cancer) patients [105]. Additionally, they demonstrated that ectopically expressed Spry2 not only significantly reduced proliferation and migration, but also blocked tumor formation *in vivo* in mice. In their study, Spry2 was shown to inhibit proliferation of mutant K-Ras-transformed NSCLC cells without inhibiting Erk1/2 activation, suggesting that Spry2 restricts tumor formation by modulating other pathways [105]. Another Spry isoform, Spry 4, also displayed inhibitory effects on cell migration, invasion and anchorage-independent growth in NSCLC lines [107]. Conforming with this notion, Vanas et al. reported that cell proliferation and migration in breast cancer cell lines was inhibited by Spry4 expression, indicating a tumor suppressive role of Spry4 in this tumor entity [108]. In a study led by Lo et al. it was revealed that Spry1 and Spry2 were consistently downregulated in breast cancer when compared to normal tissue. More than 90 % of the patient samples demonstrated suppressed expression of Spry1 and Spry2. Epigenetic silencing of Spry by DNA methylation and histone hypoacetylation was ruled out [109]. Faratian et al. reported that Spry1, Spry2 and Spry4 were differentially expressed across the

clinicopathological subgroups of breast cancer and implied that Spry2 is an independent prognostic factor in breast cancer [110]. Apart from these findings, other studies have proposed a downregulation not only of Spry1, but of Spry2 and Spry4 in prostate cancer [111-114]. Additionally, loss of Spry expression might be a late occurrence in the progression of cancer [59]. For instance, while low-grade prostate cancers retain Spry2 expression, metastatic cancers display a significant loss of Spry2 expression [112].

In various tumor entities it was observed that specific Spry protein family members can antagonize malignant phenotypes, while others fail to do so. Spry1 was found to promote the malignant phenotype in TNBC (triple negative breast cancer) cell lines as knock-down of Spry1 impaired cell growth, migration and metastasis formation [115]. Nevertheless, context-dependent contribution of certain Spry isoforms to tumorigenicity and metastatic potential have been reported for example in colon cancer and sarcoma, where Spry2 functioned as an oncogene [116-118].

All these studies provide evidence that Spry in malignancies functions in a cancer cell-specific and context dependent manner, therefore they might not only negatively regulate tumor progression, but positively as well.

1.5.4.1 Sprouty and brain cancer

In gliomas, the role of Spry is also multifaceted. A co-expression network analysis of the glioma transcriptome revealed that Spry proteins (Spry1, 2 and 4) likely participate in the regulation of EGFR signaling in glioma pathogenesis [119]. Kwak et al. implied that Spry2 might play a tumor suppressive role as they found that Spry2 protein levels were significantly decreased in 80% of invasive WHO Grade II-IV gliomas, but not in non-invasive Grade I and normal tissues [120]. However, another study demonstrated that Spry2 unexpectedly acted as a driver of GB cell proliferation and anchorage-independent growth. Its knock-down potentiated the response to RTK inhibitors and reduced proliferation of GB cells [121]. In a study led by Park et al., Spry2 expression and survival patterns of patients with gliomas were analyzed. Spry2 was found to be upregulated in GB, which correlated with reduced survival in GB patients. Similarly, its knock-down significantly impaired proliferation of GB cells, but not of normal astrocytes. Furthermore, abrogating Spry2 function strongly inhibited tumor growth and led to significantly prolonged survival *in vivo*, whereas overexpression promoted tumor propagation [122]. More recently, it was shown that Spry2 mediates the effect of

miR-21 on carmustine (BCNU)-resistant glioma cells [123]. In 2016, Zhang et al. performed transcriptome analyses of adult diffuse gliomas (WHO Grades II-IV) and revealed that gliomas with high expression of Spry isoforms (Spry1, 2 and 4) and low expression of NF1 and PTEN showed poor overall survival compared to tumors with a reversed expression pattern [124].

These findings indicate that Spry might play an important role in the pathogenesis of glial tumors and that they may represent potential targets for therapy.

2 Aim and objectives of the study

A considerable body of evidence indicates that alterations of RTK (receptor tyrosine kinase) signaling contribute to cancer development and progression. It is well established that many genes involved in signal transduction via RTKs are amplified or mutated in various tumors, but also negative regulators of this pathways could harbor the potential of being tumor suppressors [125].

The working hypothesis, corroborated by earlier data showing an important function of Spry3 (Sprouty3) as an antagonist of growth factor BDNF-mediated signaling in neuronal development [78], is that in brain tumors inhibition of RTK-induced signals might be deregulated on account of aberrant Spry3 activity. In consequence, the affected cancer cells show accelerated cell proliferation, limited dependency on extracellular signals and enhanced cell motility.

This study investigates a previously uncharacterized member of the Spry family, Spry3, concerning its role in cancerogenesis of brain-associated cancers:

1) The endogenous expression of Spry3 protein in different brain cancer-derived cells.

As Spry proteins are localized at sites of signaling via growth factors, the serum-dependency of endogenous Spry3 expression will be examined by determining its protein level in serum-starved and -stimulated brain cancer-derived cells. Furthermore, the correlation between the malignancy/tumor grades of the histopathological subtypes of brain cancer and Spry3 protein levels will be addressed and compared.

2) The contribution of Spry3 protein to typical transforming features by overexpression studies in selected brain cancer-derived cell lines.

By using an adenoviral expression system, overexpression and knock-down experiments will shed light on the role of Spry3 on RTK-mediated processes such as cell proliferation, migration and adhesion.

3 Material and methods

3.1 Cell biological approaches

3.1.1 Cell lines

All utilized cell lines originate from human tissue and are listed in Table 2. They were purchased from the American Type Culture Collection (ATCC), the JCRB cell bank or were established at the Institute of Cancer Research, Medical University of Vienna (ICR) [126]. Cell lines LN-40 and LN-140 were kindly provided by Dr. Tribolet (Lausanne). Cell lines from the Neuromed Campus in Linz (NML) were supplied by Dr. Walter Berger, Institute of Cancer Research; Department of Medicine I. Used growth media were prepared and supplied by the ICR.

Table 2: Detailed overview of all used cell lines including information about source, tissue origin, disease type, age, gender and used culture medium. m = male; f = female; na = not available

Cell line	Source / Alias	Tissue	Disease type	Age	Gender	Culture medium
NMC-G1	JCRB - IFO50467	brain	astrocytoma	na	f	DMEM
SW1088	ATCC - HTB-12	brain	astrocytoma	72	m	DMEM
U-373MG	ATCC – HTB-17	brain	astrocytoma	61	m	DMEM
AM-38	JCRB - IFO50492	brain	glioblastoma	36	m	EMEM +20% FCS
BTL1529	NML	brain	glioblastoma	30	f	RPMI
BTL2177	NML	brain	glioblastoma	46	f	RPMI
BTL53	NML	brain	glioblastoma	45	m	RPMI
DBTRG-05MG	ATCC - CRL-2020	brain	glioblastoma	59	f	DMEM
T98G	ATCC – CRL-1690	brain	glioblastoma	61	m	DMEM
VBT72	ICR	brain	glioblastoma	33	f	RPMI
Hs683	ATCC - HTB-138	brain	oligodendroglioma	76	m	DMEM
LN-40	Dr. Tribolet	brain	gliosarcoma	na	na	DMEM
LN-140	Dr. Tribolet	brain	gliosarcoma	na	na	DMEM
BTL1376	NML	brain	gliosarcoma	64	m	RPMI

BTL2175	NML	brain	gliosarcoma	43	f	RPMI
SK-N-DZ	ATCC - CRL-2149	brain; derived from metastatic site: bone marrow	neuroblastoma	2	f	DMEM +NEAA
SK-N-FI	ATCC - CRL-2142	brain; derived from metastatic site: bone marrow	neuroblastoma	11	m	DMEM +NEAA
MG63	ATCC - CRL-1427	bone	osteosarcoma	14	m	DMEM

Media

DMEM (Dulbecco's Modified Eagle Medium) supplemented with 10% fetal calf serum (FCS) – heat inactivated, penicillin (100 U/ml), streptomycin (100 µg/ml)

RPMI (Roswell Park Memorial Institute), supplemented with 10% fetal calf serum (FCS) – heat inactivated, penicillin (100 U/ml), streptomycin (100 µg/ml)

EMEM (Eagle's Minimum Essential Medium) supplemented with 20% fetal calf serum (FCS) – heat inactivated, penicillin (100 U/ml), streptomycin (100 µg/ml)

3.1.2 Cell culture

Cells were cultured in 10 cm diameter dishes in their respective medium containing 10% or 20% fetal calf serum (FCS) in a humidified incubator at 37°C with 7.5 % CO_2. Some media were additionally provided with 0.1 mM Non-Essential Amino Acids (NEAA). These exceptions are pointed out in Table 2.

After reaching confluency of 90%, cells were splitted at an adequate ratio between 1:2 to 1:10, depending on the requirements of experiments and cell line.

For passaging, the cell monolayer was washed with 1x PBS (phosphate buffered saline), followed by trypsinization and detaching of the cells. The enzymatic inactivation of T/E (Trypsin/EDTA) was carried out by addition of medium containing FCS. Between cell passages, medium was exchanged every 2 to 4 days. Growth medium and PBS were used at 37°C whereas T/E was used at room temperature.

1x Phosphate Buffered Saline (1x PBS)

127 mM NaCl

2.7 mM KCl

4.3 mM $Na_2HPO_4 \bullet 2H_2O$

1.4 mM KH_2PO_4

pH=7.4, in ddH2O

Trypsin/EDTA (T/E)

0.1% Trypsin

0.01% Ethylenediaminetetraacetic acid (EDTA)

0.001% Phenol red

3.1.3 Cell thawing and cryopreservation

Cells were thawed at 37°C in a water bath and immediately poured into a 10 cm diameter petri dish containing 15 mL of pre-incubated medium to further dilute the toxic dimethyl sulfoxide (DMSO). Cells were evenly spread by gently rotating the dish. Following day, growth medium was exchanged and residual DMSO removed.

For cryopreservation, logarithmically growing cells were trypsinized at 50-70% confluency and resuspended in 15 mL medium, followed by centrifugation at 800 rpm for 5 minutes. Supernatant was discarded, cells were resuspended in 1 mL FCS + 10% DMSO and transferred into a cryopreservation vial which was immediately placed into an ice box. Next, cells were stored at -80°C for two days and subsequently transferred into liquid nitrogen for long-term storage.

3.1.4 Stimulation and starvation of cells

For serum-dependent expression studies of Spry3 by Western blot analysis, cells were grown to 70-80% confluency in two 10 cm dishes each before being subjected to serum withdrawal and non-withdrawal.

For starvation, medium was aspired and cells were washed twice with 5 mL of growth medium devoid of FCS. Cells were propagated in 10 mL of growth medium without FCS. In parallel, growth medium of another set of the same cell line was replaced by 10 mL fresh medium containing the appropriate concentration of FCS.

Both set of cells were incubated for 20 h, harvested by scraping and collected into 1.5 mL Eppendorf tubes. This was achieved by medium aspiration, washing cells in 1x PBS and harvesting by scraping them off in 1 mL 1x PBS, followed by centrifugation at 1500 rpm for 5 min. The supernatant was discarded and pellets were put immediately into a portable tank containing liquid N_2. Finally, pellets were stored at -80°C.

3.1.5 Adenoviral infection of cells and determination of virus titer

To avoid cytotoxicity and determine optimal concentrations of the viruses, pilot testing was conducted beforehand in the desired cell lines using an adenovirus expressing Cyan Fluorescence Protein (CFP) as a reporter. For this purpose, a three-step serial dilution (1:100, 1:500 and 1:2500) of the virus stock diluted in serum-free medium was carried out. 100 µL of each dilution were added directly to 6 x 10^5 cells in culture medium and incubated for 48 hours. After incubation, cells were washed with 1x PBS and fluorescence microscopy pictures with a CFP filter as well as Brightfield pictures were taken at 4x magnification using Nikon Eclipse Ti microscope and NIS-Elements software.

Viral titers were determined by measuring the OD_{260} of the CFP virus as well as the other used viruses in a microvolume spectrophotometer (Nanodrop, Thermo Scientific). For this, 15 µL of virus stock solution was mixed with 100 µL 1x Tris-EDTA (TE) buffer, 0.1% Sodium dodecyl sulfate (SDS). Similarly, a blank solution for calibration was made of 7.5 µL 10 mM Tris, 7.5 µL 2x storage buffer and 100 µL 1x TE, 0.1% SDS. Mixtures were rigorously vortexed for 30 sec and centrifuged at 13000 rpm for 5 min. Supernatants were used to measure the absorbance. Absorbance values of the viruses where then normalized against values of virus expressing CFP and volumes of used virus stocks were adjusted accordingly.

For the study, 6 x 10^5 cells were counted using a Neubauer improved cell counting chamber and seeded into 10 cm diameter dishes. Next day, virus stocks were thawed on ice and cells were infected as described above with the adequate dilution of adenoviruses expressing lacZ, luciferase, CFP, Spry3 and Spry4. Additionally, two different shSpry3 expressing adenoviruses were mixed 1:1 and used for the experiments. After 20-24 hours of incubation, adenoviral solutions, except for shSpry3 with an incubation time of 72 hours, were removed by medium aspiration. Infected cells were propagated in their respective medium or processed

for subsequent experiments. All used recombinant viruses were produced by group members of Prof.Dr. Sutterlüty-Fall. The adenoviruses expressing Spry3 [127], Spry4 [128] and control proteins (luciferase, lacZ or CFP) [129] were produced as described. Daniel Valcanover assisted in preparing the adenoviruses expressing shSpry3 during his Bachelor's thesis.

2x Storage buffer

10 mM Tris, pH=8

100 mM NaCl

0.1% bovine serum albumin (BSA)

50% glycerol

3.1.6 Scratch Assay

For scratch assay, 6 x 10^5 cells were counted and seeded into a 10 cm dish using a Neubauer improved cell counting chamber. Following day, adenoviral infection of cells was performed. 20-24 hours post infection, cells were trypsinized and transferred into wells of a 6-well plate. Next day, three straight scratches per well were introduced into the monolayer using a sterile yellow pipette tip. To remove debris, cells were washed twice with 1x PBS. Finally, 3 mL of growth medium were added into each well.

To monitor the closing of the scratch, the 6-well plate was immediately placed into the VISITRON Live Cell Imaging System and one position per scratch was selected for imaging at 10x magnification using VisiView Software. The running time was set to 40-48 hours and the time interval for picture taking was set to every 30 min. Using ImageJ software, gap width was measured for every two hours by drawing five lines per scratch. To perform exact measurements, results lower than 100 µm were excluded. Migration velocity in µm/h for each virus setup was assessed using GraphPad Prism software by applying linear regression.

3.1.7 Growth Curve

To perform growth curves, 4 x 10^4 cells were infected with adenoviruses and after an appropriate incubation time, cells were trypsinized and reseeded in 6 cm dishes in triplicates. Starting the following day, cells were then counted every 24 hours for 5 days using a Neubauer improved cell counting chamber. After determination of the absolute cell number

of each triplicate, all three values were used to generate a mean and to calculate doubling times using exponential growth equations in GraphPad Prism software.

3.1.8 Clonogenic Assay

For clonogenic assay, 3 x 10^4 cells were infected with adenoviruses expressing and following an appropriate incubation time, 500 cells were reseeded in 6 cm dishes in triplicates and propagated for 20 days in their respective growth medium. Medium was then discarded and cells washed with 1x PBS, followed by fixation of cells with 4% formaldehyde for 15 min at room temperature. After fixation, cells were again washed with 1x PBS and stained with Giemsa's azur eosin methylene blue solution (Merck, Cat. No. 109204) for 5 min for visualization. Giemsa was then discarded and washed off with ddH_2O. Finally, dishes were dried at room temperature.

Dishes were documented by scanning and visible clones were counted using ImageJ software. Clones were sorted according to their size, whereby big clones were scored as five, middle ones as two and small ones as one. The summed-up score was then normalized to 100 seeded cells. However, it should be noted that this experiment was only performed once.

3.1.9 Adhesion Assay

To perform adhesion assay, 6 x 10^4 cells were infected with adenoviruses which were then reseeded after an appropriate incubation time of the viruses, as described below (see chapter 3.1.9.3).

3.1.9.1 Coating of wells

Wells of a 24-well tissue culture plate (Falcon, Multiwell Tissue Culture Plate 3047) were divided into triplicates, whereas 2 of them were coated with 350 µL collagen I solution while the remaining one was left uncoated. An hour later, the same volume of ddH_2O was added on top of the collagen and the plate was left on a plane surface overnight.

Collagen I

from calf skin**,** Type I, (0.1% solution in 0.1 M acetic acid), aseptically processed (Sigma-Aldrich); diluted to final concentration of 100 µg/mL (1:10)

3.1.9.2 Blocking of wells

Next day, the collagen was aspired and a BSA-block was performed in all wells. For this purpose, 400 µL of 5% w/v BSA in serum-free DMEM (pre-equilibrated) were added into each well. The plate was incubated at 37°C for 30 min. Afterwards, BSA solution was aspirated and wells were washed thrice with 500 µL 0.1% w/v BSA in serum-free DMEM.

3.1.9.3 Preparation and seeding of cells

Whilst blocking, cells were trypsinized, collected in 50 mL Falcon tubes and centrifuged at 1300 rpm for 5 min. Pellets were washed twice with serum-free DMEM before being subjected to counting. Cell density was adjusted to 1 x 10^6 cells/mL and after another round of centrifugation, resuspended in the appropriate volume of 25mM Hepes in serum-free DMEM (pre-equilibrated). This was followed by a recovery time of 10 min in the incubator with slightly opened tube lids. Afterwards, 5 x 10^4 cells of each viral setup were seeded in triplicates and total volume was compensated with 25mM Hepes in serum-free DMEM. The plate was incubated for 30 min at 37°C, followed by three washing steps with 0.1% w/v BSA in serum-free DMEM. Whilst washing, non-adherent cells were removed by rocking the plate gently but thoroughly.

3.1.9.4 Fixation and staining

Fixation of adherent cells followed and was achieved by adding 400 µL of 4% formaldehyde into each well for 15 min at room temperature. Then, wells were washed thrice with 1x PBS. Finally, cells were stained evenly with 350 µL of 0.5% w/v crystal violet in 2% v/v EtOH (ethanol) for 10-15 min at room temperature. Crystal violet was removed and wells were washed repeatedly and thoroughly with rising volumes of ddH_2O. The plate was dried off at room temperature and 9 microscopic photos per well were taken at 10x magnification using Nikon Eclipse Ti microscope and NIS-Elements software. Cells were counted manually using ImageJ software. Final cell count was achieved by subtracting BSA-treated counts from collagen-treated cell counts.

3.2 Biochemical approaches

3.2.1 Total protein isolation and determination of protein concentration

In furtherance of overexpression studies, cells were harvested in 1x SLB (sample loading buffer) with the aid of a scraper. Samples were collected in 1.5 mL Eppendorf tubes and boiled at 95°C for 10 min, followed by sonication for 5 minutes and storage at -20°C.

To investigate endogenous protein levels after serum induction and serum withdrawal, pellets generated as described in chapter 3.1.4 were thawed on ice, resuspended in 150-200 µL chilled protein lysis buffer and incubated for 10 minutes on ice. Protein lysates were sonicated for 5 min followed by centrifugation at 13000 x g for 15 min at 4°C. The protein containing supernatant was transferred into a new Eppendorf tube and a 2.5 µL aliquot for determination of total protein concentration was separated. The remaining supernatant was stored at -20°C.

The concentration of protein lysates was determined by using the Micro BCA Protein Assay Reagent Kit (Thermo Scientific). Protein lysates were diluted 1:200 in ddH_2O and compared to a set of BSA protein standards reaching from 0µg/ml to 200µg/ml. For this purpose, protein samples as well as BSA samples were pipetted into wells of a 96-well plate where they were mixed with reagents of the kit according to the manufacturers protocol. The plate was incubated for 2 hours at 37°C and absorbance was measured at 562 nm with a spectrophotometer (TECAN). Finally, protein concentrations were normalized to the BSA protein standard using Excel software.

Protein lysis buffer (TGH buffer)

50 mM Hepes

150 mM NaCl

1 mM EDTA

10 mM NaF

1.5 mM $MgCl_2$

10% glycerol

1% Triton X-100

in ddH2O

0.5 mM Na-Vanadate added freshly

2.5% Complete (Roche) added freshly

1 µM PMSF added freshly

1x sample loading buffer (SLB)

10% glycerol

5% 2-mercaptoethanol

2.3% SDS

62.5 mM Tris, pH=6.8

one spatula tip bromphenol blue

in ddH_2O

3.2.2 Sodium dodecyl sulfate-polyacrylamide gel electrophoresis (SDS-PAGE)

SDS-PAGE was used to separate proteins by their size. For studies of Spry3, a 13% separation gel was chosen to achieve the desired resolution and sample separation.

3.2.2.1 Casting of polyacrylamide gels

The SDS-PAGE cassette was assembled, the separation gel mixture was poured and immediately overlaid with isopropanol to ensure a straight surface area with exclusion of air bubbles. After polymerization of the separating gel, isopropanol was discarded and the surface of the gel was gently washed with ddH_2O. A stacking gel was prepared, poured onto the separating gel and a 15 mm comb was inserted. Following polymerization, the comb was carefully removed and the cassette transferred into a gel electrophoresis chamber filled with 1x running buffer.

13% Separation gel

9.75 ml Acrylamid/Bis-acrylamid (37.5:1), 30% solution in H_2O

7.5 ml 1.5 M Tris(hydroxymethyl)aminomethane, pH=8.8 (Tris)

12.3 mL ddH_2O

150 µL 20% Sodium dodecyl sulfate (SDS)

300 µL 10% Ammonium persulfate (APS)

12 µL Tetramethylethylenediamine (TEMED)

filled up with ddH_2O to 30ml

4.5% Stacking gel

1.913 mL Acrylamide/Bis-acrylamide (37.5:1), 30% solution in H_2O

1.8 mL 1.5 M Tris, pH=6.8

10.95 mL ddH_2O

75 µL 20% SDS

150 µL 10% APS

15 µL TEMED

1x Running buffer

50 mM Tris

0.19 M Glycine

3.5 mM SDS

in ddH_2O

3.2.2.2 Sample preparation and electrophoresis

Meanwhile, 250 µg of total protein lysates were prepared and mixed with adequate volumes of TGH buffer to reach a final volume of 150 µL. To ensure protein denaturation, protein samples were treated with 30 µL 4x SLB and boiled at 95°C for 10 min at a thermoshaker. Samples, which were previously treated with 1x SLB, were simply thawed and boiled as described before.

After a short spin-down, samples, 10 µL protein marker (Precision Plus Protein All Blue Prestained Protein Standards #1610373, BioRad) and two additional Spry3 overexpression samples were loaded into the slots of the stacking gel using gel-loader tips. Overexpression samples were generated as mentioned in chapter 3.1.5, but only the first and third dilutions were used.

Electrophoresis was performed at 150V in constant voltage modus. For overnight runs, electrophoresis was performed at 50V and turned up to 150V the following day to complete the run.

4x Sample loading buffer

40% Glycerol

20% β-mercaptoethanol

9.2% SDS

0.25 M Tris/HCl, pH= 6.8

Bromophenol blue (one spatula tip)

in ddH_2O

3.2.3 Western Blot

The detection of desired proteins was carried out by immunoblotting. After electrophoresis, the separation gel was assembled into a wet transfer sandwich cassette consisting of a sponge, two 13x15 cm 3MM blotting paper (Whatman), separating gel, 13x15 cm nitrocellulose membrane (GE Healthcare, pore size 0.2 µm), two 13x15 cm 3MM blotting paper and sponge. Air bubbles were removed and transfer cassette was placed into a transfer apparatus filled with 1x transfer buffer. Transfer was performed overnight at 300 mA and 4°C under constant stirring to ensure consistent temperature.

1x Transfer buffer

48 mM Tris

39 mM Glycine

0.037% SDS

20% Methanol

in ddH_2O

3.2.3.1 Ponceau staining

Following day, the sandwich was disassembled and the membrane stained with Ponceau red staining solution until protein bands became visible. After a short rinse in ddH_2O, the membrane was documented by scanning, followed by trimming and labeling.
De-staining was carried out in 1x TBST on a racking table until the red color disappeared completely.

Ponceau red solution

0.1% Ponceau-red

5% Acetic acid

in ddH_2O

10x Tris-buffered saline (TBS)

250 mM Tris

1.7 M NaCl

27 mM KCl

in ddH2O

pH=7.6

1x Tris-buffered saline with Tween20 (TBST)

10% 10x TBS

0.1% Tween20

in ddH_2O

3.2.3.2 Immunoblotting

The membrane was blocked in blocking solution for 1 hour at room temperature to prevent non-specific antibody binding, followed by washing thrice in 1x TBST, 10 min each. 20 mL of primary antibody solution in the desired dilution was added onto the membrane and incubated overnight at 4°C with a closed lid, also on a racking table.

Next, the membrane was again washed thrice in 1x TBST for 10 min each, before it was incubated with the secondary antibody for 1 hour at room temperature. Subsequently, the membrane was again washed thrice in 1x TBST.

In case of Spry3 detection, membrane was washed once in 1x TBST for 10 min, then in 1x TNN for 30 min and lastly in 1x TBST for 10 min again. This was done to ensure background elimination on the blot.

Blocking solution (prepared freshly)

5% non-fat dry milk powder

in 1xTBST

1x TNN buffer (modified)

50 mM Tris-Cl, pH=7.5

250 mM NaCl

5 mM EDTA

in ddH_2O

Primary antibody solution (repeated usage, stored at 4°C)

Primary antibody in desired dilution

rabbit anti-Spry3, 1:250 dilution, established by Prof. Sutterlüty-Fall group

mouse anti-GAPDH, 1:6000 dilution, Santa Cruz (G9):sc-365062

1% BSA

0.1% NaN_3

in 1x PBS

Secondary antibody solution (prepared freshly, stored at 4°C)

anti-mouse IgG or anti-rabbit IgG, 1:5000 dilution

sheep anti-mouse, GE healthcare; conjugated to horse radish peroxidase (HRP)

donkey anti-rabbit, GE healthcare; conjugated to horse radish peroxidase (HRP)

2% non-fat dry milk powder

in 1x TBST

3.2.3.3 Detection

To visualize proteins by chemiluminescence, a detection solution consisting of 10 mL of ECL1 solution and 30 µL of ECL2 solution was prepared and spread evenly on the membrane for about a minute. The membrane was then placed between two plastic foils and air bubbles were removed. An X-ray film was placed on the top and exposure was performed in a light-tight X-ray cassette. Exposure time and quality depended mainly on the presence of protein and antibody quality. The light emitted by the chemiluminescence reaction was detected by an X-ray processor.

Usually, the membrane was washed in 1x TBST for 10 min to remove ECL solution and incubated again with a different set of antibodies of interest.

X-ray films were scanned using a special film holder with specific software setup. Protein bands visible on the X-ray film were then analyzed for their density using Image Quant software. Background correction was introduced and protein levels were normalized to a MG63 external standard and GAPDH as housekeeping control.

ECL solution 1

200 mM p-coumaric acid

1.25 mM luminol

in 0.1 M Tris, pH=8.8

ECL solution 2

3% H_2O_2 in ddH_2O

4 Results

4.1 Endogenous Spry3 expression varies in brain cancer-derived cells and is not influenced by serum availability

As an initial experiment, endogenous levels of Spry3 protein were determined in 17 brain cancer-derived cell lines. To study whether Spry3 expression is influenced by serum availability, cells were cultured in parallel in media without (-) and with (+) serum, then harvested to perform total protein isolation and subsequently Western blot analysis. As an external reference, MG63 cells were used as these cells showed moderate Spry3 levels in previous experiments (data not shown). Values of MG63 were set to 1 in each Western blot analyzed, then expression in the brain cancer-derived cell lines was calculated in relation to MG63 and normalized to GAPDH.

As depicted in Fig. 12a, most cell lines expressed detectable Spry3 protein which in some cases appeared as a double band on Western blots. In the stimulated setup of the cells, the upper/slower migrating band was often more pronounced than the lower/faster migrating band. On the contrary, cells which were cultured devoid of serum displayed a more distinct lower band, implying that stimulation may lead to posttranslational modification of Spry3 protein, hence the more pronounced upper band. For better viewing of differences in protein level, analyses of the long and short exposures blots were included. Similar observations of multiple differentially migrating bands in Spry2 Western blots were made by other groups [72, 130].

Quantification of protein levels revealed that only two of these 17 cell lines, NMC-G1 and VBT72, differed significantly in their parallel setups. VTB72 cells demonstrated diminished Spry3 levels upon serum starvation when compared to the logarithmically grown/stimulated counterpart, whereas in the NMC-G1 cell line, it was the other way around. In those cells, Spry3 expression was not diminished but enhanced in starved cells and lowered in stimulated cells. This observation of decreased Spry3 protein levels despite of serum availability was made in 6 further cell lines. With the exception of SW1088, BTL1529 and BTL1376, in which Spry3 levels were similar between the counterparts, protein levels among the parallel setups of the other cell lines were clearly variable (Fig. 12b). Hence, a serum-dependency of Spry3 expression could not be observed in brain cancer-derived cells .

To investigate if these modifications have an impact on the actions of Spry3 in following overexpression studies, DBTRG-05MG and U-373MG cell lines were selected based on their different double band configuration. As clearly visible in Fig. 12a, while DBTRG-05MG cells displayed more pronounced upper bands, U-373MG cells showed more distinct lower bands, regardless of their stimulation status. These findings suggest that Spry3 is regulated in a cell- and context-dependent manner.

a

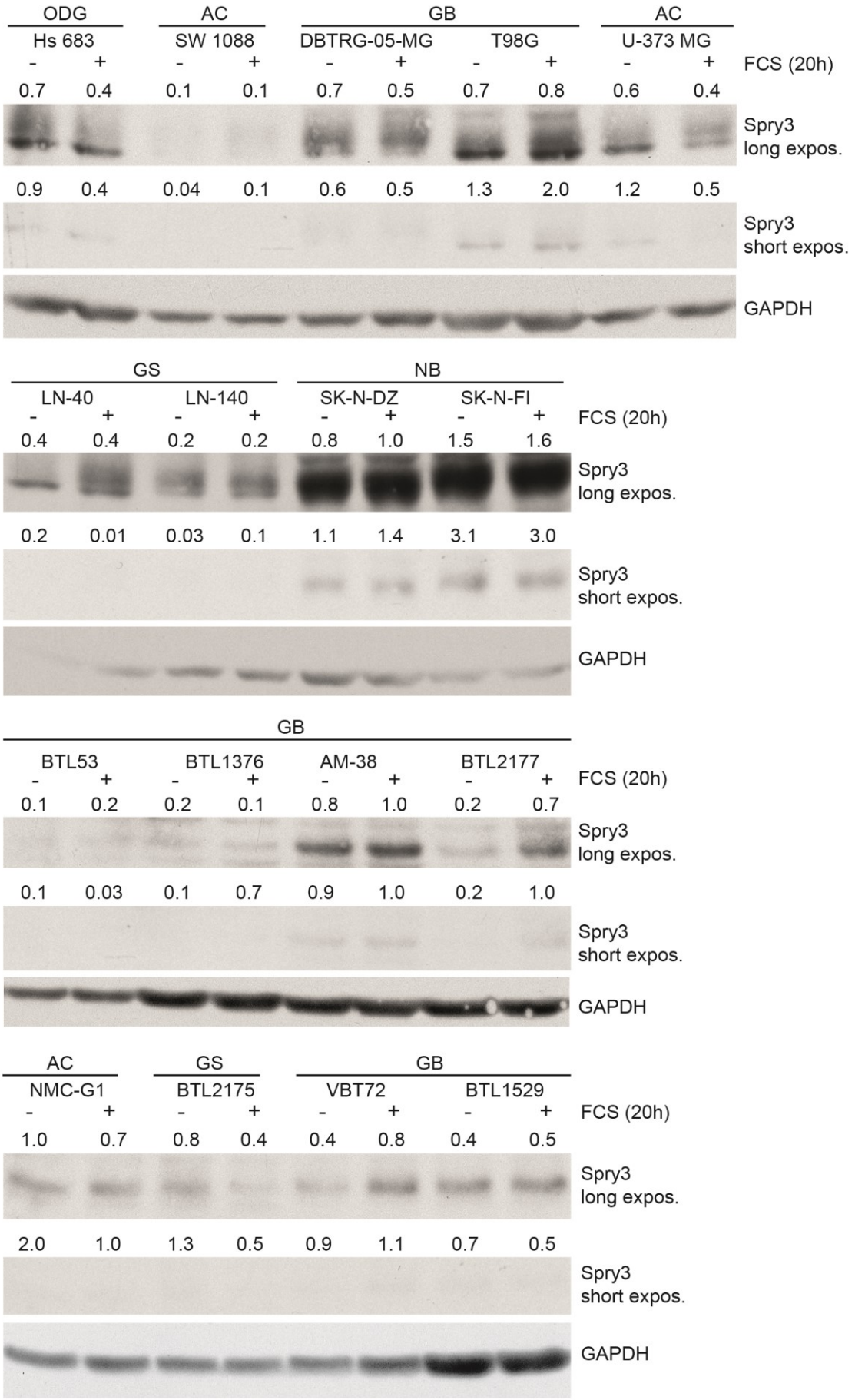
ODG
AC
GB
AC
Hs 683
SW 1088
DBTRG-05-MG
T98G
U-373 MG
- + - + - + - + - +
FCS (20h)
0.7 0.4 0.1 0.1 0.7 0.5 0.7 0.8 0.6 0.4
Spry3 long expos.
0.9 0.4 0.04 0.1 0.6 0.5 1.3 2.0 1.2 0.5
Spry3 short expos.
GAPDH
GS
NB
LN-40
LN-140
SK-N-DZ
SK-N-FI
- + - + - + - +
FCS (20h)
0.4 0.4 0.2 0.2 0.8 1.0 1.5 1.6
Spry3 long expos.
0.2 0.01 0.03 0.1 1.1 1.4 3.1 3.0
Spry3 short expos.
GAPDH
GB
BTL53
BTL1376
AM-38
BTL2177
- + - + - + - +
FCS (20h)
0.1 0.2 0.2 0.1 0.8 1.0 0.2 0.7
Spry3 long expos.
0.1 0.03 0.1 0.7 0.9 1.0 0.2 1.0
Spry3 short expos.
GAPDH
AC
GS
GB
NMC-G1
BTL2175
VBT72
BTL1529
- + - + - + - +
FCS (20h)
1.0 0.7 0.8 0.4 0.4 0.8 0.4 0.5
Spry3 long expos.
2.0 1.0 1.3 0.5 0.9 1.1 0.7 0.5
Spry3 short expos.
GAPDH

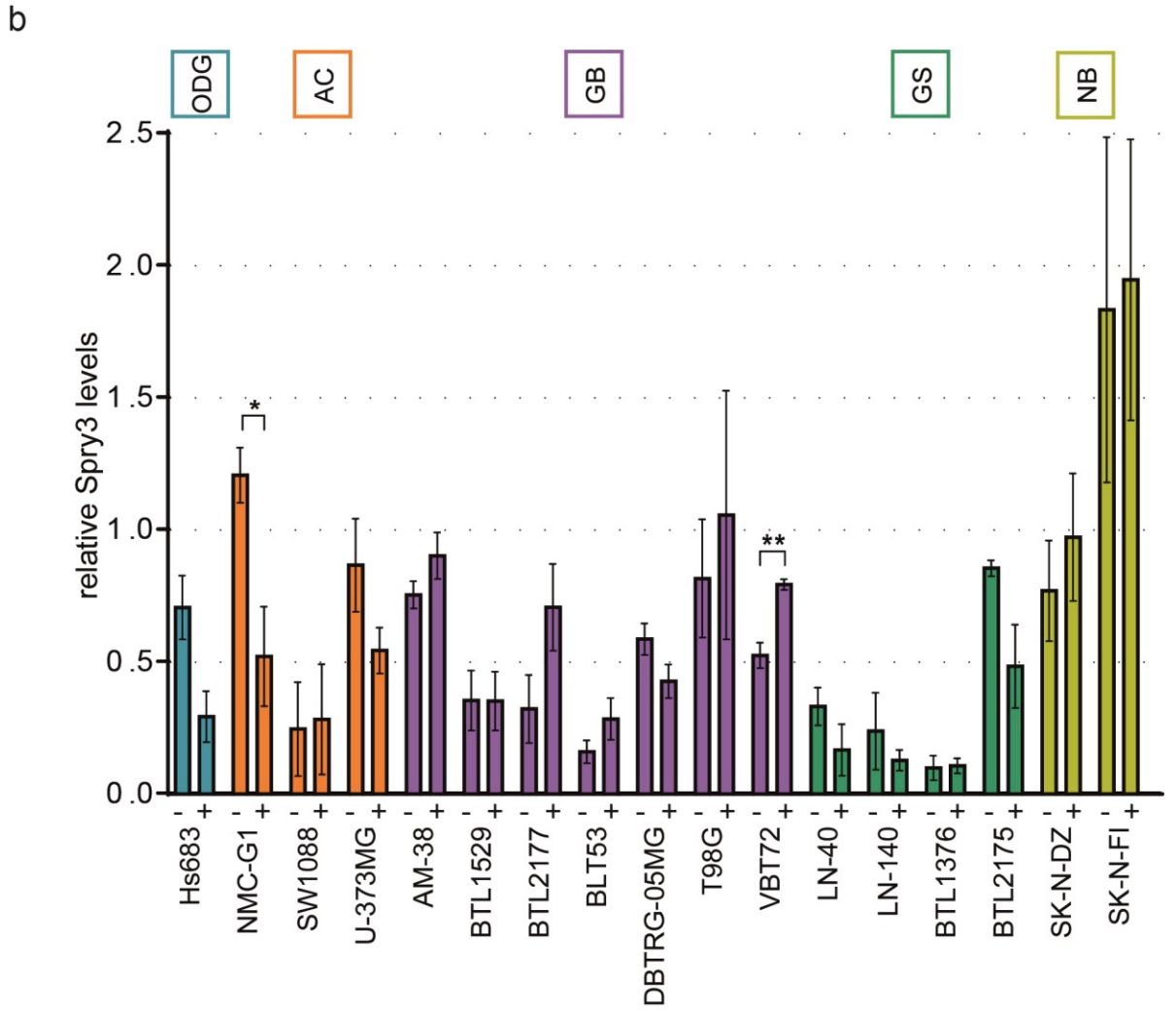

Fig. 12. Endogenous expression of Spry3 in response to serum-starvation and stimulation in brain cancer-derived cells. Cells were starved (-) and stimulated (+) for 20 hours. After total protein isolation, equal protein amounts were analyzed by Western blot using the indicated antibodies. **(a)** Representative Western blots showing Spry3 protein detection with long and short exposures are depicted for better viewing of protein levels and double bands. **(b)** Intensity of bands were calculated using ImageQuant software. Results of 2-3 Western blots were summarized and means ± SEM are presented in a column graph. Significance between cell pairs was assessed using unpaired t-test in GraphPad Prism. ODG = Oligodendroglioma, AC = Astrocytoma, GB = Glioblastoma, GS = Gliosarcoma, NB = Neuroblastoma. *$p<0.05$; **$p<0.005$.

To address whether there is a significant correlation between tumor grade and Spry3 levels, the histological subtypes from which the cells derive were compared to each other. In this instance, mean Spry3 protein levels of the starved setup were analyzed and compared.
As depicted in Fig. 13a, Spry3 was found to be differentially expressed across the clinico-pathological subgroups of brain cancer. A tendency to higher Spry3 levels could be observed in the metastatic neuroblastoma cell lines, but since this group consist of only a few samples, a clear statement is not possible. Nevertheless, statistical analysis additionally revealed that Spry3 levels in these cells were not significantly higher compared to cells of the other

groups. Interestingly, the less malignant cancer groups (oligodendroglioma, astrocytoma) demonstrated higher Spry3 protein levels than the more malignant groups (glioblastoma, gliosarcoma), although these differences were not significant.

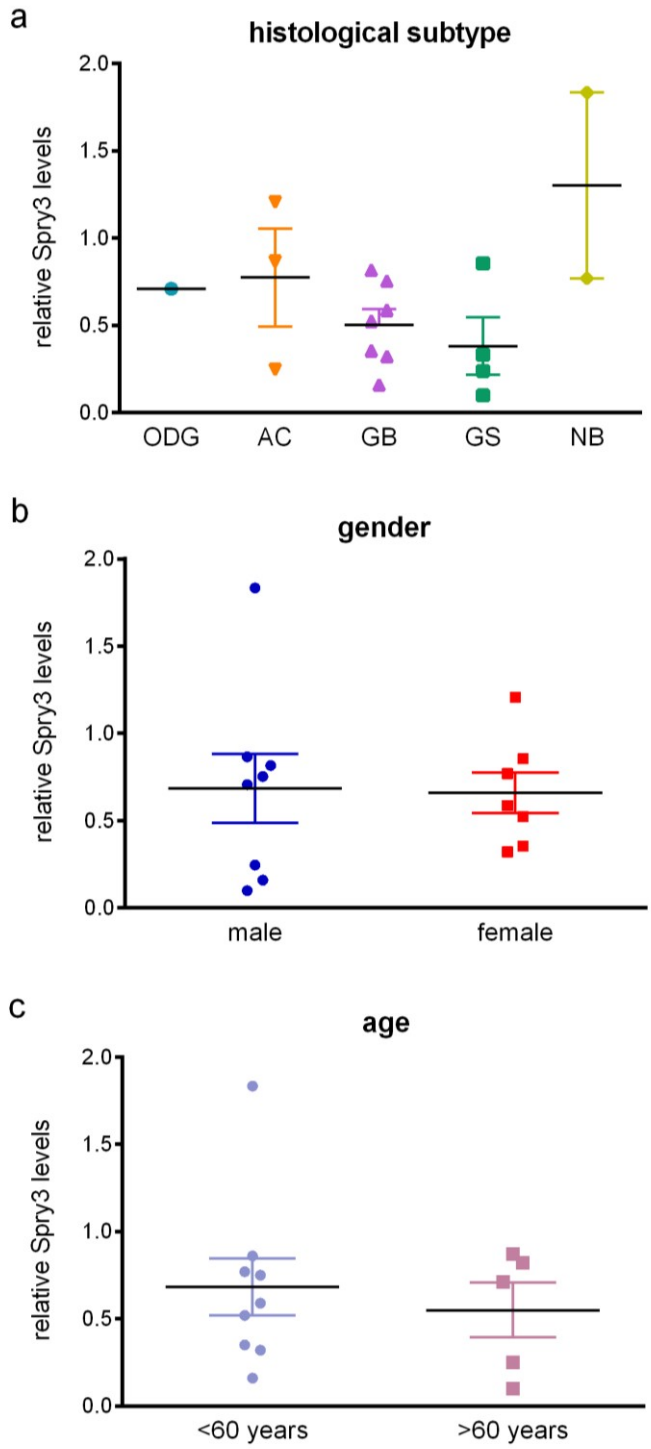

Fig. 13. Spry3 across the clinicopathological subgroups of brain cancer and relation to gender/age of patients the cells originate from. Mean Spry3 values of starved cells were summarized in a scattered dot plot showing means ± SEM. **(a)** Using GraphPad Prism's One-way ANOVA significance between histological subtypes was assessed. **(b)(c)** Unpaired t-test was used to calculate significance between the subgroups of gender and age. ODG = Oligodendroglioma, AC = Astrocytoma, GB = Glioblastoma, GS = Gliosarcoma, NB = Neuroblastoma. **p<0.05; **p<0.005*.

Further analysis of mean Spry3 values of starved cells showed that Spry3 expression correlated neither with gender (Fig. 13b) nor age of patients the cells originate from, although cells from patients under 60 years old demonstrated slightly higher Spry3 levels (Fig. 13c).

4.2 Overexpression studies

4.2.1 CFP pilot testing

To test the suitability of overexpression studies, selected cell lines were examined for their ability to be infected by adenoviral vectors. A three-step serial dilution of a CFP control virus was used as a marker for infectivity rate and cell toxicity. At 48h post infection, fluorescent and Brightfield imaging revealed that U373-MG, DBTRG-05MG clearly, and SK-N-FI to a much lower yet adequate degree, were susceptible to adenoviral infection, as they displayed sufficient infectivity while T98G and SK-N-DZ showed no CFP signal at all (Fig. 14). The second of the three-step serial dilution yielded suitable results, and to avoid any possible cell toxicity, 50 µL instead of the former used 100 µL of this dilution were used to infect cells in subsequent overexpression studies.

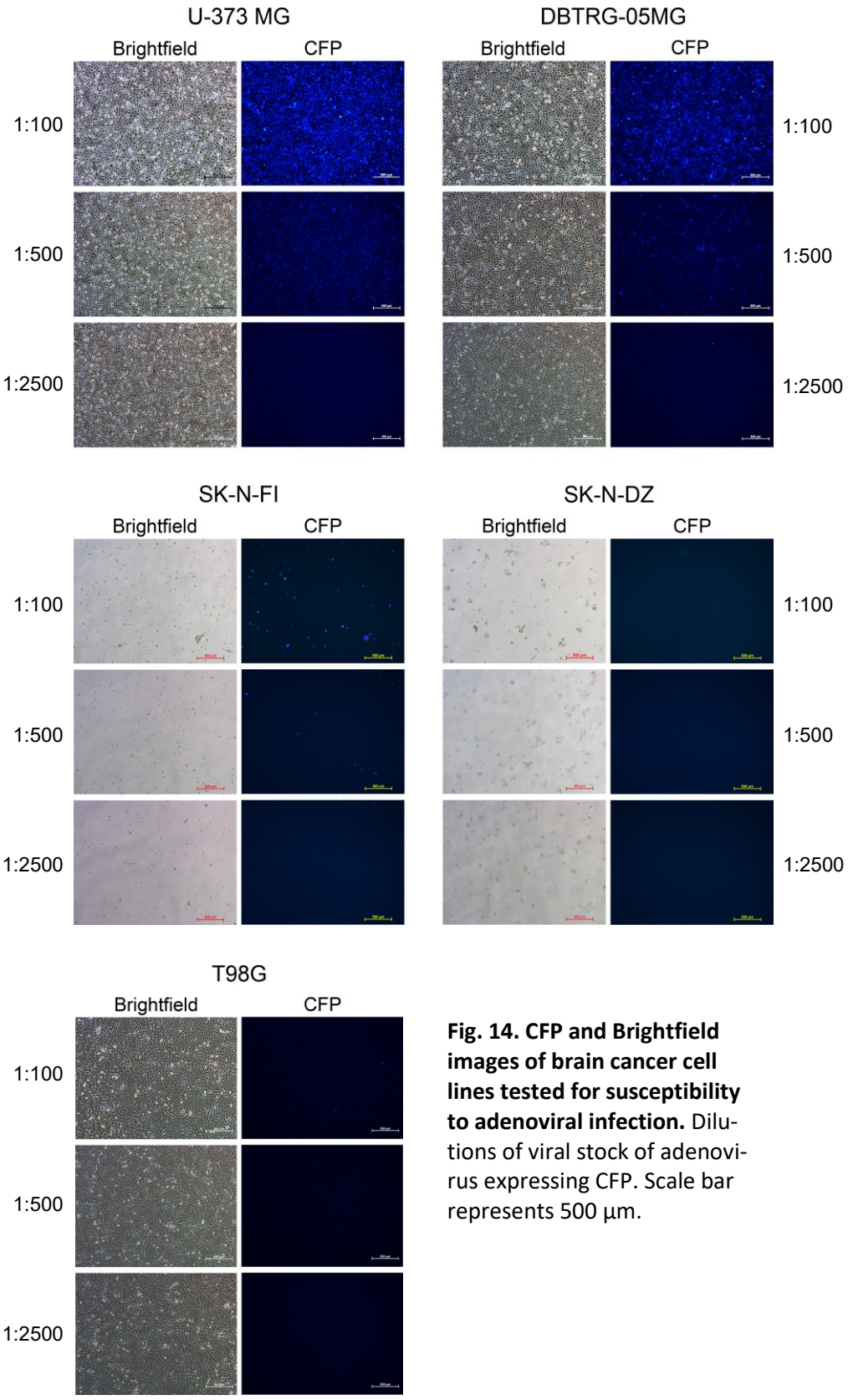

Fig. 14. CFP and Brightfield images of brain cancer cell lines tested for susceptibility to adenoviral infection. Dilutions of viral stock of adenovirus expressing CFP. Scale bar represents 500 µm.

4.2.2 Ectopic Spry3 and Spry4 expression have an opposing effect on cell migration in brain cancer-derived cells

To examine the influence of ectopic Spry3 expression on cell migration in brain cancer-derived cells, scratch assays were performed with U-373 MG and DBTRG-05MG cells. Therefore, cells were infected with adenoviruses expressing Spry3, lacZ (control) and luciferase (control). Furthermore, another member of the Spry family, Spry4, was included.

In U-373 MG cells, the time to close the gap was significantly delayed when cells expressed Spry4 (Fig. 15a-c). These cells covered a distance of 16 µm/h, while control treated cells moved about 1.5-fold faster (23 µm/h). Spry3 expressing cells displayed a distance coverage of 26 µm/h, a result significantly higher when compared to Spry4 expressing cells only, but similar to the control group.

DBTRG-05MG cells were generally faster to close the gap than U-373 MG cells. With a distance coverage of 36 µm/h, ectopic Spry3 expression, in comparison to the control and Spry4 treated groups, significantly accelerated gap closure (Fig. 15a-c). At 24 h, the closure of the wound was complete, whereas in the other groups, the closure of the scratch was less progressed. With the slowest migration rate of 21 µm/h, Spry4 overexpression inhibited gap closure significantly when compared to the Spry3 and control group (26 µm/h).

Both Spry3 and Spry4 were clearly overexpressed by the respective adenoviral system as verified by immunoblot (Fig. 15d). Moreover, the two Spry proteins influenced cell migration differently. In U-373 MG cells, the inhibitory effect of Spry4 on migration was prominent while the accelerating effect of Spry3 was only indicated, as shown in Fig. 15b. In DBTRG-05MG cells, both the accelerating effect of Spry3 and the inhibitory effect of Spry4 were clear.

Although to differing degrees and in a cell-context-dependent manner, these data demonstrate that cell migration is inhibited by Spry4 and accelerated by Spry3, indicating a tumor-suppressive and tumor-promoting role of these Spry isoforms in brain cancer-derived cells, respectively.

a

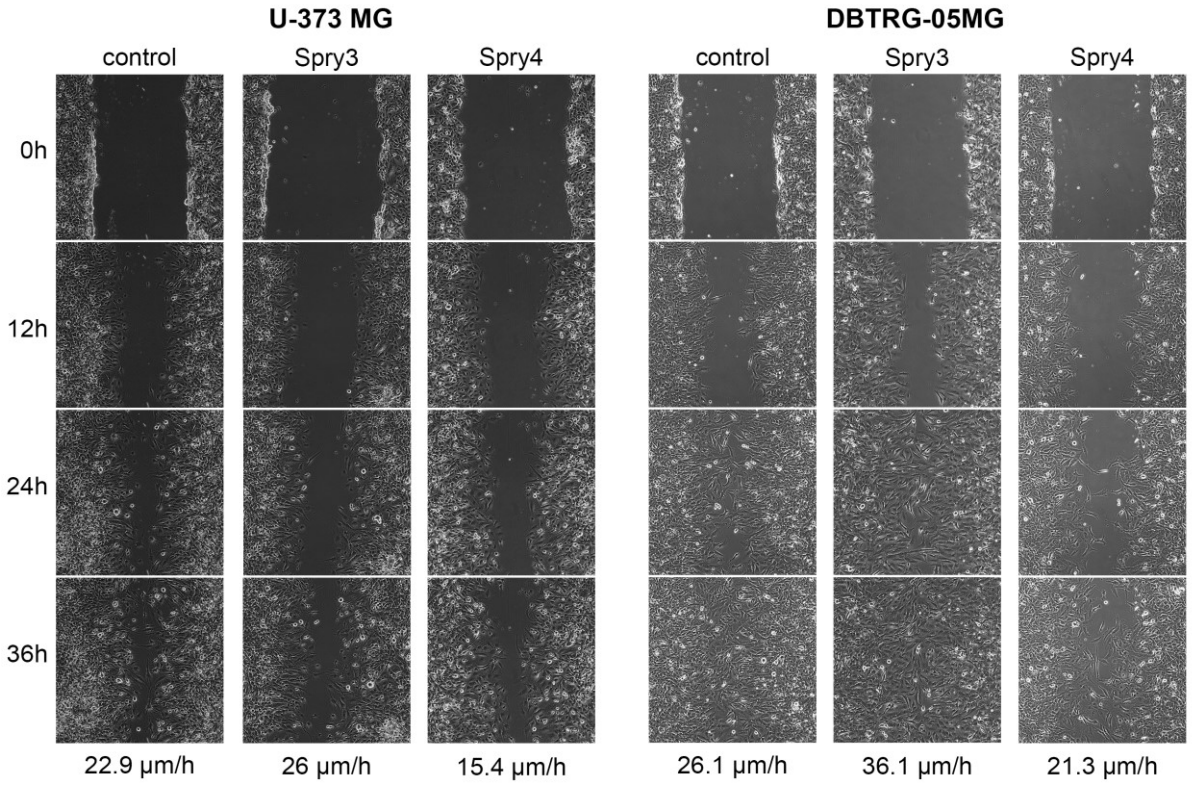
U-373 MG
DBTRG-05MG
control
Spry3
Spry4
control
Spry3
Spry4
0h
12h
24h
36h
22.9 µm/h
26 µm/h
15.4 µm/h
26.1 µm/h
36.1 µm/h
21.3 µm/h

b

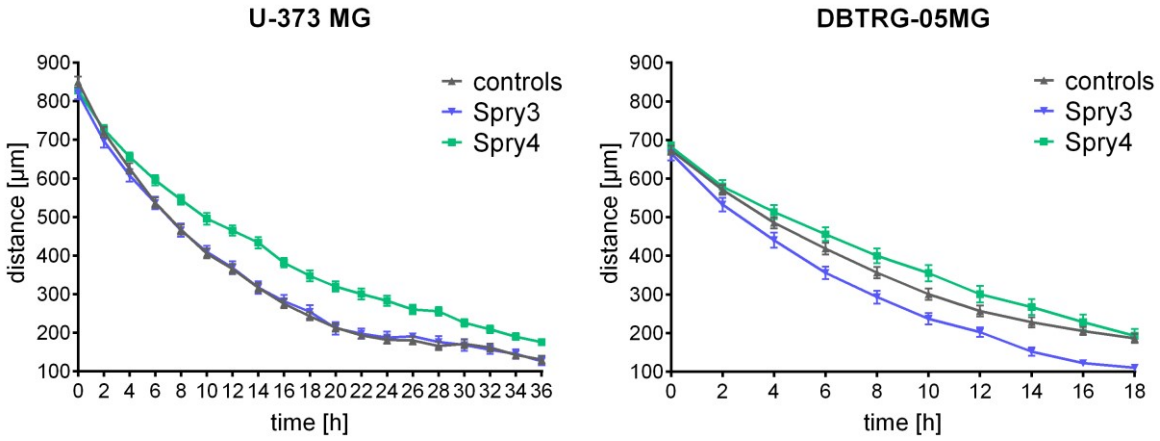
U-373 MG
DBTRG-05MG
controls
Spry3
Spry4
distance [µm]
time [h]
100
200
300
400
500
600
700
800
900
0 2 4 6 8 10 12 14 16 18 20 22 24 26 28 30 32 34 36
0 2 4 6 8 10 12 14 16 18

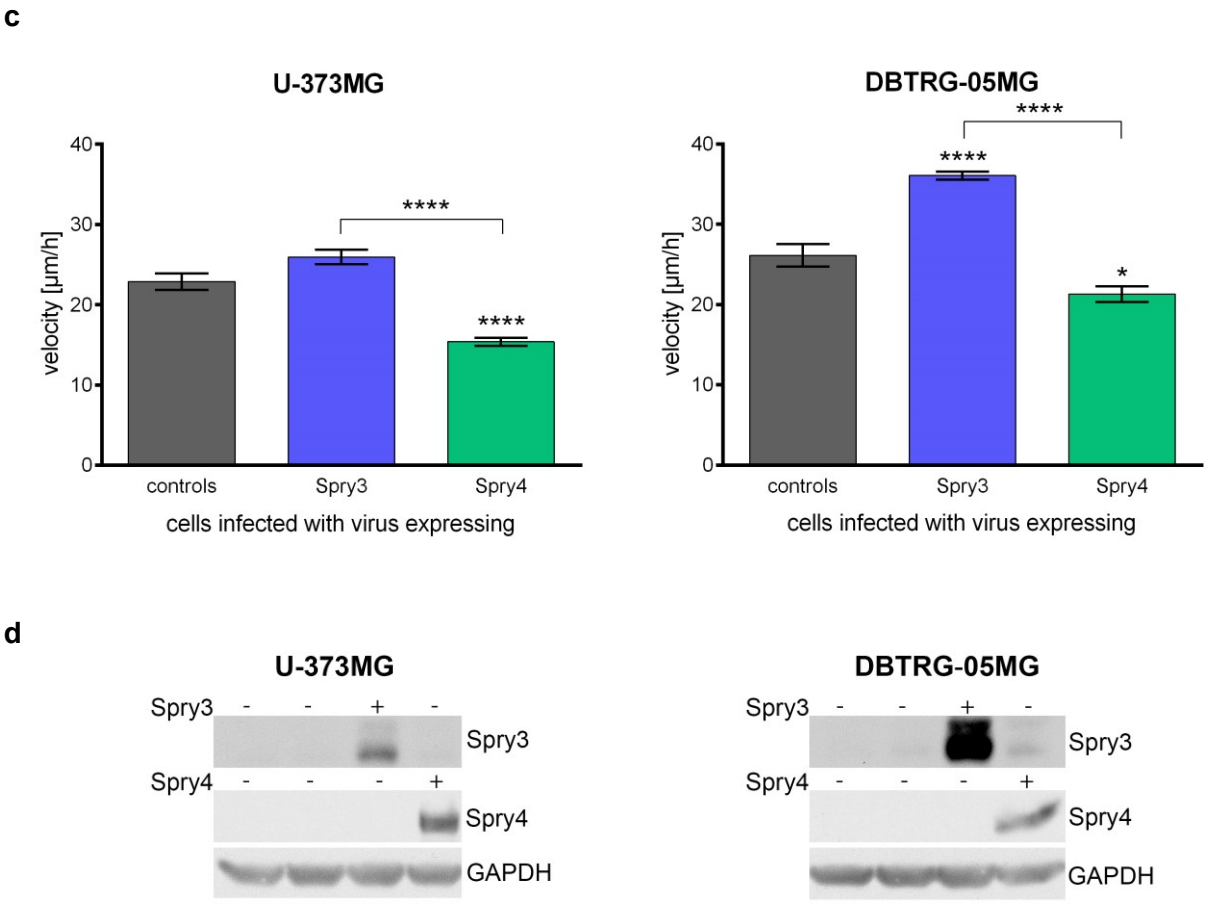

Fig. 15. Influence of Spry3 and Spry4 on cell migration. Both cell lines were infected with adenoviruses expressing the indicated proteins. **(a)** Representative scratches are pictured after 0, 12, 24 and 36 hours. **(b)** Representative curves of distance coverage per hour are depicted for each cell line. Using ImageJ, gap widths were determined by setting five measurements with the line tool for every two-hour timepoints. **(c)** Using linear regression, migration velocities from three different scratches of at least three independent experiments were calculated. Results were summarized in a graph showing means ± SEM. Significance was calculated using One-way ANOVA with Tukey correction in GraphPad Prism. **(d)** After performing the assay, cells were collected and ectopic expression of Spry proteins was verified by immunoblotting with the indicated antibodies. **p<0.05*; ***p<0.01; ***p<0.001; ****p<0.0001*.

4.2.3 Overexpression of Spry3 accelerates while Spry4 diminishes cell proliferation in brain cancer cells

To investigate the influence of Spry3 on cell proliferation in brain cancer-derived cells, Spry3, Spry4 and controls including luciferase, either lacZ or CFP were introduced into U-373 MG and DBTRG-05MG cell lines using the adenoviral system. After re-seeding 4 x 10^4 cells, growth curve analyses were performed by counting cells every 24 hours for 5 days, then curves were modeled using a semi-logarithmic scale. In the case of U-373 MG as it is apparent from Fig. 16a, the resulting almost linear curves depict that cell proliferation was more remarkable in Spry3 expressing cells than in the control and Spry4 treated groups. Lowest

increase in cell number was observed in the Spry4 expressing group. The growth promoting effect of Spry3 overexpression was even stronger in DBTRG-05MG cells. In addition to the fact that DBTRG-05MG cells proliferated at a higher rate than U-373 MG cells in general, the curve obtained from Spry3 expressing cells rose faster than the curves generated from the control and Spry4 groups. The cells expressing Spry4 yet again demonstrated the lowest proliferation rate.

To additionally study if lowering Spry3 levels can influence cell proliferation, shSpry3 was introduced to cells 72 hours prior to re-seeding. Using exponential growth equations of the generated growth curves, doubling times were calculated in GraphPad Prism software.

As can be seen from Fig. 16b, U-373 MG cells infected with Spry3 were the fastest to divide and doubled in 38 hours, significantly faster when compared to all other groups. The control group needed about 43 hours for cell doubling. Expression of shSpry3 and Spry4 significantly slowed down cell doubling when compared to the Spry3 and control group and resulted in similar times of 49 and 48 hours, respectively.

In the DBTRG-05MG cell line, ectopic expression of Spry3 also had an impact on proliferation. When compared to the control and Spry4 groups, it demonstrated significant accelerated cell doubling. Spry4 infected cells were the slowest to divide with doublings every 35 hours. This result was found to be significantly slower than the Spry3 and the control groups, which doubled in 27 and 30 hours, respectively (Fig. 16b). Contrary to expectations, cells expressing shSpry3 displayed the shortest doubling time of 26 hours. As depicted in Fig. 16c, ectopic expression of Spry3 was successful as verified by immunoblotting, but the blots also revealed that in DBTRG-05MG cells, shSpry3 did not lead to a complete knock down of Spry3, as Spry3 protein was still detectable in the shSpry3 lane.

In accordance with the observations made from migration analyses, these data demonstrate that ectopic Spry3 overexpression accelerates while Spry4 expression inhibits cell proliferation in brain cancer-derived cells, substantiating the tumorigenic and anti-oncogenic effects of Spry3 and Spry4, respectively.

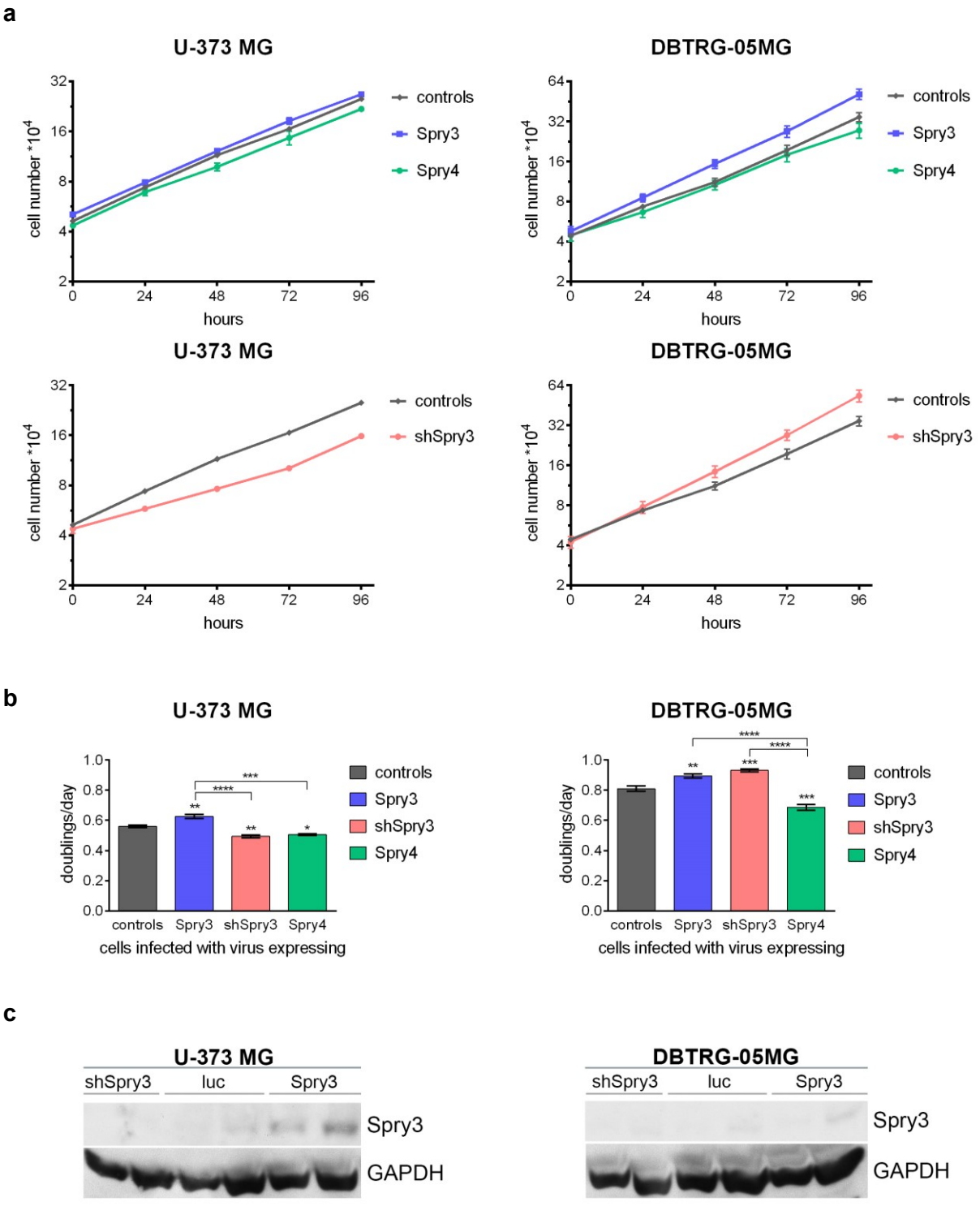

Fig. 16. Influence of ectopic expression of Spry3, shSpry3 and Spry4 on cell proliferation in brain cancer-derived cells was analyzed by performing growth curves. Both cell lines were infected with adenoviruses expressing the indicated proteins. **(a)** Representative growth curve of each cell line is shown and for better viewing, curves of shSpry3 expressing cells are depicted separately. **(b)** Doubling times of at least two independent experiments were calculated using exponential growth equations and means ± SEM are presented as doublings per day. Significance was calculated using One-way ANOVA with Tukey correction in GraphPad Prism. **(c)** Representative immunoblots which were performed with remaining aliquots of days 4 (left lane) and 5 (right lane) to verify overexpression of Spry3 are shown. Reduced Spry3 levels in samples infected with adenoviral vector expressing shSpry3 were not verified by quantification. **p<0.05; **p<0.01; ***p<0.001; ****p<0.0001.*

4.2.4 Ectopically expressed Spry3 and Spry4 influence colony formation ability of brain cancer-derived cells

Colony formation assay was used to test U-373 MG and DBTRG-05MG cells for their ability to grow into a colony after being infected with adenoviruses expressing Spry3, Spry4 and CFP or either luciferase (controls). As pictured in Fig. 17a, all cells exhibited clonogenic properties, as they retained their capacity to reproduce.

In the U-373 MG cell line, cells infected with Spry3 formed about 48 clones within 20 days, significantly more than Spry4 and control treated cells, in which similar values of 34 and 37 clones were obtained, respectively (Fig. 17b).

Corroborating with growth curves experiments, the DBTRG-05MG cell line yet again showed a higher proliferation rate than U-373 MG cells, resulting in more and larger clones in general (Fig. 17a). Cells infected with the Spry3 expressing virus produced 95 clones, similar to the control treated group with 94 clones and significantly more than the Spry4 treated group in which 73 clones were counted. Expression of Spry4 led to statistically significant inhibition of colony formation in DBTRG-05MG cells (Fig. 17b).

These data demonstrate that in some brain cancer-derived cells, ectopically expressed Spry3 and Spry4 influence clone formation. Nevertheless, since this experiment was only performed in replicates, it needs validation by independent experimentations.

a

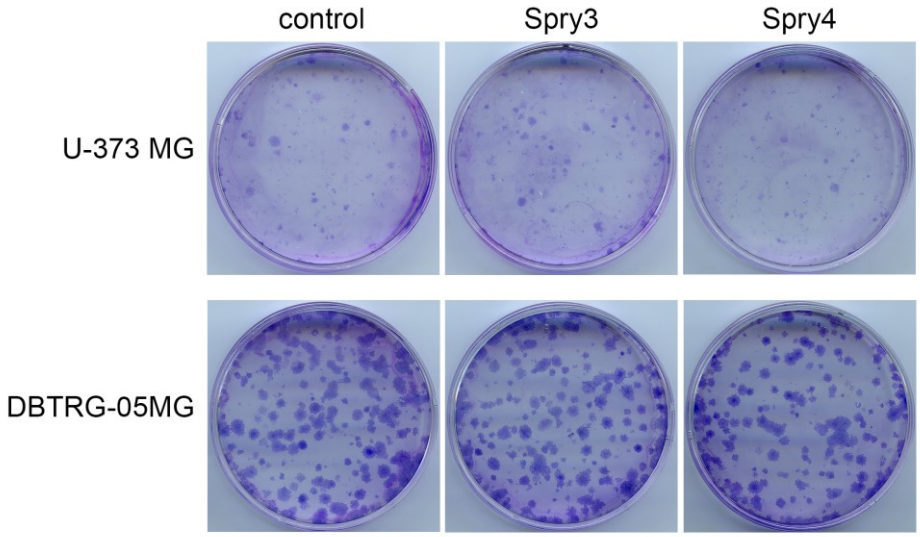

b

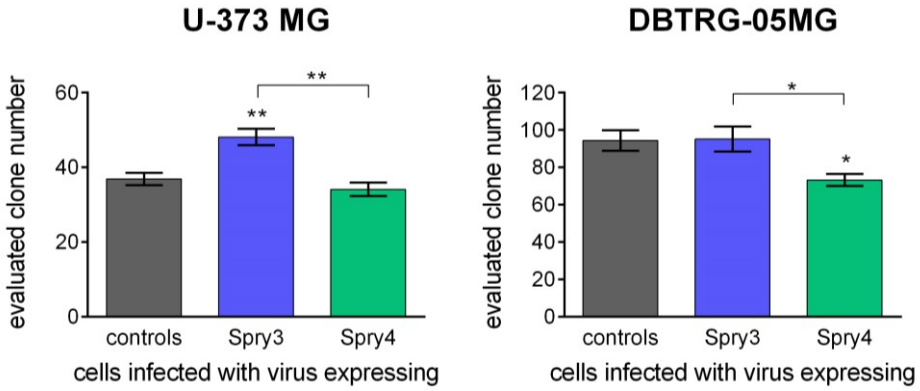

Fig. 17. Influence of ectopic expression of Spry3 and Spry4 on clone formation in brain cancer-derived cells. (a) Representative Giemsa stained dishes are pictured for each cell line and setup. **(b)** Clonogenic assay was performed once in triplicates. Clones were counted and evaluated according to their size. Scored clones were normalized to 100 seeded cells and graphed as plating efficiency ± SEM of the triplicates. Significance was calculated using unpaired t-test in GraphPad Prism. *p<*0.05*; **p<*0.01.*

4.2.5 In brain cancer cells, Spry3 inhibits adherence to collagen while Spry3 knock-down promotes cell adhesion

To study the change of cell adhesion properties of brain cancer-derived cells upon Spry3 introduction, adhesion assay was performed. SK-N-FI cells previously infected with Spry3, shSpry3, Spry4 and luc (control) were re-seeded into wells coated with collagen type I and BSA as negative control.

Adhesion of cells to collagen was observed in all cases as viewed in Fig. 18a, although cells adhered better to the collagen coated wells than to those treated only with BSA. Determination of cell numbers attached to the matrix surface revealed that the presence of ectopic Spry3 protein expression, in comparison to the other groups, significantly inhibited adhesion of SK-N-FI cells (Fig. 18b). In its presence, adherence capacity was reduced 2.0- to 2.5-fold (189 cells) when compared to the Spry4 (468 cells) and control treated groups (400 cells), respectively. Meanwhile, the differences between Spry4 and control virus expressing cells were insignificant. Although they had the same outcomes regarding the Spry- and control treated groups, the two independently performed experiments are depicted separately in Fig. 18b. Deviations were only found in the results obtained from the shSpry3 expressing cells. Even though a higher cell count of 551 cells was obtained in the first experiment, repression of Spry3 failed to influence adhesion significantly when compared to control treated cells. However, in the second experiment, adhesion of shSpry3-treated cells was 1.8-fold

(715 cells) increased by comparison with control virus treated cells. Furthermore, both shSpry3 results were significant when compared to the Spry3 group.

These findings suggest that Spry3 may play a role in cancer invasion and metastasis, as its overexpression leads to reduced cell adhesiveness. Apparently, repression of Spry3 would appear to reverse this oncogenic process, but due to the different obtained results, no clear conclusion can be made regarding its adhesion promoting abilities.

a

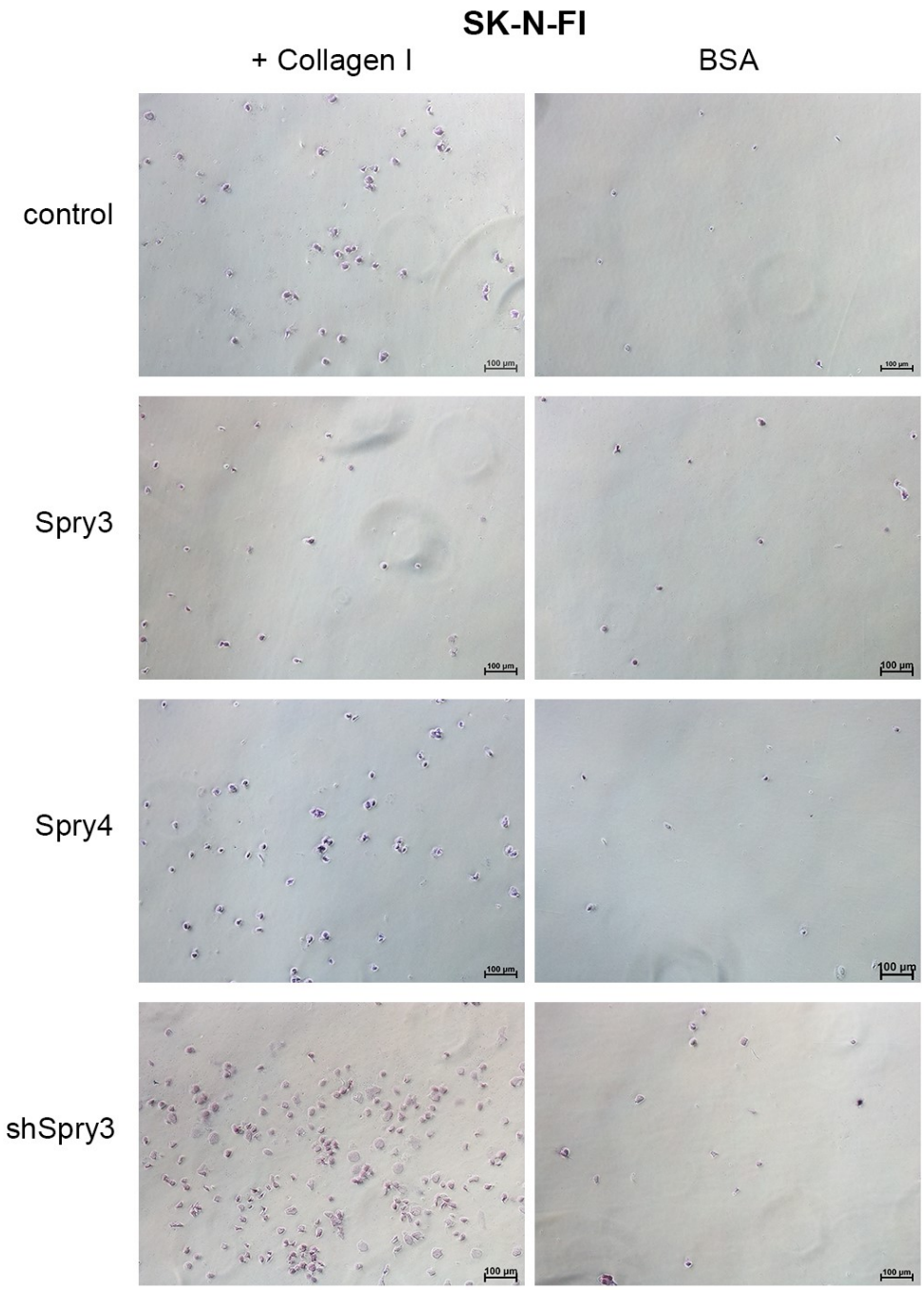

b

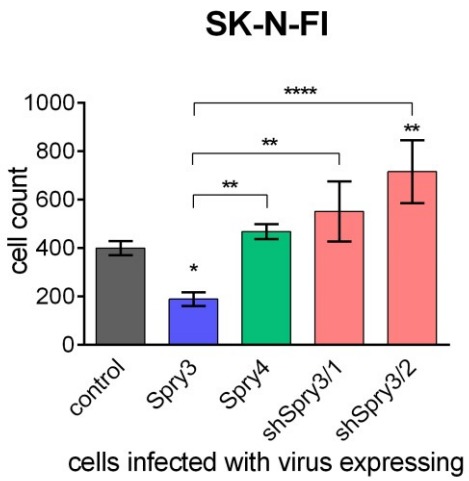

Fig. 18. Influence of ectopic expression of Spry3, shSpry3 and Spry4 on cell adhesion. (a) Representative microscopic pictures of adherent cells of different viral setups. After fixation and staining, cells were counted manually using ImageJ software. **(b)** Cell counts of two experiments were determined by subtracting BSA cell count from collagen count. For better viewing of the different outcomes, cell count of shSpry3 treated cells of both experiments (labelled as shSpry3/1 and shSpry3/2) are depicted separately. Results are presented as column bar with means ± SEM. Significance was assessed in GraphPad Prism using One-way ANOVA with Tukey correction.*p<*0.05*; **p<*0.01;* ***p<*0.001;* ****p<*0.0001.* Scale bar represents 100 µm.

5 Discussion

Although several reports have investigated the role of RTK signaling antagonist Spry in various cancer types, little is known about the function of the family member Spry3 in general. In this context, the aim of the study was to elucidate the role of Spry3 protein in the cancerogenesis of brain-associated cancers.

Since the expression of RTKs and their downstream actors such as the Spry proteins are known to be deregulated in brain tumors, we started our studies by analyzing endogenous Spry3 protein levels in brain cancer-derived cells of glial and non-glial origin. Given that Spry proteins localize at sites of signaling via growth factors [79], we examined the inducibility of endogenous Spry3 expression via serum by determining protein levels in cells which were cultured in the presence and absence of serum. In our study, human brain cancer cell lines generally expressed Spry3, but protein levels varied among the different cell lines, regardless of their stimulation status. This suggests that Spry3, likewise other Spry members, is regulated in a cell- and context-dependent manner but that unlike the other Spry isoforms, Spry3 expression is not subject to growth factor induction [78-80]. Comparable observations were made by Kral et al., where Spry1 protein levels in lung cancer failed to fluctuate in response to serum supplementation [131]. Moreover, we conclude that Spry3 expression does not coincide with tumor grade, as Spry3 levels also showed a divergent distribution across the clinicopathological subgroups of brain cancer. Expression might be regulated rather in a transcription factor-dependent manner, presumably by MAZ, EGR1, ZNF263 and PAX6 [82, 88-90], or in a ligand- and/or receptor-specific manner, as it was reported in the study of BDNF-TrkB signaling by Panagiotaki et al. [78].

Interestingly, we showed that Spry3 appeared as two slightly different migrating bands on Western blots. A possible cross-reaction of the antibody with other Spry isoforms can be ruled out, since the specificity of the Spry3 antibody was confirmed by former group members (data not shown). However, it is probable that this band shifts in the gel are caused by posttranslational modifications of the Spry3 protein such as palmitoylation, phosphorylation and/or others on tyrosine and/or serine residues, as it was reported for the other Spry isoforms [64]. We noted that in the stimulated setup of the cells, the upper/slower migrating band was mostly more pronounced than the lower/faster migrating band. On the contrary, cells cultured devoid of serum displayed a more distinct lower band, implying that posttranslational modification upon stimulation might be the leading cause of double bands, hence

the more pronounced upper band. In some cases, serum stimulation or deprivation even caused no to only little changes in the band pattern. Examples are found when comparing patterns between DBTRG-05MG and U-373 MG cells. It is evident that in DBTRG-05MG, Spry3, in both stimulated and starved cells, is more or less exclusively migrating as an upper form. However, in U-373 MG, Spry3 is migrating as a lower form in cells which were cultured devoid of serum, whereas in stimulated cells, Spry3 appears as both migrating forms. An explanation for the different migration behavior of Spry3 protein bands in these two cases could be due to the fact, that DBTRG-05MG cells harbor a $BRAF^{V600E}$ mutation. BRAF mutations provoke constitutive activation of the ERK pathway and are associated with disabled feedback inhibition loops [46]. Since one of the many consequences of downstream BRAF signaling is the aberrant activation of ERK, increased Spry3 levels as well as serum-induced posttranslational modification may be the consequences in this cell line. This suggestion is further supported by studies of $BRAF^{V600E}$ melanomas, where Spry1, 2, and 4 are overexpressed in an ERK-dependent manner, and the inhibition of $BRAF^{V600E}$ by vemurafenib leads to reduced levels of Spry and SPRED proteins [132]. However, we have not further investigated the underlying mechanisms of the emergence of double bands of the Spry3 protein on Western blots.

Although cancer-related reports of Spry3 expression are scarce in the literature, its expression in normal adult brain tissue is rather well documented [79, 82]. A study investigating Spry mRNA levels concluded that in hepatocellular carcinoma, expression levels of Spry1, Spry2 and Spry4 differed significantly from levels of their non-tumor tissue counterparts. While Spry1 expression was upregulated, Spry2 expression was significantly lowered in advanced hepatocellular carcinoma. However, expression levels of Spry3 were not significantly altered [133].

In the functional part of this study, Spry3 and to better elucidate its unique function, Spry4, were transiently overexpressed to investigate their potential roles in brain cancer. It was shown that Spry3 overexpression positively influenced cell migration in the glioblastoma cell line DBTRG-05MG (WHO Grade IV), while in the generally slower migrating astrocytoma cell line U-373 MG (WHO Grade III), the effect of Spry3 expression on migration was less promi-

nent. Furthermore, cell proliferation was enhanced in both cell lines upon ectopic Spry3 expression, while Spry4 inhibited both of these RTK-mediated processes.

Contrary to expectations that Spry proteins function as antagonists of RTK-mediated signaling [65, 67, 73], our results suggest that in brain cancer Spry3 promotes the tumorigenic potential while Spry4 resumes the role of a tumor-suppressor in brain cancer cells, matching the observations of earlier studies performed with Spry4 [107, 108]. Consequently, we wanted to confirm these findings by checking whether downregulation of Spry3 expression would result in tumor suppressing properties. Thus, we constructed an shRNA directed against Spry3 and examined if Spry3 expression was repressible in those two cell lines. As a result, Spry3 repression in U-373 MG cells was successful as no signals were detectable in Western blots, whereas in the DBTRG-05MG cell line, knock-down of Spry3 was not achieved. This result may be due to the generally higher proliferation rate of DBTRG-05MG cells when compared to U-373 MG in combination with the long incubation time of the shSpry3 adenoviral vector. Expression of shSpry3 might have thin out over the total time period of the experiments, leading to a faster recovery of the target gene from knock down. Nevertheless, after introducing shSpry3 to U-373 MG cells and performing growth curve experiments, we demonstrated that knock-down of Spry3 indeed inhibited cell proliferation, confirming our conclusions from the overexpression studies.

In accordance with our findings, another member of the Spry family, Spry2 was suggested to augment the malignancy of GB cells by two reports [121, 122]. Spry2 was found to be upregulated in GB, which correlated with reduced survival in GB patients [121, 122]. Furthermore, repression of its expression impaired proliferation and anchorage-independent growth of GB cells [121] but not of normal astrocytes [122]. In contrast, Spry2 was reported to reduce GDNF/RET-dependent proliferation of NB cells, whereas a Spry2 mutant (Tyr55 replaced by alanine) enhanced cell proliferation, suggesting that Spry2 regulates NB cell growth by modulating ERK activity downstream of RET tyrosine kinase [134].

In addition to its effects in brain cancer, Spry2 upregulation was also shown to promote proliferation, migration, tumor growth and invasion of colon carcinoma cells while its knock-down decreased cell migration and invasion [116]. Tumor enhancing properties were also demonstrated for Spry1 in the embryonal rhabdomyosarcoma subtype. Spry1, in the pres-

ence of mutant Ras, supported cell proliferation and survival and yet silencing of Spry1 abolished its tumorigenicity [135].

Regarding Spry4 and the concept of it acting as a tumor suppressor in brain cancer, our data are in agreement with previous studies which reported that Spry4 decelerated cell proliferation and motility in breast [108] and lung cancer [107], indicating that Spry4 might fulfill a tumor suppressive role in these tumor entities as well as in brain cancer. In addition, Zhou et al. reported that Spry4 expression inhibited cell proliferation in colon carcinomas [115], while expression of Spry1 [136] and Spry2 [116, 117] enhanced the tumorigenicity of these cancers. Interestingly, paradoxical regulatory roles of Spry2 and Spry4 have been reported by some investigators as well. Rathmanner et al. provided evidence that in osteosarcoma cells, Spry2 but not Spry4 interfered with proliferation and migration [128]. In ovarian cancer, Spry2 and Spry4 proteins were found to be downregulated but only Spry2 downregulation was associated with poor survival of patients [137]. Regarding cell migration, Spry4 expression was additionally reported to inhibit migration in pancreatic [138], prostate [114] cancers and endothelial cells [139].

The significant promoting effect of Spry3 as well as the inhibitory effect of Spry4 on cell proliferation were further verified in part in a clonogenic assay, where the long-term effects of Spry3 and Spry4 overexpression on proliferation as well as adhesion were studied. We investigated which of these events is given priority to and observed that only in the U-373 MG cell line ectopic expression of Spry3 led to increased colony numbers, whereas only in DBTRG-05MG cells, Spry4 negatively influenced clone formation. However, we observed differences in clone sizes. DBTRG-05MG cells formed larger clones in all setups, but this could be due to the higher proliferation rate of this cell line in general compared to the U-373 MG cell line. Since this experiment was only performed in replicates, these data must be interpreted with caution. Nonetheless, these results are in accordance with the findings of Vanas et al., where Spry4 overexpression was also shown to significantly inhibit clone formation in breast cancer-derived cells [108].

To study the short-term changes of cell adhesion properties, we performed adhesion assays in the high-expressing metastatic neuroblastoma SK-N-FI cell line (WHO Grade IV). We showed that Spry3 overexpression significantly inhibited adhesion of cells and similarly to

previous experiments, knock-down reversed this effect in one of two experiment significantly, resulting in increased adhesion rates. Coincidently, Spry4 overexpression had no effect on adhesion in this cell line. These findings further support the idea of the role of Spry3 as an oncogene in brain cancer. Spry3 may not only contribute to tumorigenesis by increasing proliferation and migration events, but also by promoting invasion and metastasis.
However, a study reported by Jaggi et al. showed that in pancreatic cells of mice, Spry4 inhibited cell adhesion and migration without an involvement in tumor growth and progression [138]. Furthermore, it was shown that Spry4 overexpression, besides inhibiting in vivo angiogenesis, inhibited migration and adhesion of endothelial cells, while its repression resulted in increased cell migration [139].

Specific Spry protein family members were shown not only to antagonize malignant phenotypes, but to promote them as well. Possible explanations are delivered by Park et al. and Zhang et al.. In their studies they demonstrated that Spry2 knock-down diminished cell proliferation of GB [122] and colon cancer cells [136], respectively. Both reports suggested that proliferation arrest was due to oncogenic DNA replication stress caused by increased EGF-dependent ERK and Akt signaling. Given that the results obtained from our Spry3 knock-down studies are in compliance with these findings, EGFR-dependent replication stress is likely to play a key role. Similarly to Spry2 [122], repression of Spry3 expression may cause premature S-phase entry and increased DNA damage, leading to decreased cell proliferation of brain cancer-derived cells.
A further approach to understand the mechanisms underlying the oncogenic properties of Spry proteins is presented by another report of Spry2. Holgren et al. demonstrated that Spry2 was upregulated in colon cancer and functioned as an oncogene. Spry2 transfectants showed strong upregulation of HGFR and HGF-stimulated Erk and Akt phosphorylation, leading to enhanced cell migration and invasion. In contrast, knock-down of HGFR and Spry2 significantly decreased cell proliferation, migration and invasion [116]. In our study, we obtained similar results with Spry3 transfectans and it can therefore be assumed that Spry3 in brain cancer, by upregulating RTKs and their downstream effectors, utilizes similar modes of actions as Spry2 in colon cancer.
Another possible explanation is that like Spry1 and Spry2, Spry3 binds to c-Cbl and inhibits c-Cbl mediated RTK degradation, resulting in RTK stabilization and thus, sustained signaling

activity [76]. In the case of Spry2, it was shown that in mammalian cells, Spry2 associated with c-Cbl, thereby blocking the binding between EGFR and c-Cbl and inhibiting c-Cbl-mediated EGFR ubiquitination. On the contrary, Spry4, which at least in some cases fails to bind c-Cbl, would not block EGFR downregulation [140].

Another RTK-stabilizing capacity of Spry proteins was reported by He et al., where Spry1 was found to selectively promote the malignant phenotype in TNBC (triple negative breast cancer) cell lines. In detail, knock-down of Spry1 impaired cell growth, migration and metastasis formation. Furthermore, knock-down of Spry1 attenuated EGF mediated Akt phosphorylation in contrast to knock-down of Spry4, which potentiated this pathway. They reported that Spry1 constitutively anchors to the cell membrane and thus promotes the malignant phenotype likely through stabilizing EGFR and/or facilitating EGFR activation including the formation of down-stream signaling complexes [115]. It is therefore likely that increased proliferation and migration rates might be the result of Spry3 upregulating the expression of RTKs by similar mechanisms.

Concerning their role as negative regulators of RTK-mediated signaling, many reports point out that Spry proteins interfere with the activation of MAPK signaling. During development, Spry proteins interfere with cell signaling in the presence of various growth factors, but especially in response to the FGF family [141]. Overexpression of Spry1 [64, 70], Spry2 [60, 64, 66, 70] and Spry4 [66, 95, 142] were shown to inhibit FGF- and VEGF-induced proliferation, migration or differentiation by limiting pathways leading to ERK activation. The dependency of Spry suppression mechanisms on specific growth factor receptors is further elucidated by studies of Spry4, which was shown to have a broader suppression activity, as it also functioned as an inhibitor for PLC-dependent signaling [143]. In hippocampal neurons, repression of Spry2 and Spry4 expression strongly promoted axon outgrowth, which was further increased by FGF2 treatment. In addition, FGF2 reduced expression of Spry2 by 33% while the expression of Spry4 was reduced by 44% [144]. Spry2 expression in osteoblasts, as an early response to stimulation by FGF1, was reported to act as a feedback inhibitor of FGF1-induced responses [145].

In the context of cancer, Spry1, despite of elevated levels of FGF ligands and FGFRs, was found to be decreased in 40% of prostate cancers, implying that a loss of Spry1 may potentiate the ability of FGFs to enhance tumorigenic properties of prostate cancer cells [111]. An-

other report revealed that in breast cancer, Spry4 exerted inhibitory effects on cell proliferation and migration. They further demonstrated that Spry4 overexpression led to decreased ERK phosphorylation, suggesting that its tumor-suppressing capacities originate from a reduction of MAPK activation [108]. Since the finding mentioned above are in consistency with our results on the inhibitory properties of Spry4 expression, it is likely that in brain cancer-derived cells, similar mechanisms of Spry4 contribute to the inhibition of RTK-mediated processes such as cell proliferation and migration.

6 Conclusion

Together this study has shown that the cellular context in brain cancer is not appropriate for Spry3 to interfere with RTK-mediated processes like proliferation, migration and adhesion. On the contrary, Spry3 enhanced the tumorigenic potential of brain cancer associated cells, while Spry4 exerted tumor suppressing properties. Several questions remain unanswered at present. It will be of interest to examine if and which RTKs in brain cancer cells are target to upregulation by Spry3 overexpression. Additionally, cellular localization, binding partners of Spry3 and functional consequences of these interactions should be addressed in future investigations. To better understand the underlying physiological functions, research is also needed to determine important phosphorylation sites of Spry3 and how phosphorylation events modulate the oncogenic potential of Spry3. Akt and Erk levels including their changes upon growth factor stimulation would be interesting to assess in brain cancer cells as well as in Spry3 transfectants. On this basis, our findings suggest the role of Spry3 is to promote the malignant phenotype in brain cancer.

7 Abbreviations

2-HG	D-2-hydroxyglutarate
AC	Astrocytoma
Akt	Protein kinase B (PKB)
APS	Ammonium persulfate
ATRX	Alpha Thalassemia/Mental Retardation Syndrome X-Linked
BDNF	brain-derived neurotrophin factor
BSA	bovine serum albumin
c-Cbl	canonical casitas B-lineage lymphoma
CDK4	Cyclin Dependent Kinase 4
CDKN2A/B	Cyclin Dependent Kinase Inhibitor 2A/B
CFP	Cyan Fluorescence Protein
c-KIT	KIT Proto-Oncogene Receptor Tyrosine Kinase
CNS	Central Nervous System
CpG	5'cytosine-phosphate-guanine-3'
CRD	cysteine-rich domain
ddH_2O	double-distilled water
DMEM	Dulbecco's Modified Eagle Medium
DMSO	dimethyl sulfoxide
dSpry	Drosophila Sprouty
DYRK1A	dual-specificity tyrosine-phosphorylated and -regulated kinase 1A
EGF	epidermal growth factor, Siehe
EGFR	Epidermal Growth Factor Receptor
EGR1	Early Growth Response Protein 1
Elk-1	ETS Like-1 protein
EMEM	Eagle's Minimum Essential Medium
ERK	Extracellular signal-regulated kinases
FCS	fetal calf serum
FGF	fibroblast growth factor
FGFR	Fibroblast Growth Factor Receptor
FoxO	Forkhead Box O
Gap1	GTPase-activating protein 1
GB	Glioblastoma

G-CIMP	glioma CpG island methylator phenotype
GDNF	glial-derived growth factor
GDP	Guanosine diphosphate
GEF	Guanine nucleotide exchange factor
GPCR	G-protein-coupled receptor
Grb2	Growth Factor Receptor Bound Protein 2
GS	Gliosarcoma
GSK3	Glycogen Synthase Kinase 3
GTP	Guanosine-5'-triphosphate
HGF	hepatocyte growth factor
HGFR	Hepatocyte Growth Factor Receptor
IDH	Isocitrate dehydrogenase
IGFR	Insulin Like Growth Factor Receptor
IP_3	inositol (1,4,5)-trisphosphate
IR	Insulin Receptor
IRS	insulin receptor substrate
JM	juxtamembrane
JNK	c-Jun N-terminal kinase
MAP2K	MEK (MAP/ERK kinase), MAPKK
MAP3K	MAPKK kinase
MAPK	Mitogen-Activated Protein Kinase
MAZ	Myc-Associated Zinc Finger Protein
MDM2/4	Mouse double minute 2/4 homolog
MEK	MAPK/ERK Kinase
MEKK	MEK kinase
MKP	MAPK phosphatase
MLK3	Mitogen-Activated Protein Kinase Kinase Kinase
Mnk1	MAP Kinase Interacting Serine/Threonine Kinase 1
mTORC1/2	mechanistic target of rapamcyin complex 1/2
mut	mutated
NB	Neuroblastoma
NEAA	Non-Essential Amino Acids
NEDD4	neural precursor cell expressed developmentally downregulated protein 4
NF1/2	Neurofibromin 1/2

NSCLC	non-small cell lung cancer
OD	Optical density
ODG	Oligodendroglioma
PAX6	Paired Box Protein Pax-6
PBS	phosphate buffered saline
PDGF	platelet-derived growth factor
PDGFR	Platelet Derived Growth Factor Receptor
PDK1	phosphoinositide-dependent protein kinase 1
PHD	Pleckstrin Homology domain
PHLPP	PH domain leucine-rich repeat protein phosphatase
PI3K	phosphatidyl inositol 3-kinase
PIP_2	phosphatidylinositol 4,5-bisphosphate
PIP_3	phosphatidylinositol 3,4,5-bisphosphate
PKC	protein kinase C
PLC-γ	phospholipase C gamma
PP2A	Protein phosphatase 2A
PTB	phosphotyrosine-binding
PTEN	Phosphatase And Tensin Homolog
PTP1B	Protein tyrosine phosphatase 1B
Raf	Serine/Threonine-Protein Kinase
Ras	Rat Sarcoma
RB	Retinoblastoma
RBD	Raf1-binding domain
RPMI	Roswell Park Memorial Institute
RTK	Receptor tyrosine kinase
SCF	stem cell factor
SDS	Sodium dodecyl sulfate
SDS-PAGE	Sodium dodecyl sulfate-polyacrylamide gel electrophoresis
SH2/3	SRC Homology 2/3 Domain
Shp2	SH2-domain containing tyrosine phosphatase 2
SIAH2	Seven In Absentia Homolog 2
SLB	sample loading buffer
Sos	Son of Sevenless
Spry	Sprouty

SRM	serine-rich motif
T/E	Trypsin/EDTA
TCGA	The Cancer Genome Atlas
TEMED	Tetramethylethylenediamine
TESK1	testicular protein kinase 1
TK	tyrosine kinase
TM	transmembrane helix
TNBC	triple negative breast cancer
TP53	Tumor Protein P53
TrkB	tyrosine receptor kinase B
TSC1	TSC Complex Subunit 1
TSC2	TSC Complex Subunit 2
VEGF	vascular endothelial growth factor
VEGFR	Vascular Endothelial Growth Factor Receptor
WES	whole-exome sequencing
WHO	World Health Organization
wt	wildtype
ZNF263	Zinc Finger Protein 263
α-KG	α-ketoglutarate

8 List of figures

9 List of tables

10 References

1. Noone AM HN, Krapcho M, Miller D, Brest A, Yu M, Ruhl J, Tatalovich Z, Mariotto A, Lewis DR, Chen HS, Feuer EJ, Cronin KA (eds). SEER Cancer Statistics Review, 1975-2015, National Cancer Institute. Bethesda, MD, https://seer.cancer.gov/csr/1975_2015/, based on November 2017 SEER data submission, posted to the SEER web site, April 2018. Accessed February, 2019.
2. Mueller S, Chang S. Pediatric brain tumors: current treatment strategies and future therapeutic approaches. *Neurotherapeutics : the journal of the American Society for Experimental NeuroTherapeutics* 2009;6(3):570-86 doi: 10.1016/j.nurt.2009.04.006.
3. Muscat JE, Hinsvark M, Malkin M. Mobile telephones and rates of brain cancer. *Neuroepidemiology* 2006;27(1):55-6 doi: 10.1159/000094381.
4. Alexiou GA, Sioka C. Mobile phone use and risk for intracranial tumors. *J Negat Results Biomed* 2015;14:23 doi: 10.1186/s12952-015-0043-7.
5. Inskip PD, Hoover RN, Devesa SS. Brain cancer incidence trends in relation to cellular telephone use in the United States. *Neuro-oncology* 2010;12(11):1147-51 doi: 10.1093/neuonc/noq077.
6. Schuz J, Jacobsen R, Olsen JH, Boice JD, Jr., McLaughlin JK, Johansen C. Cellular telephone use and cancer risk: update of a nationwide Danish cohort. *J Natl Cancer Inst* 2006;98(23):1707-13 doi: 10.1093/jnci/djj464.
7. Preston DL, Ron E, Yonehara S, et al. Tumors of the nervous system and pituitary gland associated with atomic bomb radiation exposure. *Journal of the National Cancer Institute* 2002;94(20):1555-63
8. Ron E. Cancer risks from medical radiation. *Health physics* 2003;85(1):47-59
9. Thompson DE, Mabuchi K, Ron E, et al. Cancer incidence in atomic bomb survivors. Part II: Solid tumors, 1958-1987. *Radiation research* 1994;137(2 Suppl):S17-67
10. Johansson G, Andersson U, Melin B. Recent developments in brain tumor predisposing syndromes. *Acta Oncologica* 2016;55(4):401-11 doi: 10.3109/0284186X.2015.1107190.
11. Hamilton SR, Liu B, Parsons RE, et al. The molecular basis of Turcot's syndrome. *N Engl J Med* 1995;332(13):839-47 doi: 10.1056/NEJM199503303321302.
12. Bondy ML, Scheurer ME, Malmer B, et al. Brain tumor epidemiology: consensus from the Brain Tumor Epidemiology Consortium. *Cancer* 2008;113(7 Suppl):1953-68 doi: 10.1002/cncr.23741.
13. Malmer B, Henriksson R, Gronberg H. Different aetiology of familial low-grade and high-grade glioma? A nationwide cohort study of familial glioma. *Neuroepidemiology* 2002;21(6):279-86 doi: 10.1159/000065528.
14. Paunu N, Lahermo P, Onkamo P, et al. A novel low-penetrance locus for familial glioma at 15q23-q26.3. *Cancer research* 2002;62(13):3798-802
15. Kruchko C, Ostrom QT, Boscia A, Truitt G, Gittleman H, Barnholtz-Sloan JS. CBTRUS Statistical Report: Primary Brain and Other Central Nervous System Tumors Diagnosed in the United States in 2011–2015. *Neuro-Oncology* 2018;20(suppl_4):iv1-iv86 doi: 10.1093/neuonc/noy131 %J Neuro-Oncology.
16. Wang L, Sun J, Li Z, et al. Gliosarcomas with the BRAF V600E mutation: a report of two cases and review of the literature. *Journal of clinical pathology* 2017;70(12):1079-83 doi: 10.1136/jclinpath-2017-204620.

17. Nakagawara A, Li Y, Izumi H, Muramori K, Inada H, Nishi M. Neuroblastoma. *Japanese journal of clinical oncology* 2018;48(3):214-41 doi: 10.1093/jjco/hyx176.
18. Martínez-González A. Targetting Hypoxia in Brain Tumors: From Mathematics to Bedside, 2014
19. Louis DN, Ohgaki H, Wiestler OD, et al. The 2007 WHO classification of tumours of the central nervous system. *Acta neuropathologica* 2007;114(2):97-109 doi: 10.1007/s00401-007-0243-4.
20. Louis DN, Perry A, Reifenberger G, et al. The 2016 World Health Organization Classification of Tumors of the Central Nervous System: a summary. *Acta Neuropathol* 2016;131(6):803-20 doi: 10.1007/s00401-016-1545-1.
21. Malta TM, de Souza CF, Sabedot TS, et al. Glioma CpG island methylator phenotype (G-CIMP): biological and clinical implications. *Neuro-Oncology* 2017;20(5):608-20 doi: 10.1093/neuonc/nox183 %J Neuro-Oncology.
22. Ohgaki H, Kleihues P. The Definition of Primary and Secondary Glioblastoma. 2013;19(4):764-72 doi: 10.1158/1078-0432.CCR-12-3002 %J Clinical Cancer Research.
23. Watanabe T, Nobusawa S, Kleihues P, Ohgaki H. IDH1 mutations are early events in the development of astrocytomas and oligodendrogliomas. *The American journal of pathology* 2009;174(4):1149-53 doi: 10.2353/ajpath.2009.080958.
24. Liu X-Y, Gerges N, Korshunov A, et al. Frequent ATRX mutations and loss of expression in adult diffuse astrocytic tumors carrying IDH1/IDH2 and TP53 mutations. 2012;124(5):615-25 doi: 10.1007/s00401-012-1031-3.
25. Jiao Y, Killela PJ, Reitman ZJ, et al. Frequent ATRX, CIC, FUBP1 and IDH1 mutations refine the classification of malignant gliomas. *Oncotarget* 2012;3(7):709-22 doi: 10.18632/oncotarget.588.
26. Cancer Genome Atlas Research N. Comprehensive genomic characterization defines human glioblastoma genes and core pathways. *Nature* 2008;455(7216):1061-8 doi: 10.1038/nature07385.
27. Brennan CW, Verhaak RG, McKenna A, et al. The somatic genomic landscape of glioblastoma. *Cell* 2013;155(2):462-77 doi: 10.1016/j.cell.2013.09.034.
28. Hedger G, Sansom MS, Koldso H. The juxtamembrane regions of human receptor tyrosine kinases exhibit conserved interaction sites with anionic lipids. *Sci Rep* 2015;5:9198 doi: 10.1038/srep09198.
29. R. Critchley W, Pellet-Many C, Ringham B, Harrison M, C. Zachary I, Ponnambalam S. *Receptor Tyrosine Kinase Ubiquitination and De-Ubiquitination in Signal Transduction and Receptor Trafficking*, 2018.
30. Lemmon MA, Schlessinger J. Cell signaling by receptor tyrosine kinases. *Cell* 2010;141(7):1117-34 doi: 10.1016/j.cell.2010.06.011.
31. Hubbard SR, Miller WT. Receptor tyrosine kinases: mechanisms of activation and signaling. *Curr Opin Cell Biol* 2007;19(2):117-23 doi: 10.1016/j.ceb.2007.02.010.
32. Bertrand S, Le Pétillon Y, Somorjai I, Escrivà H. *Developmental cell-cell communication pathways in the cephalochordate amphioxus: Actors and functions*, 2017.
33. Lake D, Correa SA, Muller J. Negative feedback regulation of the ERK1/2 MAPK pathway. *Cell Mol Life Sci* 2016;73(23):4397-413 doi: 10.1007/s00018-016-2297-8.
34. Wennerberg K, Rossman KL, Der CJ. The Ras superfamily at a glance. *J Cell Sci* 2005;118(Pt 5):843-6 doi: 10.1242/jcs.01660.
35. Cargnello M, Roux PP. Activation and function of the MAPKs and their substrates, the MAPK-activated protein kinases. *Microbiol Mol Biol Rev* 2011;75(1):50-83 doi: 10.1128/MMBR.00031-10.

36. Roskoski R, Jr. ERK1/2 MAP kinases: structure, function, and regulation. *Pharmacological research* 2012;66(2):105-43 doi: 10.1016/j.phrs.2012.04.005.
37. Kondoh K, Nishida E. Regulation of MAP kinases by MAP kinase phosphatases. *Biochim Biophys Acta* 2007;1773(8):1227-37 doi: 10.1016/j.bbamcr.2006.12.002.
38. Yoon S, Seger R. The extracellular signal-regulated kinase: multiple substrates regulate diverse cellular functions. *Growth factors (Chur, Switzerland)* 2006;24(1):21-44 doi: 10.1080/02699050500284218.
39. Roberts PJ, Der CJ. Targeting the Raf-MEK-ERK mitogen-activated protein kinase cascade for the treatment of cancer. *Oncogene* 2007;26(22):3291-310 doi: 10.1038/sj.onc.1210422.
40. Eskilsson E, Rosland GV, Talasila KM, et al. EGFRvIII mutations can emerge as late and heterogenous events in glioblastoma development and promote angiogenesis through Src activation. *Neuro-oncology* 2016;18(12):1644-55 doi: 10.1093/neuonc/now113.
41. An Z, Aksoy O, Zheng T, Fan QW, Weiss WA. Epidermal growth factor receptor and EGFRvIII in glioblastoma: signaling pathways and targeted therapies. *Oncogene* 2018;37(12):1561-75 doi: 10.1038/s41388-017-0045-7.
42. Inda MM, Bonavia R, Mukasa A, et al. Tumor heterogeneity is an active process maintained by a mutant EGFR-induced cytokine circuit in glioblastoma. *Genes & development* 2010;24(16):1731-45 doi: 10.1101/gad.1890510.
43. Johansson G, Andersson U, Melin B. Recent developments in brain tumor predisposing syndromes. *Acta Oncol* 2016;55(4):401-11 doi: 10.3109/0284186X.2015.1107190.
44. Jeuken J, van den Broecke C, Gijsen S, Boots-Sprenger S, Wesseling P. RAS/RAF pathway activation in gliomas: the result of copy number gains rather than activating mutations. *Acta neuropathologica* 2007;114(2):121-33 doi: 10.1007/s00401-007-0239-0.
45. Lo HW. Targeting Ras-RAF-ERK and its interactive pathways as a novel therapy for malignant gliomas. *Curr Cancer Drug Targets* 2010;10(8):840-8
46. Wan PT, Garnett MJ, Roe SM, et al. Mechanism of activation of the RAF-ERK signaling pathway by oncogenic mutations of B-RAF. *Cell* 2004;116(6):855-67
47. Davies H, Bignell GR, Cox C, et al. Mutations of the BRAF gene in human cancer. *Nature* 2002;417(6892):949-54 doi: 10.1038/nature00766.
48. Knobbe CB, Reifenberger J, Reifenberger G. Mutation analysis of the Ras pathway genes NRAS, HRAS, KRAS and BRAF in glioblastomas. *Acta neuropathologica* 2004;108(6):467-70 doi: 10.1007/s00401-004-0929-9.
49. Basto D, Trovisco V, Lopes JM, et al. Mutation analysis of B-RAF gene in human gliomas. *Acta neuropathologica* 2005;109(2):207-10 doi: 10.1007/s00401-004-0936-x.
50. Pfister S, Janzarik WG, Remke M, et al. BRAF gene duplication constitutes a mechanism of MAPK pathway activation in low-grade astrocytomas. *The Journal of clinical investigation* 2008;118(5):1739-49 doi: 10.1172/JCI33656.
51. Myung JK, Cho H, Park CK, Kim SK, Lee SH, Park SH. Analysis of the BRAF(V600E) Mutation in Central Nervous System Tumors. *Transl Oncol* 2012;5(6):430-6 doi: 10.1593/tlo.12328.
52. Manning BD, Toker A. AKT/PKB Signaling: Navigating the Network. *Cell* 2017;169(3):381-405 doi: 10.1016/j.cell.2017.04.001.
53. Mendoza MC, Er EE, Blenis J. The Ras-ERK and PI3K-mTOR pathways: cross-talk and compensation. *Trends in biochemical sciences* 2011;36(6):320-8 doi: 10.1016/j.tibs.2011.03.006.

54. Mao H, Lebrun DG, Yang J, Zhu VF, Li M. Deregulated signaling pathways in glioblastoma multiforme: molecular mechanisms and therapeutic targets. *Cancer Invest* 2012;30(1):48-56 doi: 10.3109/07357907.2011.630050.
55. Singh RK, Kumar S, Gautam PK, et al. Protein kinase C-alpha and the regulation of diverse cell responses. *Biomolecular concepts* 2017;8(3-4):143-53 doi: 10.1515/bmc-2017-0005.
56. Fukami K, Nakamura Y. Regulation and physiological functions of mammalian phospholipase C. *The Journal of Biochemistry* 2017;161(4):315-21 doi: 10.1093/jb/mvw094 %J The Journal of Biochemistry.
57. Hacohen N, Kramer S, Sutherland D, Hiromi Y, Krasnow MA. sprouty encodes a novel antagonist of FGF signaling that patterns apical branching of the Drosophila airways. *Cell* 1998;92(2):253-63
58. Mailleux AA, Tefft D, Ndiaye D, et al. Evidence that SPROUTY2 functions as an inhibitor of mouse embryonic lung growth and morphogenesis. *Mechanisms of Development* 2001;102(1-2):81-94 doi: 10.1016/s0925-4773(01)00286-6.
59. Mason JM, Morrison DJ, Basson MA, Licht JD. Sprouty proteins: multifaceted negative-feedback regulators of receptor tyrosine kinase signaling. *Trends in cell biology* 2006;16(1):45-54 doi: 10.1016/j.tcb.2005.11.004.
60. Yigzaw Y, Cartin L, Pierre S, Scholich K, Patel TB. The C terminus of sprouty is important for modulation of cellular migration and proliferation. *J Biol Chem* 2001;276(25):22742-7 doi: 10.1074/jbc.M100123200.
61. Wong ES, Lim J, Low BC, Chen Q, Guy GR. Evidence for direct interaction between Sprouty and Cbl. *J Biol Chem* 2001;276(8):5866-75 doi: 10.1074/jbc.M006945200.
62. Fong CW, Leong HF, Wong ES, Lim J, Yusoff P, Guy GR. Tyrosine phosphorylation of Sprouty2 enhances its interaction with c-Cbl and is crucial for its function. *The Journal of biological chemistry* 2003;278(35):33456-64 doi: 10.1074/jbc.M301317200.
63. Christofori G. Split personalities: the agonistic antagonist Sprouty. *Nat Cell Biol* 2003;5(5):377-9 doi: 10.1038/ncb0503-377.
64. Impagnatiello MA, Weitzer S, Gannon G, Compagni A, Cotten M, Christofori G. Mammalian sprouty-1 and -2 are membrane-anchored phosphoprotein inhibitors of growth factor signaling in endothelial cells. *J Cell Biol* 2001;152(5):1087-98 doi: 10.1083/jcb.152.5.1087.
65. Cabrita MA, Jaggi F, Widjaja SP, Christofori G. A functional interaction between sprouty proteins and caveolin-1. *J Biol Chem* 2006;281(39):29201-12 doi: 10.1074/jbc.M603921200.
66. Sasaki A, Taketomi T, Wakioka T, Kato R, Yoshimura A. Identification of a dominant negative mutant of Sprouty that potentiates fibroblast growth factor- but not epidermal growth factor-induced ERK activation. *J Biol Chem* 2001;276(39):36804-8 doi: 10.1074/jbc.C100386200.
67. Ozaki K, Miyazaki S, Tanimura S, Kohno M. Efficient suppression of FGF-2-induced ERK activation by the cooperative interaction among mammalian Sprouty isoforms. *Journal of cell science* 2005;118(Pt 24):5861-71 doi: 10.1242/jcs.02711.
68. Kim HJ, Bar-Sagi D. Modulation of signalling by Sprouty: a developing story. *Nature reviews. Molecular cell biology* 2004;5(6):441-50 doi: 10.1038/nrm1400.
69. Mason JM, Morrison DJ, Bassit B, et al. Tyrosine phosphorylation of Sprouty proteins regulates their ability to inhibit growth factor signaling: a dual feedback loop. *Molecular biology of the cell* 2004;15(5):2176-88 doi: 10.1091/mbc.e03-07-0503.

70. Hanafusa H, Torii S, Yasunaga T, Nishida E. Sprouty1 and Sprouty2 provide a control mechanism for the Ras/MAPK signalling pathway. *Nature cell biology* 2002;4(11):850-8 doi: 10.1038/ncb867.
71. Fong CW, Leong HF, Wong ESM, Lim J, Yusoff P, Guy GR. Tyrosine Phosphorylation of Sprouty2 Enhances Its Interaction with c-Cbl and Is Crucial for Its Function. *Journal of Biological Chemistry* 2003;278(35):33456-64
72. Rubin C, Litvak V, Medvedovsky H, Zwang Y, Lev S, Yarden Y. Sprouty fine-tunes EGF signaling through interlinked positive and negative feedback loops. *Current biology : CB* 2003;13(4):297-307
73. Lao DH, Chandramouli S, Yusoff P, et al. A Src homology 3-binding sequence on the C terminus of Sprouty2 is necessary for inhibition of the Ras/ERK pathway downstream of fibroblast growth factor receptor stimulation. *The Journal of biological chemistry* 2006;281(40):29993-30000 doi: 10.1074/jbc.M604044200.
74. Schmelzle K, Kane S, Gridley S, Lienhard GE, White FM. Temporal dynamics of tyrosine phosphorylation in insulin signaling. *Diabetes* 2006;55(8):2171-9 doi: 10.2337/db06-0148.
75. Cabrita MA, Christofori G. Sprouty proteins, masterminds of receptor tyrosine kinase signaling. *Angiogenesis* 2008;11(1):53-62 doi: 10.1007/s10456-008-9089-1.
76. DaSilva J, Xu L, Kim HJ, Miller WT, Bar-Sagi D. Regulation of sprouty stability by Mnk1-dependent phosphorylation. *Molecular and cellular biology* 2006;26(5):1898-907 doi: 10.1128/MCB.26.5.1898-1907.2006.
77. Kral R, Doriguzzi A, Mayer CE, Krenbek D, Setinek U, Sutterluty-Fall H. Differential Effects of Variations at Codon 106 on Sprouty2 Functions in Lung Cancer-Derived Cells. *Journal of cellular biochemistry* 2016;117(8):1822-32 doi: 10.1002/jcb.25482.
78. Panagiotaki N, Dajas-Bailador F, Amaya E, Papalopulu N, Dorey K. Characterisation of a new regulator of BDNF signalling, Sprouty3, involved in axonal morphogenesis in vivo. *Development (Cambridge, England)* 2010;137(23):4005-15 doi: 10.1242/dev.053173.
79. Minowada G, Jarvis LA, Chi CL, et al. Vertebrate Sprouty genes are induced by FGF signaling and can cause chondrodysplasia when overexpressed. *Development (Cambridge, England)* 1999;126(20):4465-75
80. de Maximy AA, Nakatake Y, Moncada S, Itoh N, Thiery JP, Bellusci S. Cloning and expression pattern of a mouse homologue of drosophila sprouty in the mouse embryo. *Mech Dev* 1999;81(1-2):213-6 doi: https://doi.org/10.1016/S0925-4773(98)00241-X.
81. Zhang S, Lin Y, Itaranta P, Yagi A, Vainio S. Expression of Sprouty genes 1, 2 and 4 during mouse organogenesis. *Mechanisms of development* 2001;109(2):367-70
82. Ning Z, McLellan A, Ball M, et al. Regulation of SPRY3 by X chromosome and PAR2-linked promoters in an autism susceptibility region. *Human molecular genetics* 2015;24 doi: 10.1093/hmg/ddv231.
83. Lo TL, Fong CW, Yusoff P, et al. Sprouty and cancer: the first terms report. *Cancer letters* 2006;242(2):141-50 doi: 10.1016/j.canlet.2005.12.032.
84. Ozaki K, Kadomoto R, Asato K, Tanimura S, Itoh N, Kohno M. ERK pathway positively regulates the expression of Sprouty genes. *Biochemical and biophysical research communications* 2001;285(5):1084-8 doi: 10.1006/bbrc.2001.5295.
85. Abe M, Naski MC. Regulation of sprouty expression by PLCgamma and calcium-dependent signals. *Biochemical and biophysical research communications* 2004;323(3):1040-7 doi: 10.1016/j.bbrc.2004.08.198.

86. Edwin F, Anderson K, Ying C, Patel TB. Intermolecular interactions of Sprouty proteins and their implications in development and disease. *Mol Pharmacol* 2009;76(4):679-91 doi: 10.1124/mol.109.055848.
87. Hall AB, Jura N, DaSilva J, Jang YJ, Gong D, Bar-Sagi D. hSpry2 is targeted to the ubiquitin-dependent proteasome pathway by c-Cbl. *Current biology : CB* 2003;13(4):308-14
88. Gross I, Morrison DJ, Hyink DP, et al. The receptor tyrosine kinase regulator Sprouty1 is a target of the tumor suppressor WT1 and important for kidney development. *The Journal of biological chemistry* 2003;278(42):41420-30 doi: 10.1074/jbc.M306425200.
89. Ding W, Bellusci S, Shi W, Warburton D. Functional analysis of the human Sprouty2 gene promoter. *Gene* 2003;322:175-85
90. Ding W, Bellusci S, Shi W, Warburton D. Genomic structure and promoter characterization of the human Sprouty4 gene, a novel regulator of lung morphogenesis. *American journal of physiology. Lung cellular and molecular physiology* 2004;287(1):L52-9 doi: 10.1152/ajplung.00430.2003.
91. Lao DH, Yusoff P, Chandramouli S, et al. Direct binding of PP2A to Sprouty2 and phosphorylation changes are a prerequisite for ERK inhibition downstream of fibroblast growth factor receptor stimulation. *The Journal of biological chemistry* 2007;282(12):9117-26 doi: 10.1074/jbc.M607563200.
92. Edwin F, Singh R, Endersby R, Baker SJ, Patel TB. The tumor suppressor PTEN is necessary for human Sprouty 2-mediated inhibition of cell proliferation. *The Journal of biological chemistry* 2006;281(8):4816-22 doi: 10.1074/jbc.M508300200.
93. Gross I, Bassit B, Benezra M, Licht JD. Mammalian sprouty proteins inhibit cell growth and differentiation by preventing ras activation. *The Journal of biological chemistry* 2001;276(49):46460-8 doi: 10.1074/jbc.M108234200.
94. Tefft D, Lee M, Smith S, Crowe DL, Bellusci S, Warburton D. mSprouty2 inhibits FGF10-activated MAP kinase by differentially binding to upstream target proteins. *American journal of physiology. Lung cellular and molecular physiology* 2002;283(4):L700-6 doi: 10.1152/ajplung.00372.2001.
95. Sasaki A, Taketomi T, Kato R, et al. Mammalian Sprouty4 suppresses Ras-independent ERK activation by binding to Raf1. *Nature cell biology* 2003;5(5):427-32 doi: 10.1038/ncb978.
96. Martinez N, Garcia-Dominguez CA, Domingo B, et al. Sprouty2 binds Grb2 at two different proline-rich regions, and the mechanism of ERK inhibition is independent of this interaction. *Cellular signalling* 2007;19(11):2277-85 doi: 10.1016/j.cellsig.2007.07.008.
97. Aranda S, Alvarez M, Turro S, Laguna A, de la Luna S. Sprouty2-mediated inhibition of fibroblast growth factor signaling is modulated by the protein kinase DYRK1A. *Molecular and cellular biology* 2008;28(19):5899-911 doi: 10.1128/MCB.00394-08.
98. Leeksma OC, Van Achterberg TA, Tsumura Y, et al. Human sprouty 4, a new ras antagonist on 5q31, interacts with the dual specificity kinase TESK1. *European journal of biochemistry* 2002;269(10):2546-56
99. Tsumura Y, Toshima J, Leeksma OC, Ohashi K, Mizuno K. Sprouty-4 negatively regulates cell spreading by inhibiting the kinase activity of testicular protein kinase. *The Biochemical journal* 2005;387(Pt 3):627-37 doi: 10.1042/BJ20041181.
100. Chandramouli S, Yu CY, Yusoff P, et al. Tesk1 interacts with Spry2 to abrogate its inhibition of ERK phosphorylation downstream of receptor tyrosine kinase signaling.

The Journal of biological chemistry 2008;283(3):1679-91 doi: 10.1074/jbc.M705457200.
101. Wong ES, Fong CW, Lim J, et al. Sprouty2 attenuates epidermal growth factor receptor ubiquitylation and endocytosis, and consequently enhances Ras/ERK signalling. *The EMBO journal* 2002;21(18):4796-808
102. Ng C, Jackson RA, Buschdorf JP, Sun Q, Guy GR, Sivaraman J. Structural basis for a novel intrapeptidyl H-bond and reverse binding of c-Cbl-TKB domain substrates. *The EMBO journal* 2008;27(5):804-16 doi: 10.1038/emboj.2008.18.
103. Takahashi T, Yamaguchi S, Chida K, Shibuya M. A single autophosphorylation site on KDR/Flk-1 is essential for VEGF-A-dependent activation of PLC-gamma and DNA synthesis in vascular endothelial cells. *The EMBO journal* 2001;20(11):2768-78 doi: 10.1093/emboj/20.11.2768.
104. Fong CW, Chua MS, McKie AB, et al. Sprouty 2, an inhibitor of mitogen-activated protein kinase signaling, is down-regulated in hepatocellular carcinoma. *Cancer research* 2006;66(4):2048-58 doi: 10.1158/0008-5472.CAN-05-1072.
105. Sutterluty H, Mayer CE, Setinek U, et al. Down-regulation of Sprouty2 in non-small cell lung cancer contributes to tumor malignancy via extracellular signal-regulated kinase pathway-dependent and -independent mechanisms. *Molecular cancer research : MCR* 2007;5(5):509-20 doi: 10.1158/1541-7786.MCR-06-0273.
106. Lee SA, Ho C, Roy R, et al. Integration of genomic analysis and in vivo transfection to identify sprouty 2 as a candidate tumor suppressor in liver cancer. *Hepatology (Baltimore, Md.)* 2008;47(4):1200-10 doi: 10.1002/hep.22169.
107. Tennis MA, Van Scoyk MM, Freeman SV, Vandervest KM, Nemenoff RA, Winn RA. Sprouty-4 inhibits transformed cell growth, migration and invasion, and epithelial-mesenchymal transition, and is regulated by Wnt7A through PPARgamma in non-small cell lung cancer. *Molecular cancer research : MCR* 2010;8(6):833-43 doi: 10.1158/1541-7786.MCR-09-0400.
108. Vanas V, Muhlbacher E, Kral R, Sutterluty-Fall H. Sprouty4 interferes with cell proliferation and migration of breast cancer-derived cell lines. *Tumour biology : the journal of the International Society for Oncodevelopmental Biology and Medicine* 2014;35(5):4447-56 doi: 10.1007/s13277-013-1587-0.
109. Lo TL, Yusoff P, Fong CW, et al. The ras/mitogen-activated protein kinase pathway inhibitor and likely tumor suppressor proteins, sprouty 1 and sprouty 2 are deregulated in breast cancer. *Cancer research* 2004;64(17):6127-36 doi: 10.1158/0008-5472.CAN-04-1207.
110. Faratian D, Sims AH, Mullen P, et al. Sprouty 2 is an independent prognostic factor in breast cancer and may be useful in stratifying patients for trastuzumab therapy. *PloS one* 2011;6(8):e23772 doi: 10.1371/journal.pone.0023772.
111. Kwabi-Addo B, Wang J, Erdem H, et al. The expression of Sprouty1, an inhibitor of fibroblast growth factor signal transduction, is decreased in human prostate cancer. *Cancer research* 2004;64(14):4728-35 doi: 10.1158/0008-5472.CAN-03-3759.
112. McKie AB, Douglas DA, Olijslagers S, et al. Epigenetic inactivation of the human sprouty2 (hSPRY2) homologue in prostate cancer. *Oncogene* 2005;24(13):2166-74 doi: 10.1038/sj.onc.1208371.
113. Fritzsche S, Kenzelmann M, Hoffmann MJ, et al. Concomitant down-regulation of SPRY1 and SPRY2 in prostate carcinoma. *Endocrine-related cancer* 2006;13(3):839-49 doi: 10.1677/erc.1.01190.

114. Wang J, Thompson B, Ren C, Ittmann M, Kwabi-Addo B. Sprouty4, a suppressor of tumor cell motility, is down regulated by DNA methylation in human prostate cancer. *The Prostate* 2006;66(6):613-24 doi: 10.1002/pros.20353.
115. Zhou X, Xie S, Yuan C, et al. Lower Expression of SPRY4 Predicts a Poor Prognosis and Regulates Cell Proliferation in Colorectal Cancer. *Cellular physiology and biochemistry : international journal of experimental cellular physiology, biochemistry, and pharmacology* 2016;40(6):1433-42 doi: 10.1159/000453195.
116. Holgren C, Dougherty U, Edwin F, et al. Sprouty-2 controls c-Met expression and metastatic potential of colon cancer cells: sprouty/c-Met upregulation in human colonic adenocarcinomas. *Oncogene* 2010;29(38):5241-53 doi: 10.1038/onc.2010.264.
117. Barbachano A, Ordonez-Moran P, Garcia JM, et al. SPROUTY-2 and E-cadherin regulate reciprocally and dictate colon cancer cell tumourigenicity. *Oncogene* 2010;29(34):4800-13 doi: 10.1038/onc.2010.225.
118. Lito P, Mets BD, Kleff S, O'Reilly S, Maher VM, McCormick JJ. Evidence that sprouty 2 is necessary for sarcoma formation by H-Ras oncogene-transformed human fibroblasts. *The Journal of biological chemistry* 2008;283(4):2002-9 doi: 10.1074/jbc.M709046200.
119. Ivliev AE, t Hoen PA, Sergeeva MG. Coexpression network analysis identifies transcriptional modules related to proastrocytic differentiation and sprouty signaling in glioma. *Cancer Res* 2010;70(24):10060-70 doi: 10.1158/0008-5472.CAN-10-2465.
120. Kwak HJ, Kim YJ, Chun KR, et al. Downregulation of Spry2 by miR-21 triggers malignancy in human gliomas. *Oncogene* 2011;30(21):2433-42 doi: 10.1038/onc.2010.620.
121. Walsh AM, Kapoor GS, Buonato JM, et al. Sprouty2 Drives Drug Resistance and Proliferation in Glioblastoma. *Molecular cancer research : MCR* 2015;13(8):1227-37 doi: 10.1158/1541-7786.MCR-14-0183-T.
122. Park JW, Wollmann G, Urbiola C, et al. Sprouty2 enhances the tumorigenic potential of glioblastoma cells. *Neuro Oncol* 2018;20(8):1044-54 doi: 10.1093/neuonc/noy028.
123. Yuan ZS, Cao Y, Li ZY. IGFBP2 induces SPRY1 expression via NF-kappaB signaling pathway in glioblastoma multiforme (GBM). *European review for medical and pharmacological sciences* 2017;21(22):5072-80 doi: 10.26355/eurrev_201711_13821.
124. Zhang W, Lv Y, Xue Y, et al. Co-expression modules of NF1, PTEN and sprouty enable distinction of adult diffuse gliomas according to pathway activities of receptor tyrosine kinases. *Oncotarget* 2016;7(37):59098-114 doi: 10.18632/oncotarget.10359.
125. Regad T. Targeting RTK Signaling Pathways in Cancer. *Cancers (Basel)* 2015;7(3):1758-84 doi: 10.3390/cancers7030860.
126. Benke S, Agerer B, Haas L, et al. Human tripartite motif protein 52 is required for cell context-dependent proliferation. *Oncotarget* 2018;9(17):13565-81 doi: 10.18632/oncotarget.24422.
127. Sutterluty H, Chatelain E, Marti A, et al. p45SKP2 promotes p27Kip1 degradation and induces S phase in quiescent cells. *Nature cell biology* 1999;1(4):207-14 doi: 10.1038/12027.
128. Rathmanner N, Haigl B, Vanas V, Doriguzzi A, Gsur A, Sutterluty-Fall H. Sprouty2 but not Sprouty4 is a potent inhibitor of cell proliferation and migration of osteosarcoma cells. *FEBS letters* 2013;587(16):2597-605 doi: 10.1016/j.febslet.2013.06.040.
129. Vanas V, Haigl B, Stockhammer V, Sutterluty-Fall H. MicroRNA-21 Increases Proliferation and Cisplatin Sensitivity of Osteosarcoma-Derived Cells. *PloS one* 2016;11(8):e0161023 doi: 10.1371/journal.pone.0161023.

130. Lim J, Wong ES, Ong SH, Yusoff P, Low BC, Guy GR. Sprouty proteins are targeted to membrane ruffles upon growth factor receptor tyrosine kinase activation. Identification of a novel translocation domain. *J Biol Chem* 2000;275(42):32837-45 doi: 10.1074/jbc.M002156200.
131. Kral RM, Mayer CE, Vanas V, Gsur A, Sutterluty-Fall H. In non-small cell lung cancer mitogenic signaling leaves Sprouty1 protein levels unaffected. *Cell biochemistry and function* 2014;32(1):96-100 doi: 10.1002/cbf.2976.
132. Lito P, Pratilas CA, Joseph EW, et al. Relief of profound feedback inhibition of mitogenic signaling by RAF inhibitors attenuates their activity in BRAFV600E melanomas. *Cancer Cell* 2012;22(5):668-82 doi: 10.1016/j.ccr.2012.10.009.
133. Sirivatanauksorn Y, Sirivatanauksorn V, Srisawat C, Khongmanee A, Tongkham C. Differential expression of sprouty genes in hepatocellular carcinoma. *Journal of surgical oncology* 2012;105(3):273-6 doi: 10.1002/jso.22095.
134. Ishida M, Ichihara M, Mii S, et al. Sprouty2 regulates growth and differentiation of human neuroblastoma cells through RET tyrosine kinase. *Cancer Sci* 2007;98(6):815-21 doi: 10.1111/j.1349-7006.2007.00457.x.
135. Schaaf G, Hamdi M, Zwijnenburg D, et al. Silencing of SPRY1 triggers complete regression of rhabdomyosarcoma tumors carrying a mutated RAS gene. *Cancer Res* 2010;70(2):762-71 doi: 10.1158/0008-5472.CAN-09-2532.
136. Zhang Q, Wei T, Shim K, et al. Atypical role of sprouty in colorectal cancer: sprouty repression inhibits epithelial-mesenchymal transition. *Oncogene* 2017;36(28):4088 doi: 10.1038/onc.2017.56.
137. Masoumi-Moghaddam S, Amini A, Wei AQ, Robertson G, Morris DL. Sprouty 2 protein, but not Sprouty 4, is an independent prognostic biomarker for human epithelial ovarian cancer. *International journal of cancer* 2015;137(3):560-70 doi: 10.1002/ijc.29425.
138. Jaggi F, Cabrita MA, Perl AK, Christofori G. Modulation of endocrine pancreas development but not beta-cell carcinogenesis by Sprouty4. *Mol Cancer Res* 2008;6(3):468-82 doi: 10.1158/1541-7786.MCR-07-0255.
139. Gong Y, Yang X, He Q, et al. Sprouty4 regulates endothelial cell migration via modulating integrin beta3 stability through c-Src. *Angiogenesis* 2013;16(4):861-75 doi: 10.1007/s10456-013-9361-x.
140. Haglund K, Schmidt MHH, Wong ES, Guy GR, Dikic I. Sprouty2 acts at the Cbl/CIN85 interface to inhibit epidermal growth factor receptor downregulation. *EMBO Rep* 2005;6(7):635-41 doi: 10.1038/sj.embor.7400453.
141. Guy GR, Jackson RA, Yusoff P, Chow SY. Sprouty proteins: modified modulators, matchmakers or missing links? *The Journal of endocrinology* 2009;203(2):191-202 doi: 10.1677/JOE-09-0110.
142. Lee SH, Schloss DJ, Jarvis L, Krasnow MA, Swain JL. Inhibition of angiogenesis by a mouse sprouty protein. *J Biol Chem* 2001;276(6):4128-33 doi: 10.1074/jbc.M006922200.
143. Ayada T, Taniguchi K, Okamoto F, et al. Sprouty4 negatively regulates protein kinase C activation by inhibiting phosphatidylinositol 4,5-biphosphate hydrolysis. *Oncogene* 2009;28(8):1076-88 doi: 10.1038/onc.2008.464.
144. Hausott B, Vallant N, Schlick B, et al. Sprouty2 and -4 regulate axon outgrowth by hippocampal neurons. *Hippocampus* 2012;22(3):434-41 doi: 10.1002/hipo.20910.

145. Yang X, Webster JB, Kovalenko D, et al. Sprouty genes are expressed in osteoblasts and inhibit fibroblast growth factor-mediated osteoblast responses. *Calcified tissue international* 2006;78(4):233-40 doi: 10.1007/s00223-005-0231-4.

11 Appendix

11.1 Kurzfassung

Essenzielle biologische Prozesse wie Proliferation, Differenzierung, Migration und Zellzyklus sind meist eine zelluläre Antwort auf Wachstumsfaktorstimuli, die durch Rezeptor-Tyrosin-Kinase-vermittelt sind. Sprouty (Spry) Proteine sind evolutionär konservierte Modulatoren dieser Signalwege, die durch ihre Interaktion mit weiteren Effektoren, Mediatoren und Regulatoren die Intensität und Dauer der intrazellulären Signale koordinieren. Dementsprechend ist deren Deregulierung häufig in der Pathophysiologie von Krebs zu finden. Die in dieser Arbeit präsentierte Studie untersucht Sprouty3 (Spry3), ein bisher kaum charakterisiertes Mitglied der Familie, in Bezug auf seine Rolle bei der Krebsentstehung von Hirntumoren.
Wir zeigen, dass die Spry3 Expression, anders als die der anderen Spry-Isoformen, keiner Wachstumsfaktorinduktion unterliegt. Des Weiteren wird das Spry3 Protein auf Western-Blots als Doppelband-Muster detektiert. Häufig sind langsamer wandernde Banden in jenen Zellen anzutreffen, die in Gegenwart von Serum kultiviert wurden, was darauf hinweist, dass das Spry3 Protein einer serumabhängigen Modifikation unterliegt. Dazu passend wird ersichtlich, dass die Spry3 Expression nicht mit dem Tumorgrad einhergeht, da die Spry3 Proteinlevels keine signifikanten Unterschiede in der Verteilung zwischen den klinisch-pathologischen Untergruppen von Hirntumoren aufweisen.
Hirnzelllinien wurden hinsichtlich ihres unterschiedlichen Bandenmusters auf Western Blots, der endogenen Levels von Spry3 und des klinisch-pathologischen Subtyps für Überexpressionsstudien ausgewählt, insofern sie auch fähig waren, Adenoviren aufzunehmen, ohne auf deren Expression zu reagieren. Mit Hilfe eines adenoviralen Expressionssystems wurden Spry3 und als weitere Spry-Kontrolle auch Spry4, in den Zellen überexprimiert und der Effekt von Spry Proteinen auf die Migration, Proliferation, Adhäsion und Klonogenität der Zellen wurde analysiert.
Betrachtet man die Migrationsresultate, beschleunigt die Spry3 Expression die Migration von DBTRG-05MG (Glioblastom, WHO IV) Zellen signifikant, während in U-373 MG (Astrozytom, WHO III) eine erhöhte Migrationsgeschwindigkeit nur angedeutet wird. Gegenteilig dazu führt die Spry4 Expression zu einer Inhibierung der Migration beider Zelllinien.

Zusätzlich zeigen wir, dass die Spry3 Überexpression die Proliferationsrate beider Zelllinien erhöht, während die Spry4 Expression die Zellverdopplung inhibiert. Übereinstimmend mit dieser Beobachtung demonstrieren wir, dass der Knock-down von Spry3 in U-373 MG dann auch zu einer signifikanten Inhibierung der Zellproliferation führt.
Außerdem deuten nicht weiter verifizierte Daten an, dass die Überexpression von Spry3 in U-373 MG Zellen die Klonogenität fördert, während Spry4 auf das Wachstum von DBTRG-05MG Zellen inhibierend wirkt.
Zusätzlich wird gezeigt, dass Spry3-überexprimierende SK-N-FI (Neuroblastom, WHO IV) Zellen eine signifikante Verminderung der Zelladhäsion aufweisen, während die Überexpression von Spry4 keinen Einfluss auf die Adhäsion nimmt. Auch hier kehrt der Spry3 Knock-down diesen Effekt um, was sich in einer signifikanten Förderung der Adhäsion auswirkt.
Zusammenfassend zeigen wir, dass die Spry3 Expression keiner Wachstumsfaktorinduktion unterliegt. Darüber hinaus berichten wir erstmalig, dass Spry3 tumorpromovierende Eigenschaften in Gehirnzellen ausübt, während der Knock-down von Spry3 dieselben Eigenschaften inhibiert. Ganz im Gegensatz zu der Wirkung von Spry3 vermag Spry4 dem malignen Phänotyp in Hirnkrebszellen entgegenzuwirken. Daher leisten unsere Daten einen wichtigen Beitrag zum Verständnis der Rolle von Spry-Proteinen in Hirntumoren.

11.2 Abstract

Essential biological processes such as proliferation, differentiation, migration and cell cycle are mostly a coordinated cellular response to growth factor stimuli interpreted by receptor tyrosine kinase-mediated signaling pathways. Sprouty (Spry) proteins are evolutionarily conserved proteins affecting signal duration and intensity of transmitted signals via their interplay with effectors, mediators, and regulators. Accordingly, the deregulation of Spry is frequently found in cancers and thereby influences the malignant phenotype. This study investigates a previously uncharacterized member of the Spry family, Sprouty3 (Spry3), concerning its role in cancerogenesis of brain-associated cancers.

In this work, we show that unlike it is the case for other Spry isoforms, the expression of Spry3 is not subject to growth factor induction in human brain cancer cells. Furthermore, we demonstrate that Spry3 expression does not coincide with advanced tumor progression.

For overexpression studies, brain cell lines were selected for their different band pattern on Western blots, the endogenous level of Spry3 and clinicopathological subtype, inasmuch as their ability to accept adenoviruses without reacting to their expression. Using the adenoviral system, Spry3 and, as another Spry control, Spry4, were transiently overexpressed and the effect of Spry proteins on migration, proliferation, adhesion and clonogenicity was analyzed. With respect to migration, ectopically expressed Spry3 significantly accelerates cell migration in DBTRG-05MG cells (glioblastoma, WHO IV), while in U-373 MG cells (astrocytoma, WHO III) velocity rates remain largely unaffected. In contrast, Spry4 significantly inhibits cell migration in both cell lines analyzed. In addition, we show that Spry3 overexpression accelerates cell proliferation in both cell lines. In accordance, by using a shRNA directed against Spry3, repression of Spry3 expression in U-373 MG results in a significant inhibition of cell proliferation. In contrast to the tumor promoting activity of Spry3, Spry4 also exerts an inhibitory effect in this assay. Regarding the effects on clone formation ability, our data suggest that overexpression of Spry3 promotes clonogenicity in U-373 MG cells. In DBTRG-05MG, Spry4 impairs clone formation ability in these cells. Concerning their effects on adhesion, it can be shown that Spry3 significantly reduces adhesion of SK-N-FI cells (neuroblastoma, WHO IV), while overexpression of Spry4 protein has no effect. Again, Spry3 knockdown counteracts this effect, resulting in a significant promotion of adhesion.

In summary, we demonstrate that Spry3 expression is not subject to growth factor induction. In addition, we report for the first time that increased Spry3 levels have tumor-promoting properties in brain cells, while a reduction of Spry3 as achieved by a shRNA-mediated knock-down has opposite effects. We further conclude that Spry4 counteracts the malignant phenotype in brain cancer-derived cells. Therefore, our data make an important contribution to the understanding of the role of Spry proteins in brain cancer.

11.3 Vector maps

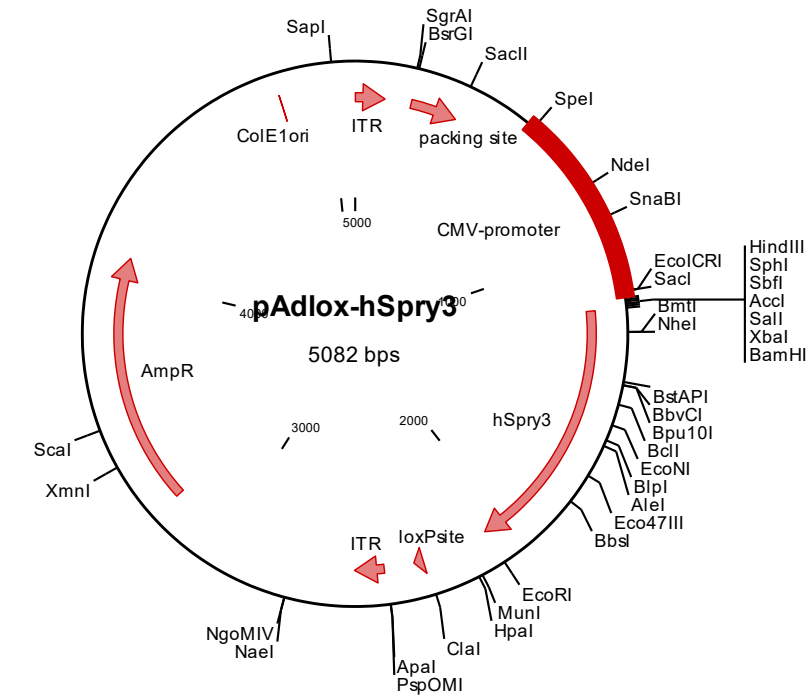

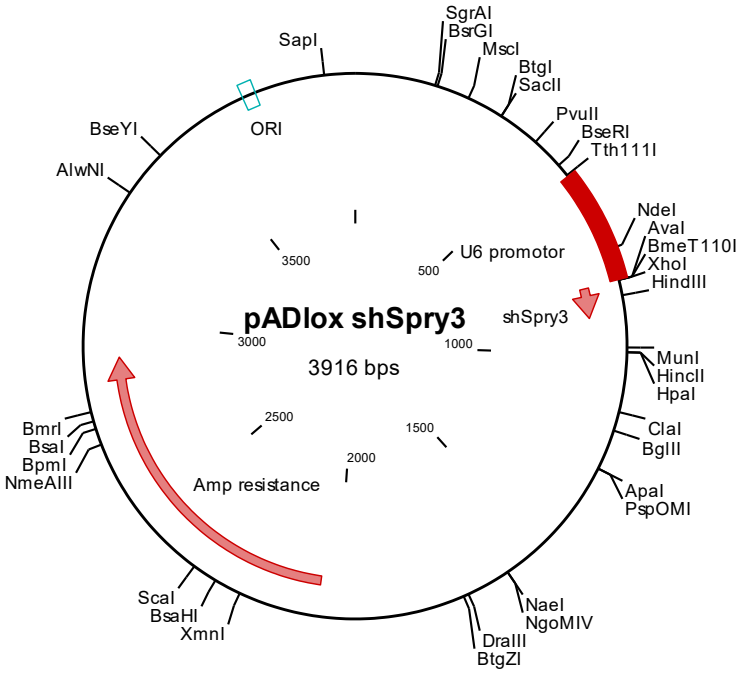

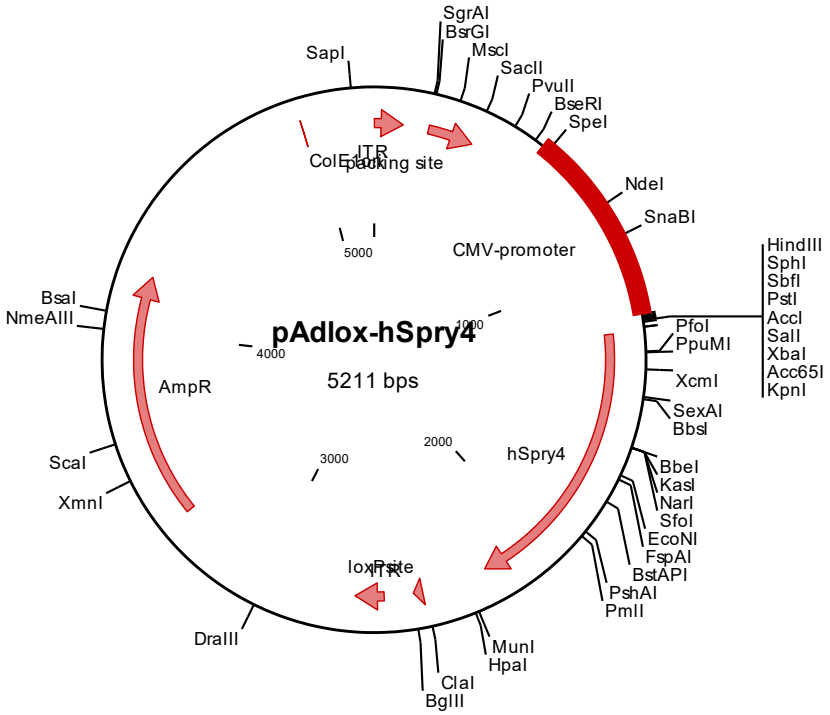
pAdlox-hSpry4
5211 bps
CMV-promoter
hSpry4
AmpR
ITR
ColE1 ori
packing site
loxP site
ITR
5000
1000
2000
3000
4000
SgrAI
BsrGI
MscI
SacII
PvuII
BseRI
SpeI
NdeI
SnaBI
HindIII
SphI
SbfI
PstI
AccI
SalI
XbaI
Acc65I
KpnI
PfoI
PpuMI
XcmI
SexAI
BbsI
BbeI
KasI
NarI
SfoI
EcoNI
FspAI
BstAPI
PshAI
PmlI
MunI
HpaI
ClaI
BglII
DraIII
ScaI
XmnI
BsaI
NmeAIII
SapI

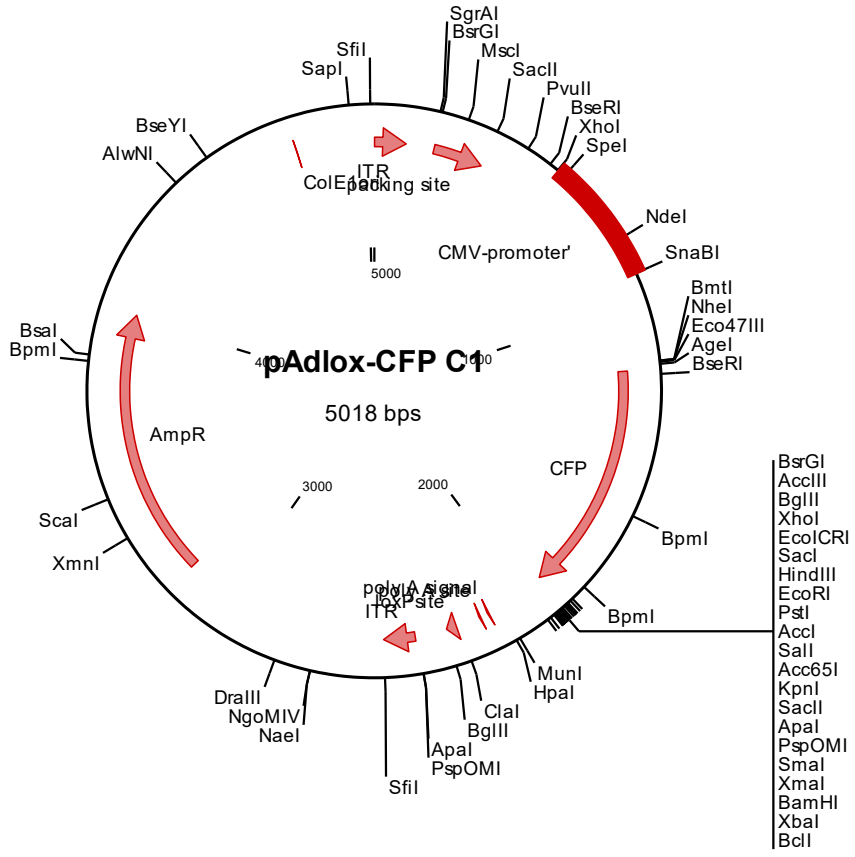
pAdlox-CFP C1
5018 bps
CMV-promoter'
CFP
AmpR
ITR
ColE1 ori
packing site
loxP site
polyA signal
5000
1000
2000
3000
4000
SgrAI
BsrGI
MscI
SacII
PvuII
BseRI
XhoI
SpeI
NdeI
SnaBI
BmtI
NheI
Eco47III
AgeI
BseRI
BpmI
BsrGI
AccIII
BglII
XhoI
EcoICRI
SacI
HindIII
EcoRI
PstI
AccI
SalI
Acc65I
KpnI
SacII
ApaI
PspOMI
SmaI
XmaI
BamHI
XbaI
BclI
MunI
HpaI
ClaI
BglII
ApaI
PspOMI
SfiI
DraIII
NgoMIV
NaeI
ScaI
XmnI
BsaI
BpmI
BseYI
AlwNI
SapI
SfiI

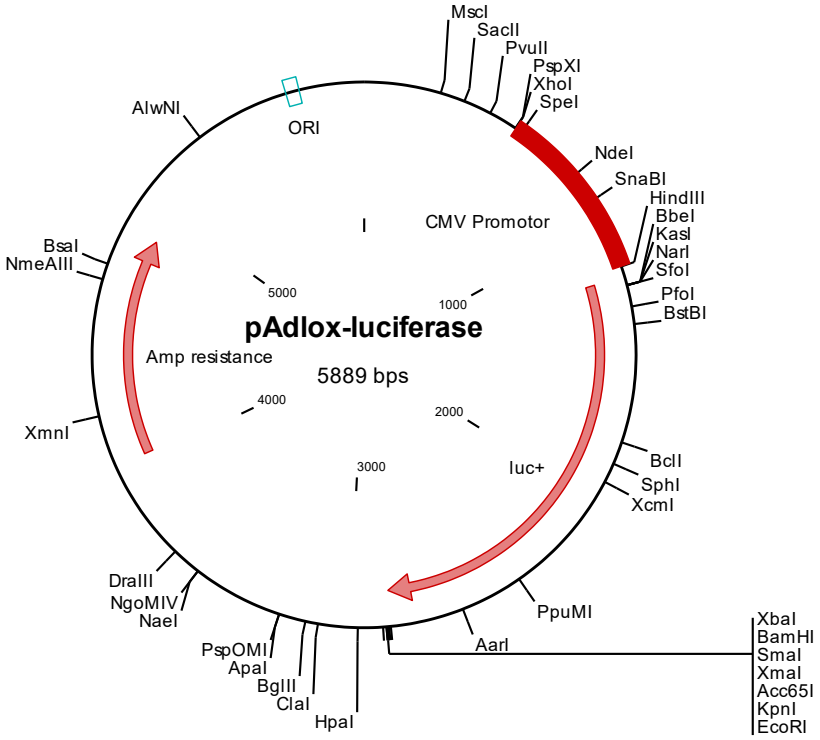
MscI
SacII
PvuII
PspXI
XhoI
SpeI
NdeI
SnaBI
HindIII
BbeI
KasI
NarI
SfoI
PfoI
BstBI
BclI
SphI
XcmI
XbaI
BamHI
SmaI
XmaI
Acc65I
KpnI
EcoRI
PpuMI
AarI
PspOMI
ApaI
BglII
ClaI
HpaI
DraIII
NgoMIV
NaeI
XmnI
BsaI
NmeAIII
AlwNI
ORI
CMV Promotor
5000
1000
pAdlox-luciferase
Amp resistance
5889 bps
4000
2000
3000
luc+